Gene Expression Signature and Pro-Angiogenic Function of Tie2-Expressing Macrophages

Thesis

Ferdinando Pucci, MSc

Gene expression signature and pro-angiogenic function of Tie2-expressing macrophages

PhD candidate

In fulfillment of the Open University requirements for the degree of Doctor of Philosophy in Molecular and Cellular Biology

Director of studies	External supervisor
Michele De Palma	Claire Lewis

Vita-Salute San Raffaele University

Milan, Italy

18 October 2010

Date of Submission: 30 August 2010
Date of Award: 14 October 2010.

ProQuest LLC.
789 East Eisenhower Parkway
P.O. Box 1346
Ann Arbor, MI 48106 – 1346

Table of Contents

Discussion

Appendix – RNA interference

Material and methods

Illustration Index

Index of Tables

Abstract

Chronic inflammation and activation of angiogenesis sustain tumor progression. Recent data indicate that tumor-infiltrating myeloid cells support tumor angiogenesis by regulating multiple pro-angiogenic pathways. However, the functional heterogeneity of myeloid cells – macrophages in particular – may be greater than currently appreciated, and the relative contribution of distinct myeloid cell types to tumor angiogenesis is currently poorly known. Our laboratory identified a subset of tumor-associated macrophages (TAMs) that are required for tumor angiogenesis – the Tie2-expressing macrophages (TEMs). TEMs appear pre-committed to a pro-angiogenic function already when they circulate as monocytes and their elimination from tumor-bearing mice blunts tumor angiogenesis without affecting the recruitment of other myeloid subsets to the tumors. Yet, both the molecular bases of TEMs pro-angiogenic activity and the functional role of the TIE2 receptor in TEM biology are currently unknown. To investigate the molecular identity of TEMs, I developed protocols to purify TEMs and TIE2– TAMs from tumors and compared the gene expression profile of these 2 tumor macrophage subsets. I found that the TEM gene signature is consistent with enhanced pro-angiogenic and tissue-remodelling activity. From such analyses, novel surface markers were established that easily and unambiguously identify TEMs in tumors. Furthermore, I found that circulating Ly6C– monocytes and tumor-infiltrating TEMs express similar gene signatures, suggesting possible developmental relationships between the two myeloid subsets. TEMs, but not other tumor-infiltrating myeloid cells, express the angiopoietin receptor TIE2. To study the functional role of TIE2 in TEMs, I developed a novel lentiviral vector-based, conditional gene knock down platform. Remarkably, *Tie2* knock-down in TEMs significantly inhibited angiogenesis and microvascular perfusion in a spontaneous tumor model, recapitulating several features of TEM elimination. In conclusion, these studies provided a molecular characterization of TEMs and related myeloid cells and identified TIE2 as a critical regulator of their proangiogenic function in tumors.

Introduction

1 Innate immunity: historical perspective

In 1908, Ilya Metchnikoff (1845–1916) and Paul Ehrlich (1854–1915) were jointly awarded the Nobel Prize in Physiology or Medicine, in recognition of their pioneering work on immunity (Mechnikov 1908; Ehrlich 1908). This event led to the birth of immunology as an academic discipline and the beginning of dichotomous thinking regarding innate and adaptive immunity. Ilya Metchnikoff, the father of cellular immunity, described the phagocytic activity carried out by macrophages (Mφs) and neutrophils (which he called microphages). He reported that Mφs are present in different organs, and that phagocytosis is used not only for host nutritional activity and scavenging of degenerated and apoptotic cells (processes that he called *physiological inflammation*), but is also used during *pathological inflammation*, a host defence mechanism against invading pathogens (Chang 2009). Similarly, Paul Ehrlich is considered the father of the humoral theory of immunity. He hypothesized that living cells express *side-chains* that can recognize a particular toxin, *like a key in a lock* (Kaufmann 2008). Ehrlich theorized that a cell under threat can express additional side-chains

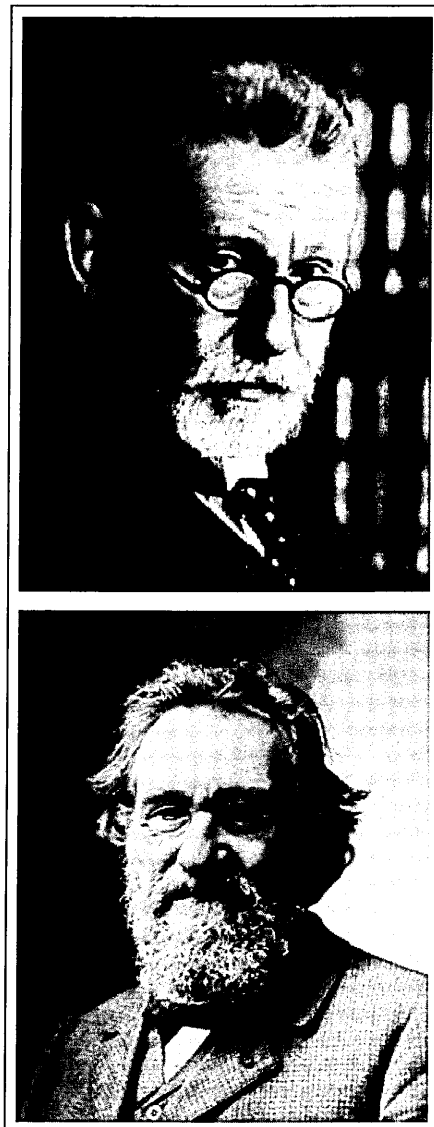

Illustration 1: Paul Ehrlich (top) and Ilya Metchnikoff (bottom). Source: nobelprize.org

to bind the toxin, and that these can be released from the cell surface to become the antibodies that are circulated through the body. It was these antibodies that Ehrlich first described as *magic bullets* in search of toxins. In the early 1900s, Ehrlich's *magic bullets* were used for the first time to treat established tumors using an immunotherapy strategy (Chang 2009).

Following Metchnikoff description of Mφs in Metazoans as early as 1892, cell types with similar features were reported thereafter. Under the name of *clasmatocytes*, Ranvier gave a histologic characterization of the Mφs in mammals; similar cells in the peritoneum were termed by Marschand *adventitial cells*. Maximow found these cells distributed in the connective tissue of mammals and termed them *resting wandering cells*. A similar type of cell was designated by Foot as *endothelial phagocyte* and by Kiyono as *histiocyte*. It is, therefore, apparent that all these terms refer to a similar cell type (Fry 1936).

1.1 Reticulo-endothelial system

Cells sharing a common origin, morphology, and function may be considered as belonging to a single entity and as constituting a "system". In 1924, Aschoff developed the "Mφ system" concept and, based on functional similarities, he grouped several kinds of cells in what he called the reticulo-endothelial system (RES) (van Furth et al. 1972). According to Aschoff, the properties which justify

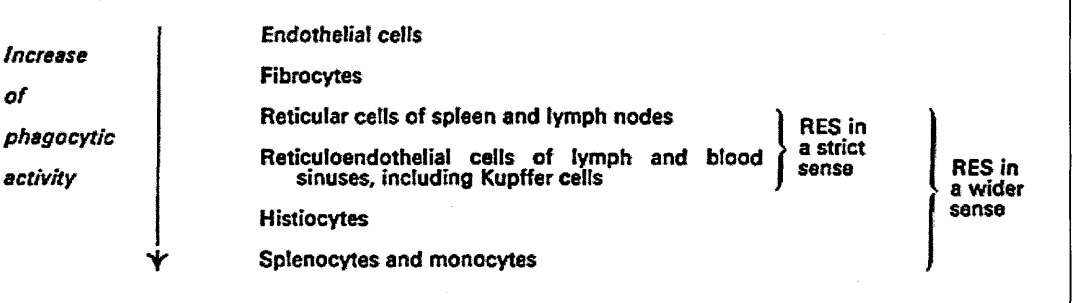

Illustration 2: The reticuloendothelial system (RES) of Aschoff (from van Furth et al. 1972)

inclusion in the RES are best defined as a pre-eminent capacity for ingestion, concentration, and storage of foreign and autogenous substances of particulate nature, such as micro-organisms, cell debris and body fluids (Fry 1936). The cells discussed by Aschoff and ranked in increasing order of phagocytic activity are shown in Illustration 2.

The least phagocytic cells are endothelial cells (ECs), which form a thin layer of cells that line the interior surface of blood vessels, assembling a non-thrombogenic surface between circulating blood in the lumen and the rest of the vessel wall. Endothelial tissue is mesoderm-derived and is a specialized type of simple squamous epithelium. The presence of vimentin rather than keratin filaments allows to distinguish endothelial from epithelial cells.

More phagocytic than ECs are the fibrocytes and reticular cells. Fibrocytes and fibroblasts are believed to be two states of a same cell, the latter being the activated state. Similar to endothelium, fibrocytes are mesoderm derived and thus express vimentin. Fibroblasts produce glycoproteins and glycosaminoglycans, but also collagenous, reticular and elastic fibers, found in the extracellular matrix of connective tissue. Reticular fibers are composed of type III collagen and are produced also by reticular cells, but unlike fibroblasts, reticular cells retain reticular fibers intracellularly. This cellular scaffolding is called cytoreticulum, and allows the creation of non-fibrillar, wholly cellular stroma (found in thymus and spleen germinal centers, where T and B cells develop, respectively).

By far the most phagocytic cells are Mφs (histiocytes) and monocytes, which also originate from mesoderm, as do all hematopoietic cells (HCs). Both monocytes and Mφs play a central role in inflammation, which is a tightly regulated process initiated following tissue injury or infection. The main function of inflammation is to eliminate the pathogenic insult and to remove damaged tissue, with the aim of

restoring tissue homeostasis. The concerted action of several cell types— ECs, neutrophils, monocytes and Mφs — is crucial to the effective elimination of intruders and cell debris (Soehnlein & Lindbom 2010). Mouse models with genetically depleted Mφs provided functional evidence for the important trophic function of Mφs in tissue development and regeneration, namely in ductal branching, bone, Langerhans islets and renal development, neural networking, angiogenesis and the maintenance of reproductive function (Pollard 2009; Ovchinnikov 2008; De Palma et al. 2005).

1.2 Mononuclear phagocyte system

It is now established that there is no direct ontogenic relationship between all the cellular components of the RES, especially not between ECs and Mφs (Goerdt et al. 1996). For this reason, during a conference on mononuclear phagocytes (MP) held in Leiden, The Netherlands, in 1969, a new classification of these cells based on ontogeny was proposed for discussion. All highly phagocytic mononuclear cells and their precursors were grouped in the Mononuclear Phagocyte System (Illustration 3). The functional criteria initially adopted to justify the inclusion of a cell type in the MP system were:

1. phagocytosis mediated by immunoglobulins with or without complement (i.e. immune phagocytosis by "professional phagocytes", to distinguish them from "facultative phagocytic cells" such as fibroblasts, reticular cells, and ECs);
2. the ability to attach firmly to a glass surface;
3. belong to the mononuclear phagocyte lineage, i.e. to originate from a precursor cell in the bone marrow (BM), to be transported via the peripheral blood as monocyte, and eventually to become a tissue Mφ (van Furth et al.

1972).

These criteria (van Furth et al. 1972), together with the knowledge available at the time, allowed the inclusion in the MP system of Mφs from many different organs

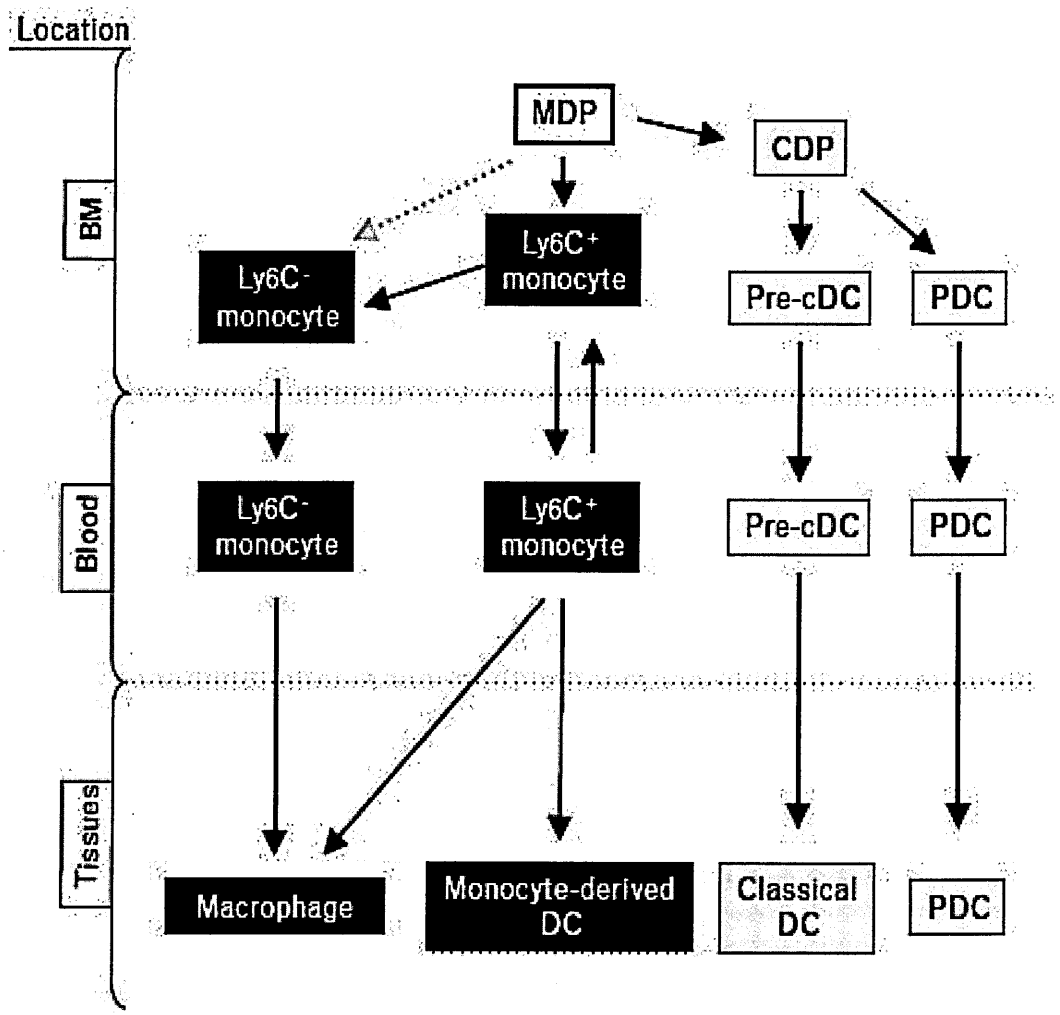

Illustration 3: The MP system in mice. Monocyte DCs progenitors (MDP) give rise to Ly6C+ monocytes, and to classical DCs progenitors (CDP). It remains to be shown whether MDPs give rise directly to Ly6C– monocytes (dotted line). Ly6C+ monocytes convert in the BM to give rise to Ly6C– monocytes. The two monocyte subsets; Ly6C+ and Ly6C– egress from the BM and enter the peripheral circulation. Under steady state conditions, Ly6C– monocytes might contribute to the tissue Mφ compartment. Ly6C+ monocytes can under inflammatory conditions give rise to Mφs and dendritic cells. CDPs give in the BM rise to pre-classical dendritic cells and plasmacytoid DCs (PDC). Pre-classical dendritic cells (Pre-cDC) circulate in blood and enter lymphoid tissue, where they give rise to classical DC. (from Yona & Jung 2010)

(connective tissue, serous cavities, liver, lung, spleen, bone, brain) under both normal and pathological conditions. At the same time, fibroblasts, reticular and ECs were excluded. Of note, splenic and lymph node dendritic cells (DCs) were excluded from the MP system, mainly because it was believed that DCs do not originate from blood monocytes (van Furth et al. 1972). Interestingly, although it was recently confirmed that in homeostatic conditions splenic DCs develop from a BM progenitor without a monocytic intermediate (Varol et al. 2007), it is now accepted that DCs are MP specialized in antigen presentation to T cells (Hume et al. 2002).

Although neutrophils are professional phagocytes that can phagocytose opsonised bacteria, they are excluded from the MP system because they are not derived through a monocytic intermediate. The production and life cycle for MP is more complex than for neutrophils. MP of the blood and tissues survive far longer than neutrophils (a feature clinically important; patients suffer from a high risk of fatal infections following transient interruption of neutrophil production). Monocytes have a preserved capacity to augment production of granule proteins through new protein synthesis, a feature that is lost in mature neutrophils. Of historical interest in this regard, Interleukin-1 (IL1) – the *endogenous pyrogen* thought for many years to be primarily a product of neutrophils – is now known to be predominantly produced by MP, because of their greater capacity for protein synthesis and cytokine production (Dale et al. 2008). At sites of acute inflammation, monocytes accumulate more slowly, but persist longer then neutrophils, which however play a central role during initial phase of inflammation (see paragraph 3).

In the last decade, the MP system framework has been further challenged by studies on monocyte transdifferentiation (Hume et al. 2002) and ontogeny of embryonic Mφs (see paragraph 1.2.a). There has been considerable controversy

in the literature as to whether monocyte transdifferentiation in non-hematopoietic cell types is a significant mechanism in either normal homeostasis or tissue repair. At least in vitro, mature blood monocytes and inflammatory Mφs can apparently transform into vascular elements, including ECs, myofibroblasts and smooth muscle cells. The RES framework, which is based on functional similarities, would be more suited to explain these results. However, transdifferentiation is a very rare event, and the mechanism probably involves monocyte cell fusion, rather than true lineage change (Hume 2006; Wagers et al. 2002).

1.2.a Embryonic Mφs and the mononuclear phagocyte system

The MP system is largely an ontological definition for vertebrates and is useful for classifying Mφs in adults. The embryo seems to contain a Mφ population that does not fit in the MP system framework. The *primitive* embryonic Mφs (peMφs) indeed seem to originate from monopotent precursors in the yolk sac mesoderm at 7.5 days post coitum (dpc), before the development of definitive hematopoiesis. Thus, peMφs bypass the monocyte-like stage, and are observed in the yolk sac, and later on in the embryo starting at 8 dpc (Ovchinnikov 2008). Whether these peMφs persist and/or proliferate in adult tissues is not known. On the other hand, *definitive* embryonic Mφs (deMφs) form as part of the definitive hematopoiesis process (i.e. from myeloid precursors and through the monocyte stage) and thus share more properties in common with their counterparts found in the adult animal than the peMφs (Ovchinnikov 2008). Interestingly, Langerhans cells (LCs) were recently shown to develop from deMφs that colonize the epidermis before birth, differentiate in situ, and then proliferate during the first week of life to establish the LC network. Moreover, adult LCs self-renew in situ and can massively proliferate during inflammation (Chorro et al. 2009).

1.3 Local proliferation of resident tissue mononuclear phagocytes

There is increasing evidence for resident tissue Mφs to be largely maintained through local proliferation under steady state conditions. This has been reported for Mφs as diverse as alveolar Mφs (Landsman & Jung 2007), the previously mentioned LCs (Chorro et al. 2009) as well as brain microglia (Ajami et al. 2007). On the other hand, there is evidence suggesting that in the absence of inflammation, local proliferation is negligible, if any, for splenic white-pulp and metallophilic Mφs (Wijffels et al. 1994) and liver kupffer cells (Crofton et al. 1978). However, the proliferation potential of the various MP subsets is largely unknown, in particular under inflammatory conditions.

1.4 Monocyte subsets

Almost 30 years ago, two discrete subsets of human blood monocytes were identified by morphology, antigen presenting capability and the differential expression of the surface markers CD16 and CD14 (Ziegler-Heitbrock et al. 1991; Shen et al. 1983). These data provided the first clues to a potential existence of differential physiological activities of monocyte subsets. Although the discrimination and function of these populations is still a matter of intense investigation and controversy (Ziegler-Heitbrock et al. 2010), monocyte heterogeneity is now regarded to be a general theme, conserved among mammals, with monocyte subsets having been reported in cows, pigs, rats, mice and humans (Yona & Jung 2010).

Phenotypic characterization in the mouse identified two discrete blood monocyte subsets (Illustration 3), according to their expression of Ly6C, GR1, CCR2, CD62L, CD43 and CX3CR1 (Geissmann et al. 2003; Palframan et al. 2001). Ly6C+ monocytes were initially referred to as *inflammatory* monocytes because

they give rise to Mφs and DCs in a variety of infectious models. Ly6C– monocytes, the most mysterious subset, were initially termed *resident* monocytes because of their longer half-life in vivo and their ability to home to both resting and inflamed tissues (Geissmann et al. 2003; Geissmann et al. 2010). Recently, it was reported that Ly6C+ blood monocytes shuttle efficiently in the absence of inflammation from the blood back to the BM (Varol et al. 2007), suggesting that this subset is not short lived as previously thought (Geissmann et al. 2003). Intriguingly, intravital microscopy revealed that Ly6C– monocytes exhibit long-range crawling on the luminal side of the vascular endothelium (Auffray et al. 2007), a feature that led these authors to term these cells as *patrolling* monocytes. Emerging evidence suggests that the two monocyte subsets exert distinct functions and have distinct fates in vivo (Nahrendorf et al. 2007; Landsman et al. 2007; Varol et al. 2009). Although monocytes have long been considered as a developmental intermediate between BM precursors and tissue Mφs, it is now clear that many DCs and tissue Mφs do not originate from monocytes at steady state, and that monocytes exert specific effector functions during inflammation.

Inflammation rapidly mobilizes monocytes from the BM (Serbina & Pamer 2006) and the subcapsular red pulp of the spleen, where a major monocyte reservoir exists in mice (Swirski et al. 2009). These splenic reservoir monocytes are indistinguishable from circulating blood monocytes and appear to be generated in the BM (like conventional blood monocytes), rather than locally in the spleen. Following injury, both splenic reservoir monocyte subsets are mobilized to the site of inflammation in an angiotensin-mediated, CCR2-independent manner (Swirski et al. 2009), whereas emigration of Ly6C+ monocytes from BM is CCR2-dependent (Serbina & Pamer 2006). However, it is not clear whether inflammation elicited monocytes integrate into the steady state resident MP network, functioning in an identical manner to resident cells.

1.5 Heterogeneity of mononuclear phagocytes

Over the past 10 years, the main, unresolved controversy inside the MP system field regards the heterogeneity versus plasticity issue (Gordon & Taylor 2005). Since the discovery of DCs (Steinman et al. 1974) and their inclusion in the MP system, distinguishing DCs from Mφs still leads to confusion and debate in the field. Several factors contributed to this confusion:

1. the use of non-specific cell surface markers (such as CD11c);
2. the adaptability and plasticity of Mφs to the micro-heterogeneity present in different tissue environments;
3. the wrong assumption that what is true for DCs in lymphoid organs is also true in non-lymphoid organs and what is true under homeostatic conditions is also relevant in inflammation (Geissmann et al. 2010).

Some authors proposed to identify DCs as cells with sufficient migration potential to reach draining lymph nodes or T-cell zones and Mφs as tissue resident, sessile, trophic cells (Geissmann et al. 2010; Yona & Jung 2010; Pollard 2009). On top of this, it has been suggested that the critical contribution of monocytes to the MP system lies in their ability to get rapidly mobilized (from BM and splenic reservoir) and reach through the circulation any site of the organism (Yona & Jung 2010), potentially with different kinetics (Nahrendorf et al. 2007; Hart et al. 2009).

Mφs and DCs may represent two extremes inside the MP system. A similar conceptual polarity stems from studies of Mφ activation during inflammation. It was initially found that Mφs from Th1 (C57B/6 and B10D2) and Th2 (BALB/c and DBA/2) mice respond in a qualitatively different manner to the same stimuli in vitro. This Mφ polarization paradigm was referred to as M1/M2, in analogy to the Th1/Th2 model (Mills et al. 2000). M1/M2 does not simply describe activated or deactivated Mφs, but cells expressing distinct metabolic programs. M1

corresponds to the IFNg-dependent, classical activation and M2 corresponds to IL4/IL13-dependent, altenative activation of Mφs (Gordon & Martinez 2010). Fully polarized M1 and M2 Mφs obtained in vitro are believed to be the extremes of a continuum of functional states present in vivo (Mantovani et al. 2002). Since the heterogeneity and complexity of MP *in vivo* (both under homeostatic and inflammatory conditions) is still largely unknown, Mφ polarization has long been attributed to the plasticity and versatility of these cells in response to exposure to different micro-environmental signals (Mantovani et al. 2002). However, it should be emphasised that the heterogeneity of the MP system is moderately recapitulated by in vitro models. Indeed, *in vitro* generated Mφs and DCs, albeit useful to study some aspect of cell biology of phagocytosis and antigen presentation, do not represent a model to study the specialized functions of the diverse MP subsets that are present in different tissues (Geissmann et al. 2010) and that participate in inflammatory responses and tissue regeneration processes *in vivo (Soehnlein & Lindbom 2010)*. Monocyte heterogeneity may contribute, at least in part, to MP plasticity *in vivo.* For instance, Ly6C– and Ly6C+ monocytes appear to be committed to readily differentiate into M2-like and M1-like MP, respectively.

In conclusion, a technological improvement will be required to shed more light on the fate of monocyte subsets and on the process of antigen presentation *in vivo (Cavanagh & Weninger 2008)*, both in health and disease. The MP field will greatly benefit from cell specific tracking studies that use genetically encoded fluorescent reporters and intravital microscopy.

1.6 Acute versus chronic inflammation

Neutrophils, monocytes and Mφs are phagocytic cells that cooperate during the onset, progression and resolution of inflammation (Soehnlein & Lindbom 2010). In

the first step, molecular alarm signals generated in response to sterile tissue damage and/or microbial invasion are recognized by resident MP (Rock et al. 2010; Medzhitov 2007). Owing to their strategic location in close proximity to the site of injury, tissue-resident cells are the primary inducers of an inflammatory reaction. Patrolling monocytes have been proposed to take part to this phase also (Auffray et al. 2007). Following the recognition of danger signals, these tissue-resident cells synthesize leukotriene B_4 (a strong secretagogue of neutrophil granule proteins and a powerful inducer of reactive oxygen species production) and chemokines, namely CXCL1, CXCL2, TNF and IL6 (phase I). During extravasation, neutrophils sequentially release preformed granules, which sensitize neutrophils to signals present in the milieu, induce ECs activation and permeability and promote Ly6C+ monocytes recruitment (phase II) (Soehnlein et al. 2008). Although the recruitment cascade for neutrophils and monocytes is similar, the two cell populations differ in their use of cell adhesion molecules and chemokines (Ley et al. 2007). After the inflammatory stimulus (e.g. pathogens) has been eliminated by the concerted action of neutrophils and MP, to avoid excessive tissue damage the healing process is actively triggered. Several mechanisms have a role in turning off neutrophil infiltration and promoting the uptake and clearance of apoptotic cells: 1) lipid mediator class switch (Serhan et al. 2008; Ravichandran & Lorenz 2007); 2) inhibition of neutrophil infiltration (Bournazou et al. 2009; Perretti & D'Acquisto 2009); 3) chemokine inactivation (Soehnlein & Lindbom 2010); 4) down-regulation of granulopoiesis (Stark et al. 2005). Thus, inflammation is a self-limiting process, but under certain circumstances, failure in the resolution of inflammation hampers the restoration of tissue homeostasis and chronic inflammation ensues. Only recently, the mechanisms involved in this pathological diversion of the inflammatory response have started to be investigated. For instance, it has been proposed that if an adaptive immune response is activated

by persistent stimulation (longer than 7 days), a chronic inflammatory loop may establish when even adaptive immune responses (which involve T and B cell functions) fail to eradicate the stimulus. In such a scenario, the composition of the infiltrating leukocytes changes from neutrophils to a mixture of mononuclear phagocytes and T cells. Concomitantly, the inflammatory stimulus changes from the one sensed by pattern-recognition receptors of innate immune cells to the one recognized as an antigen by activating receptors on T and B cells of the adaptive immune system. Antigen-activated T cells can enhance effector functions of MP and neutrophils (for instance increasing the specificity of action by antibody mediated targeting) or recruit alternative effector cells, such as eosinophils. The specialized effector cells of adaptive immunity often succeed in eradicating a stimulus that resists clearance by innate immunity, which allows for resolution and repair. Prolonged antigenic stimulation by resistant microbes or tissue-derived auto-antigens leads to chronic inflammation with formation of an inflammatory neo-tissue (Pober & Sessa 2007), which can eventually evolve to malignancy (de Visser et al. 2005).

2 Inflammation, angiogenesis and cancer

2.1 The hallmarks of cancer

Several lines of evidence indicate that tumorigenesis in humans is a multistep process and that these steps reflect genetic alterations that drive the progressive transformation of normal human cells into highly malignant derivatives. Taken together, observations of human cancers and animal models argue that tumor development proceeds via a process formally analogous to Darwinian evolution, in which a succession of genetic changes, each conferring one or another type of growth advantage, leads to the progressive conversion of normal human cells into

cancer cells. The vast catalog of cancer cell genotypes is believed to be a manifestation of six essential alterations in cell physiology that collectively dictate malignant growth (Illustration 4). These six capabilities are shared in common by most and perhaps all types of human tumors (Hanahan & Weinberg 2000).

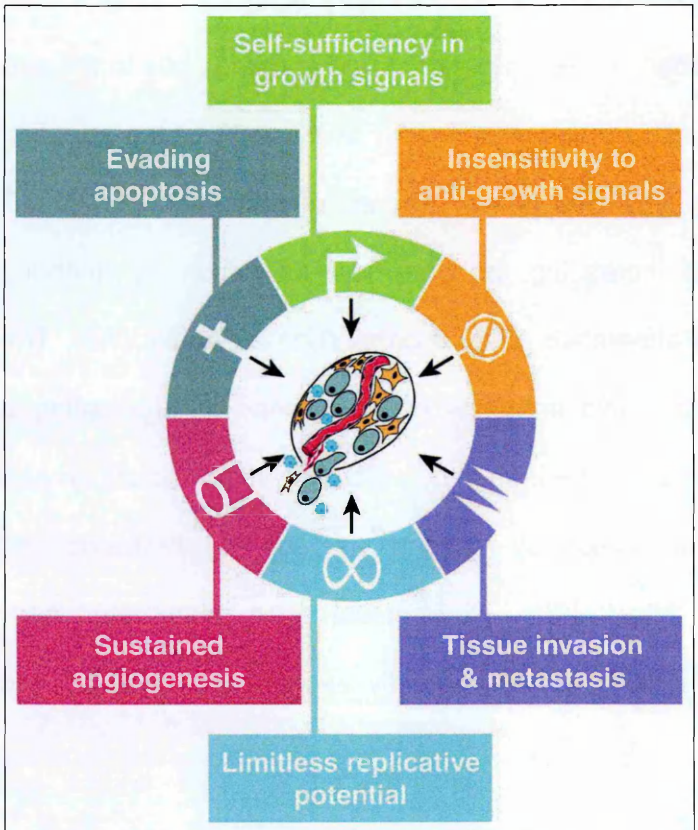

Illustration 4: Acquired Capabilities of Cancer (from Hanahan & Weinberg 2000)

Whereas acquired capabilities such as evading apoptosis, insensitivity to anti-growth signals and limitless replicative potential are clearly cell autonomous (Hanahan & Weinberg 2000), the remaining three, i.e. self-sufficiency in growth signals, tissue invasion and metastasis and sustained angiogenesis can receive a direct, variable contributions from the micro-environment, tumor-associated Mφs (TAMs) in particular (Qian & Pollard 2010). Although it has been proposed that inflammation represents the 7th hallmark of cancer (Mantovani 2009), angiogenesis is intimately linked to chronic inflammation and can account for it.

2.2 Tumor angiogenesis

Angiogenesis, a physiological process involving the growth of new blood vessels from pre-existing ones, is universally recognized as a hallmark of cancer (see paragraph 2.1). Angiogenesis is an obligate and rate-limiting factor for tumor

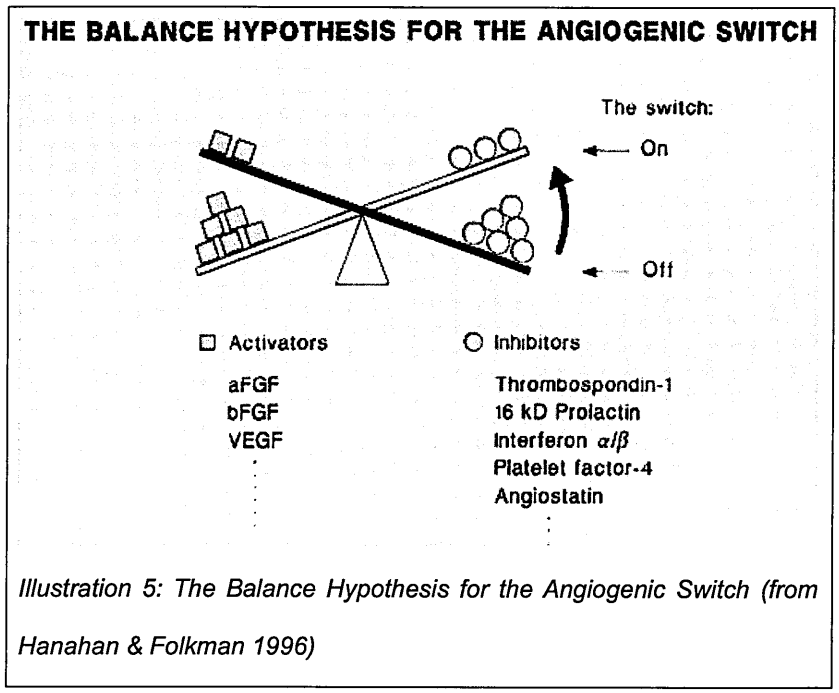

Illustration 5: The Balance Hypothesis for the Angiogenic Switch (from Hanahan & Folkman 1996)

growth (Folkman et al. 2000). Indeed, the oxygen and nutrients supplied by the vasculature are crucial for cell function and survival, obligating virtually all cells in a tissue to reside within 100 µm of a capillary blood vessel. Because of this dependence on nearby capillaries, and since proliferating cells within a tissue do not have an intrinsic ability to stimulate blood vessel growth, incipient neoplasias must develop angiogenic ability in order to progress to a larger size (Hanahan & Weinberg 2000). According to the balance hypothesis (Hanahan & Folkman 1996), the switch to the angiogenic phenotype involves a change in the local equilibrium between positive and negative regulators of angiogenesis (Illustration 5). The ability to induce and sustain angiogenesis seems to be acquired in a discrete step during tumor development, in pre-neoplastic lesions, prior to the appearance of full-blown tumors (Hanahan & Folkman 1996).

2.3 Inflammation and cancer

Back in 1863, Rudolph Virchow documented the association between the *lymphoreticular infiltrate* present at chronically inflamed tissues and the site of origin of human cancer (Plytycz & Seljelid 2003). Such an observation was

resurrected in recent years with the popular concept that inflammation and cancer are causally linked (Balkwill & Mantovani 2001). This concept is based both on epidemiological data linking chronic inflammation to a higher cancer risk and experimental evidence that certain inflammatory cells, such as TAMs, may facilitate tumor development (Mantovani & Sica 2010). It has been estimated that a significant proportion of chronic inflammatory diseases (such as inflammatory bowel desease, gastric ulcer, hepatitis) progress to cancer in predisposed patients (Coussens & Werb 2002). Chronic inflammation can cause initiating mutations in susceptible cell populations just like chemical carcinogens do. MP and neutrophils can induce DNA damage in proliferating cells, through their generation of reactive oxygen and nitrogen species that are produced normally by these cells to fight infection (Maeda & Akaike 1998). These species react to form peroxynitrite, a mutagenic agent. Hence, repeated tissue damage and multiple cycles of tissue regeneration of tissue (Illustration 6), in the presence of highly reactive nitrogen and oxygen species released from inflammatory cells, may accelerate the accumulation of genetic and epigenetic alterations that affect the expression or function of proto-oncogenes and tumour suppressor genes in somatic cells (Hussain et al. 2003).

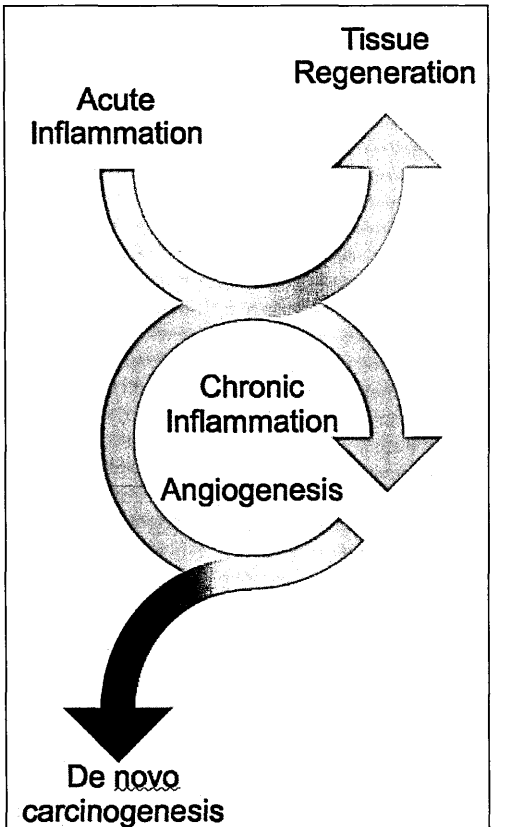

Illustration 6: Model for the link between inflammation, angiogenesis and cancer. Personal interpretation.

In 1880, seventeen years after Virchow's association between cancer and inflammation, Julius Cohnheim was the first to state that *there is no inflammation without blood vessels* (Doerr 1985). In non-inflamed

tissues, vascular ECs maintain blood fluidity, regulate blood flow, control vessel wall permeability and keep circulating leukocytes quiescent. The activation of ECs involves rapidly acting, pre-synthesized and stored molecules (type I activation), in addition to a subsequently slower transcriptionally regulated response program (type II activation) (Pober & Cotran 1990). The angiopoietin–Tie2 system is emerging as a key regulator of EC homeostasis and activation. Angiopoietin-2, one of the two main Tie2 ligands, functions as an immediate autocrine switch of vascular responsiveness to exogenous stimuli and angiogenesis (see paragraph 4.2) (Fiedler & Augustin 2006). Activated ECs trigger neutrophil recruitment (Fiedler et al. 2006), and thus play a central role in the first phase of inflammation (see paragraph 1.6). Thus, ECs activation is not only prerequisite for initiating angiogenesis, but also for triggering inflammation and inflammation-associated diseases (Illustration 6).

3 Myeloid cells and tumor angiogenesis

Oncogene activation and/or tumour suppressor gene inactivation can alter the expression of angiogenesis activators and inhibitors in transformed cells. However, these events may not be sufficient to trigger the angiogenic switch. In this regard, there is a growing interest in understanding the complex interactions between BM-derived myeloid-lineage cells and angiogenesis in tumors. Such interest has been revived recently by the observation that tumor-infiltrating myeloid cells convey pro-angiogenic programs that can counteract the activity of anti-angiogenic drugs in mouse tumor models (Shojaei & Ferrara 2008). Several studies highlighted the importance of BM-derived HCs in tumour angiogenesis (Bergers et al. 2000; Coussens et al. 2000; De Palma et al. 2003). HC subsets that have been directly implicated in tumour angiogenesis include mast cells (Coussens et al. 1999), TAMs (Lin et al. 2001), Tie2-expressing macrophages (TEMs) (De Palma et al.

2003) and Gr1+ CD11b+ myeloid derived suppressor cells (MDSCs) (Yang et al. 2004a). Other HCs types, such as platelets, neutrophils, DCs, eosinophils and hematopoietic progenitors may also participate in the angiogenic process, but it remains to be established whether they directly promote angiogenesis, rather than having a function in supporting tissue inflammation and remodelling (De Palma & Naldini 2006). However, the relative contribution of each of the aforementioned myeloid cell types to tumor angiogenesis has been limited so far by our little understanding of their developmental, phenotypic and functional identity in the context of the tumor micro-environment.

3.1 Monocytes/Macrophages

These cells are released from the bone marrow as pro-monocytes, mature into monocytes in the circulation, infiltrate tumors, and differentiate further into TAMs (Mantovani et al. 2008; Lewis & Pollard 2006). Once in tumors, Mφs express a wide array of pro-angiogenic factors, including vascular endothelial growth factor (VEGF)-A and matrix metalloproteinase (MMP)-9 (Coussens et al. 2000; Giraudo et al. 2004; Lewis et al. 2000). Evidence for their role in tumor angiogenesis has been established by several different experimental approaches. By using MMTV-PyMT mammary tumor-prone mice carrying a colony stimulating factor-1 (*Csf1*) null mutation ($Csf1^{OP/OP}$), Lin and co-workers (Lin et al. 2001; Lin et al. 2006) demonstrated that the absence of CSF-1 markedly decreased Mφ infiltration in pre-malignant tumors, and this, in turn, resulted in inhibition of tumor angiogenesis and delayed metastasis. Furthermore, inhibition of tumor-derived TAM chemoattractants, ablation of TAMs by DNA vaccination, or pharmacological neutralization of TAM-produced pro-angiogenic molecules also impaired tumor angiogenesis in various tumor models (Fischer et al. 2007; Luo et al. 2006; Giraudo et al. 2004). It should be noted, however, that in *Ccr2*-deficient, K14-HPV

cervical tumor-prone mice, the genetic depletion of TAMs unleashed a compensatory neutrophil response that rescued tumor angiogenesis and progression (Pahler et al. 2008). This interesting observation highlights a certain degree of functional redundancy among tumor-infiltrating Mφs and neutrophils, that may vary in a tissue- or organ-specific fashion.

TAM depletion from tumors removes all of the many aspects of Mφ involvement in tumor progression. These include, in addition to the production of VEGF-A and other pro-angiogenic factors, the release of cellular mediators that promote immuno-suppression and enhance tumor cell survival, migration and invasion (Mantovani et al. 2008; Lewis & Pollard 2006; Condeelis & Pollard 2006). To specifically analyse the role of myeloid cell-derived VEGF-A in tumor angiogenesis, Stockmann and co-workers (Stockmann et al. 2008) crossed mice carrying *loxP*-flanked *Vegfa* alleles to mice carrying a lysozyme M promoter-driven *Cre* recombinase. Interestingly, the authors found that the targeted deletion of VEGF-A in myeloid cells failed to inhibit angiogenesis and tumor growth or decrease the overall amount of VEGF-A expressed in tumors. Rather, it attenuated the vascular abnormalities commonly observed in tumors and improved tumor perfusion (a phenomenon previously referred to as "vascular normalization" (Jain 2005)). These results suggest that VEGF-A production by TAMs promotes the formation of chaotic, poorly functional tumor-associated vasculature – at least in the murine tumor models used.

It is rapidly emerging that TAMs may comprise distinct Mφ subsets (Coffelt et al. 2010a; Qian & Pollard 2010). Egeblad and co-workers(Egeblad et al. 2008) developed and applied multicolor imaging techniques (Hoffman & Yang 2006) to analyze the recruitment and behavior of Mφs and related myeloid cells in different tumor microenvironments in live mice. MMTV-PyMT mice were crossed with a

transgenic mouse line expressing GFP under the control of the promoter of the *Csf1r* gene, which is specifically expressed in monocyte/Mφ-lineage cells. The movement of GFP+ cells within tumors was then visualized along with fluorescently labeled dextran (to label blood vessels and Mφs that endocytose dextran) and fluorescently labeled monoclonal antibodies (to better identify the myeloid cell subsets involved). Based on their motility, expression of surface markers (such as mannose receptor, MRC1/CD206) and ability to phagocytose dextran, the Mφs could be classified into distinct sub-populations, including low-migratory MRC1+ dextran+ Mφs found in the peri-tumor areas and sessile MRC1– dextran– Mφs found within the tumor mass (Egeblad et al. 2008). This real-time analysis of myeloid cell location, behavior and gene expression within intact, live tumors, showed that the functional heterogeneity of tumor-infiltrating myeloid cells – Mφs in particular – may be greater than anticipated by the analysis of static markers on fixed tissues. As of today, at least four distinct TAM subsets have been identified and profiled from tumors (Qian & Pollard 2010; Pucci et al. 2009)

Monocytes are highly plastic cells and it is generally believed that their intra-tumoral differentiation toward distinct Mφ subsets is regulated by the contextual assortment of cytokines, chemokines and growth factors present in the tumor microenvironment. For instance, IL-4, IL-13 and IL-10 are thought to directly stimulate the growth-promoting and pro-angiogenic functions of TAMs, a process known as alternative Mφ activation or M2 polarization (Mantovani et al. 2002) (see paragraph 1.5 on page 12). However, it is also possible that distinct monocyte subsets give rise to distinct Mφ sub-populations in tumors (Pucci et al. 2009). Whether the different monocyte/Mφ subsets found in tumors (Coffelt et al. 2010a; Qian & Pollard 2010) represent distinct lineages (Pucci et al. 2009) or more plastic differentiation states (Mantovani et al. 2002), and whether they are related to each other by a precursor-to-mature cell relationship, is the object of current

investigations.

3.2 Polymorphonuclear phagocytes

Granulocytes, neutrophils in particular, and mast cells are regarded as a key source of pro-angiogenic factors in certain experimental tumors. An early study examining the importance of MMP9 and VEGF-A in pancreatic tumors of RIP1-Tag2 mice noted that inflammatory cells are the main producers of these two pro-angiogenic molecules in tumors (Bergers et al. 2000). Neutrophils, together with monocytes/Mφs, have since been identified as the predominant source of MMP9 and other pro-angiogenic molecules in RIP1-Tag2 mice (Nozawa et al. 2006; Shojaei et al. 2008). Although neutrophils are found in lower frequency than Mφs in RIP1-Tag2 insulinomas, their elimination by means of anti-GR1 antibodies (which, however, also bind Ly6C+ inflammatory monocytes; see paragraph 1.4 on page 10) in this tumor model reduces the levels of MMP9 in the tumors, which in turn inhibits the association of VEGF with VEGF receptor-2 (VEGFR-2) on ECs, thus suppressing angiogenesis.

MDSCs are a heterogeneous population of myeloid cells that encompasses immature monocytes, granulocytes, DCs and their precursors. The defining characteristics of MDSCs are largely based on their ability to suppress innate and adaptive immunity and expression of CD11b and GR1 (Gabrilovich & Nagaraj 2009; Capuano et al. 2009), whereas expression of other phenotypic markers by MDSCs varies due to their diversity and inclusion of myeloid cells at various stages of differentiation. Recent attempts at narrowing down specific subsets of these cells conclude that this group of cells can be divided into monocytic (mononuclear-MDSCs) and neutrophilic (polymorphonuclear-MDSCs) and DC subsets, which express phenotypic markers characteristic of each respective subset (Umemura et al. 2008; Youn et al. 2008). There is also some evidence

indicating that these subsets may have different functions in tumors (Movahedi et al. 2008), but the predominant phenotype and differentiation status of these cells once they migrate into premalignant tissue and tumors is unclear and is likely dependent on the tumor model and tumor type. While MDSCs are believed to promote tumor progression through immunosuppression and other mechanisms, these cells (or subsets of them, such as neutrophils) may also influence angiogenesis (Shojaei et al. 2007; Yang et al. 2004b) an effect mediated, at least in part, by their release of pro-angiogenic factors. In this regard, Shojaei and co-workers (Shojaei et al. 2007) found that tumor refractoriness to anti-VEGF therapy correlates with the marked accumulation of CD11b+ GR1+ myeloid cells within certain mouse tumors. This finding suggests that some tumors may co-opt VEGF-independent, pro-angiogenic programs that are executed by the tumor-infiltrating myeloid cells. Yet, an immuno-suppressive function has not been conclusively demonstrated for the pro-angiogenic CD11b+ GR1+ cells, raising the question of whether or not they can truly be referred to as MDSCs.

A number of experimental animal models have shown mast cells to be important for tumor angiogenesis (Crivellato et al. 2008). Mast cells accumulate during the pre-malignant stages of tumor progression and at the periphery of invasive tumors. They have direct pro-angiogenic activity due to their production of MMPs, particularly MMP-9, and secretion of other pro-angiogenic molecules such as basic fibroblast growth factor (FGF), VEGF, and IL-8. In addition, mast cells indirectly stimulate angiogenesis by secreting mast cell-specific serine proteases that activate pro-MMPs and stimulate stromal fibroblasts to synthesize collagens (De Palma & Coussens 2008). Tumors grown in transgenic mice deficient in mast cells exhibit delayed tumor vascularization and progression. For instance, premalignant angiogenesis is abated in a mast cell-deficient, skin tumor-prone K14-HPV transgenic mouse (Coussens et al. 1999), as well as during pancreatic islet cell

carcinogenesis (Soucek et al. 2007), melanoma progression (Starkey et al. 1988), and adenomatous colon polyposis (Gounaris et al. 2007).

In conclusion, the promiscuous cell markers routinely used to identify myeloid cells in tumors, together with the limited availability of mouse models and experimental tools that allow dissecting the contribution of each of the distinct myeloid cell types potentially involved, have confounded the interpretation of the role of myeloid cells in tumor angiogenesis. High-resolution, single-cell live imaging analysis of tumor-infiltrating myeloid cells is unraveling an unexpected degree of functional heterogeneity (Egeblad et al. 2008). Whereas further studies will likely establish the developmental and functional overlap of some of the aforementioned pro-angiogenic myeloid cell types, it is increasingly appreciated that TAMs comprise functionally and perhaps developmentally distinct subsets.

3.3 TIE2-expressing macrophages (TEMs)

While the origin and growth pattern of tumor cells differ enormously from tumor to tumor, angiogenesis involves genetically stable host tissues and follows recurrent patterns. Moreover, angiogenesis occurs under few physiological conditions of adult individuals and angiogenic vessels display different features from those of established blood vessels. Indeed, it is well known that tumor vessels appear structurally immature, exhibit poor association between ECs and supporting cells and are often leaky and haemorrhagic (Hashizume et al. 2000). In addition, ECs of tumor vessels display distinctive protein expression profiles, such as the specific expression or the up-regulation of matrix proteases, adhesion molecules and receptor tyrosine kinases (St Croix et al. 2000). For these reasons, newly forming tumour vessels have long been regarded as a target that could be exploited for the delivery of cancer therapeutics (Folkman 1971).

To specifically target exogenous genes to tumor angiogenesis, De Palma et al.

generated lentiviral vectors (LVs) with EC-specific expression (De Palma et al. 2003). LVs containing promoter and enhancer sequences from the mouse *Tie2* gene (Tie2p/e) proved to be the most EC-specific in vitro. Direct injection of Tie2p/e-GFP LVs into mammary tumor allografts resulted in targeted and efficient expression of the Tie2p/e vector in tumor ECs. Unexpectedly, the Tie2p/e vector also targeted gene expression to a subset of stromal cells expressing the pan-leukocyte marker CD45 and mostly localized at the tumor periphery (De Palma et al. 2003). The transplant of BM cells transduced *ex vivo* with Tie2p/e-GFP LVs into irradiated mice showed that only a small fraction of blood leukocytes and marrow cells are weakly Tie2p/e-GFP+. The circulating Tie2p/e-GFP+ cells are myeloid-lineage (CD45+, CD11b+, CD19–) cells, and were initially termed Tie2-expressing mononuclear cells (TEMs) (De Palma et al. 2003). Once recruited to the tumors, TEMs express a CD45+ CD31– CD11b+ F4/80+ phenotype and mostly localize at the tumor periphery and/or associate with small blood vessels dispersed within the tumor parenchyma (Illustration 7). Remarkably, GFP expression is detected only in tumors but not in non-angiogenic organs such as spleen, lung, liver, heart or brain. However, TEMs are also recruited to sites of non-tumor angiogenesis, namely in the granulation tissue surrounding regenerating hepatic lobules following hepatectomy and during wound healing. Of note, the Tie2p/e LVs is very weak in leukocytes, indicating minimal expression of TIE2 in the circulating monocytes. Thus, alternate surface markers that easily and unambiguously identify TEMs are highly desired.

At the time of these studies (De Palma et al. 2003), a new concept in the field of tumor biology was emerging. BM derived endothelial progenitor cells (EPCs) were reported to contribute substantially to tumor vessels by vasculogenesis, the process of de novo formation of blood vessels from angioblast-like EPCs (Lyden et al. 2001). Although TEMs do not incorporate into newly formed tumor vessels, they

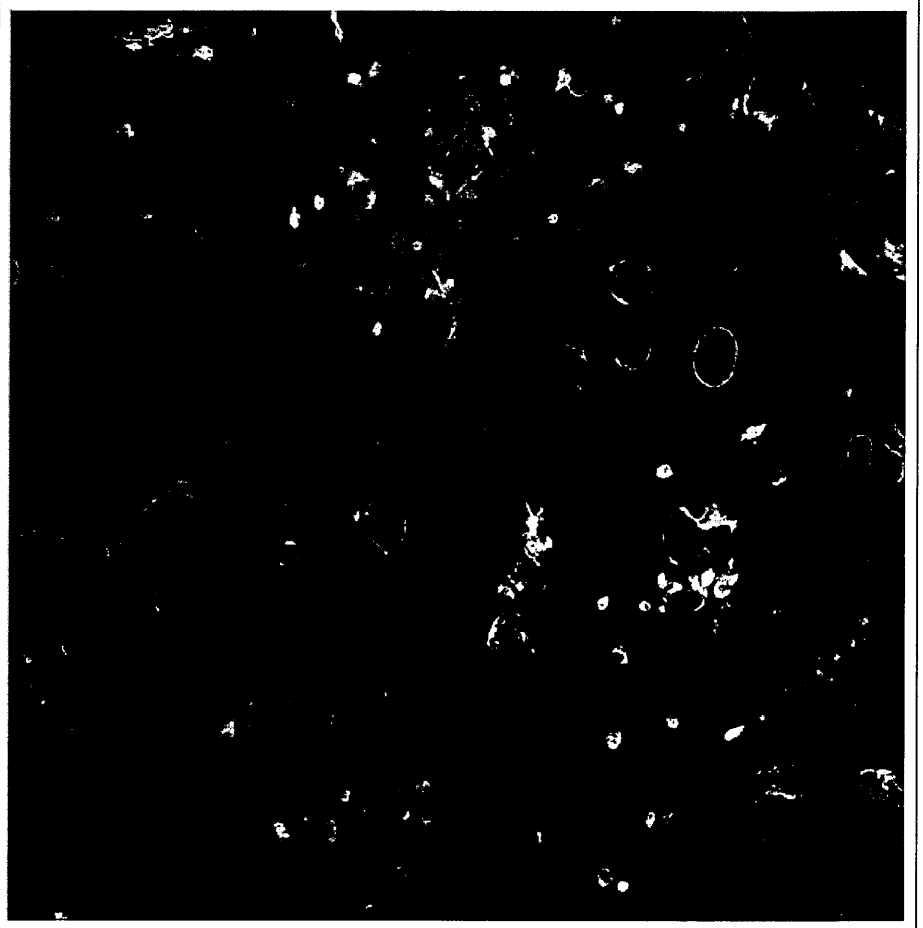

Illustration 7: TEMs in a tumor section. Immunofluorescence staining of a tumor section from a Tie2p/e-GFP BM chimera mouse. Of note, the perivascular position of Tie2p/e-GFP+ TEMs, which contrast to the widespread distribution of CD11b+ myeloid cells (in blue). Blood vessels are in red. De Palma et al. 2008.

share several surface markers with ECs, TIE2 in primis (Prater et al. 2007; De Palma & Naldini 2006). This, together with the close proximity between tumor ECs and TEMs, may have erroneously led several authors to regard TEMs as BM-derived ECs, i.e. EPCs. Thus, to study TEM biology, the choice of markers employed to identify them is of paramount importance.

3.3.a TEMs are pre-committed to a angiogenic function

The peculiar peri-vascular localization of TEMs suggests a potential role in the regulation of tumor angiogenesis. Indeed, conditional TEM depletion by employing the Tymidine Kinase (TK) suicide gene abates the recruitment of TEMs to the developing tumors and markedly inhibits tumor angiogenesis (De Palma et al. 2005). Interestingly, TEM elimination does not affect the overall number of TAMs and granulocytes, making it unlikely that TEMs comprise precursors of TAMs (Illustration 8). Rather, these studies suggest that TEMs represent a distinct TAM

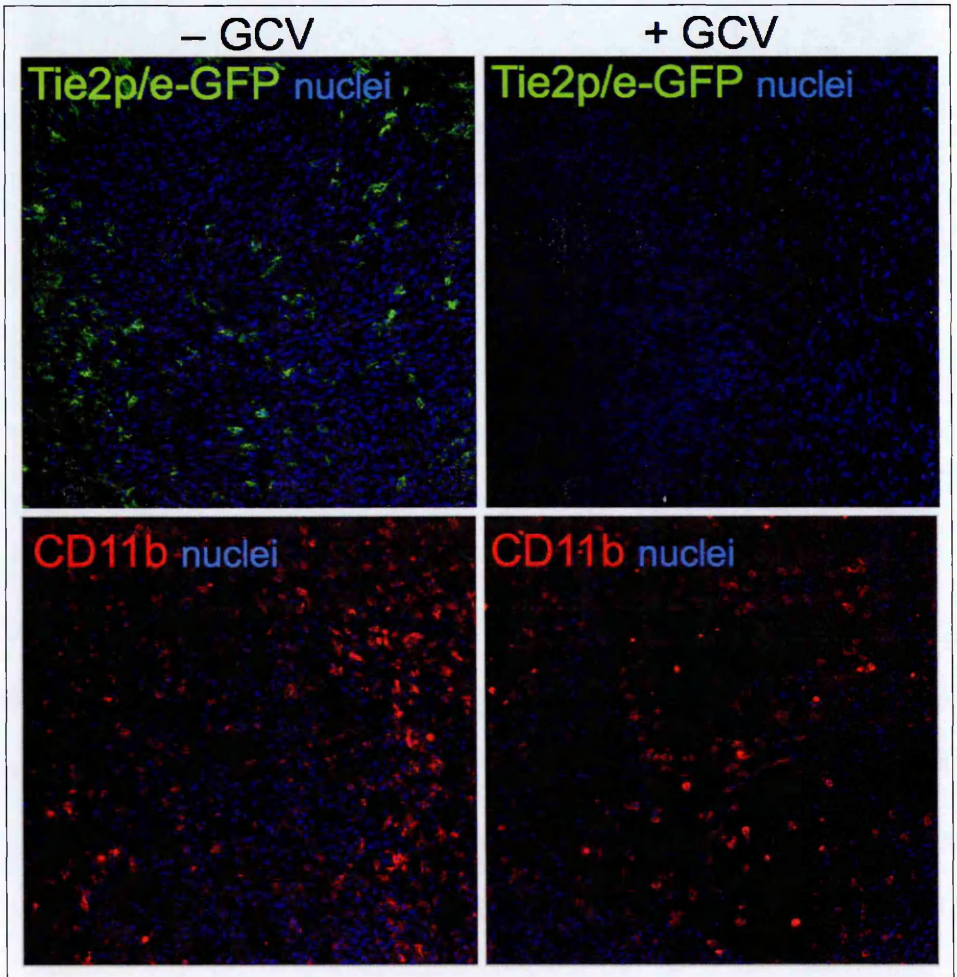

Illustration 8: TEM depletion experiment. Tumor-bearing Tie2p/e-TK-GFP BM chimera mice were treated (right panels) or not (left panels) with Gancyclovir (GCV) in order to deplete TEMs. Of note, after virtually complete TEM depletion, the presence of tumor-infiltrating CD11b+ myeloid cells is not affected. De Palma et al. 2005.

subset with inherent, non-redundant pro-angiogenic activity. TEMs hold this pro-angiogenic activity already when they circulate in the peripheral blood, before reaching the tumour site (De Palma et al. 2005). Recent data confirmed that human TEMs, similar to their murine counterpart, are already pre-committed to a pro-angiogenic function in the circulation (Coffelt et al. 2010b). Thus, TEMs are a pre-committed MP subset with innate pro-angiogenic activity. In this regard, the identification of pro-angiogenic TEMs among the heterogeneous TAM population challenges the notion that transition of tumour Mφ phenotype between growth-inhibitory and growth-promoting activity is exclusively and contextually modulated by the tumour micro-environment (Mantovani et al. 2002). Nevertheless, the molecular bases of the pro-angiogenic activity of TEMs and the role of TIE2 in TEM biology need to be elucidated.

Regarding putative TEM precursors, it has been reported that TIE2 is expressed by long term repopulating hematopoietic stem cells (HSC) and mediates their quiescence in the BM niche (Arai et al. 2004). This may explain why TK-based TEM depletion did not cause obvious myelotoxicity in mice, as this conditional cell elimination system only kills proliferating cells (De Palma et al. 2005). However, the BM progenitor/precursor of circulating and tumor-infiltrating TEMs remains to be identified.

3.3.b Exploiting TEMs to deliver therapeutics to tumors

Based on the unique tumor-homing specificity of TEMs among myeloid-lineage cells and the selective expression of the *Tie2* gene in TEMs among the progeny of BM-derived HSCs, our laboratory explored the possibility of targeting an anti-tumor cytokine (i.e. IFNa) to tumors by exogenously expressing it in TEMs (De Palma et al. 2008). Whereas HSCs constitutively expressing IFNa failed to engraft, Tie2p/e-IFNa transduced HSCs were able to successfully reconstitute mice long-term.

Although IFNa was not detectable in the plasma of Tie2p/e-IFNa mice, when challenged orthotopically with human glioma cells, these mice were resistant to tumor growth. Interestingly, by exploiting the species difference between the tumor and the host (human and mouse, respectively), we were able to show that the IFNa response of host-derived components of the tumor is sufficient to inhibit human glioma growth (De Palma et al. 2008).

In mice developing spontaneous metastatic mammary tumors (MMTV-PyMT), TEM mediated delivery of IFNa substantially (50%) reduced tumor volume. Tumor specific activation of type I IFN inducible genes was the molecular evidence for the selective targeting of the IFN response to mammary tumors but not to other organs. TEM-mediated IFNa delivery enhanced the recruitment and promoted the activation of both innate and adaptive immune cells. Finally, effective metastasis suppression in Tie2p/e-IFNa BMT mice was observed (De Palma et al. 2008).

In summary, TEM-mediated delivery of bioactive peptides is a safe, specific and effective way to contrast tumor growth and metastasis. Of note, the tumor microenvironment, if properly elicited, is able to reject the tumor.

3.3.c Human TEMs

Recently, our and other laboratories reported the existence of TEMs in human blood and cancer (Murdoch et al. 2007; Venneri et al. 2007; Pulaski et al. 2009; Coffelt et al. 2010b). In human cancer specimens, TEMs are a minor proportion of the bulk of tumor-infiltrating leukocytes – which mostly comprise TAMs and granulocytes. TEMs are found both in peri-vascular and avascular viable (hypoxic) areas of human tumors and are largely missing in non-neoplastic tissues adjacent to tumors. In addition to tumors, TEMs can be detected at low frequency in the human peripheral blood (Venneri et al. 2007; Murdoch et al. 2007; Coffelt et al. 2010b). Similar to murine cells, human TEMs isolated from peripheral blood also

have pro-angiogenic activity (Venneri et al. 2007; Coffelt et al. 2010b). Lewis and co-workers showed that circulating human TEMs are already pre-programmed in the circulation to be more pro-angiogenic than TIE2− monocytes. Additionally, angiopoietin-2 markedly enhanced the pro-angiogenic activity of human TEMs by up-regulating their expression of the pro-angiogenic gene thymidine phosphorylase.

4 TIE2 receptor

In the mouse and human system, the TIE2 receptor is almost exclusively expressed by ECs, HSCs and TEMs. The *Tek* gene encodes for the TIE2 protein. TIE2 is a receptor tyrosine kinase which possesses a unique extracellular domain containing 3 immunoglobulin-like loops which fold together with 3 epidermal growth factor-like repeats and three fibronectin type III repeats (Illustration 9) (Barton et al. 2006). Studies with dominant-negative and null mice reveal that loss of *Tie2* gene function results in embryonic death at 9.5 dpc as a consequence of an underdeveloped vasculature (Sato et al. 1995; Dumont et al. 1994). TIE2 is expressed at high levels in blood and lymphatic ECs, whereas HSCs and tumor-infiltrating TEMs express much lower levels (up to 100-fold less).

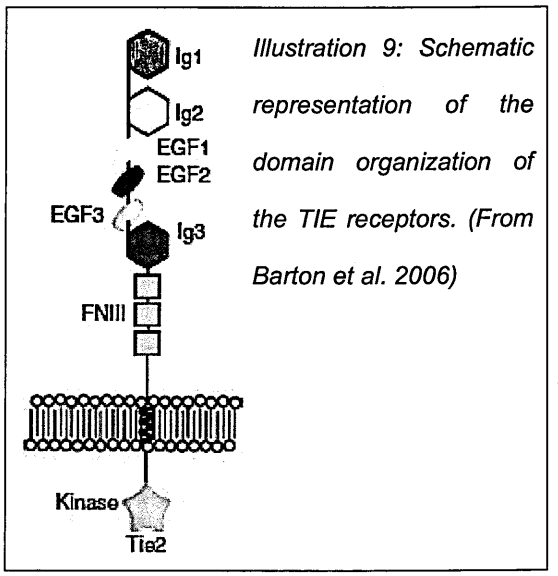

Illustration 9: Schematic representation of the domain organization of the TIE receptors. (From Barton et al. 2006)

4.1 Signalling mechanism

Initially described as an orphan receptor (Dumont et al. 1992), TIE2 was subsequently shown to interact with all four of the angiopoietins (ANG1 – ANG4)

(Valenzuela et al. 1999). The different angiopoietins, although having high sequence homology, elicit different responses from the TIE2 receptor. Indeed, ANG1 is a constitutive receptor agonist, while ANG2 is a context-dependent one (Ward & Dumont 2002). The four known angiopoietins each contain an N terminus that modulates angiopoietin clustering and a C terminus that mediates the interaction with TIE2 (Davis et al. 2003). Ligand oligomerization is necessary for receptor activation. Indeed, all angiopoietins exist primarily as tetramers, hexamers and higher order oligomers in solution (Ward & Dumont 2002; Seegar et al. 2010). Ligand-induced oligomerization of the extracellular regions of TIE2 leads to activation of the intracellular tyrosine kinase domain, which creates binding sites for Src homology 2 and phosphotyrosine binding domain containing proteins (Lemmon & Schlessinger 2010).

TIE1, although a close homolog of TIE2, does not interact directly with the angiopoietins, and its in vivo ligands are yet to be identified. A recent study using catalytically inactive TIE2 demonstrated that TIE1 phosphorylation is dependent on a functional TIE2 (Yuan et al. 2007). Recently, it has been proposed that TIE1 is an inhibitory co-receptor. Specifically, in cells expressing both TIE1 and TIE2, the receptors form heterodimers that inhibit Tie2 activation and clustering. Binding of ANG1 to TIE2 promotes heterodimer dissociation, TIE2 clustering, and signalling initiation. On the other hand, ANG2 is unable to dissociate the inhibitory TIE2-TIE1 complexes upon binding TIE2 and, therefore, does not induce TIE2 clustering and signaling, yet behaves as a competitive antagonist by blocking further binding of ANG1. Indeed, both ANG1 and ANG2 bind to the same region of Tie2 (Barton et al. 2006). Alternatively, in cells that do not express TIE1, all angiopoietins promote TIE2 clustering and activation (Seegar et al. 2010). This model proposes that the balance of TIE1 and TIE2 expression modulates the functional potential of ANG2, and by analogy, vascular homeostasis. However, this model is based on studies

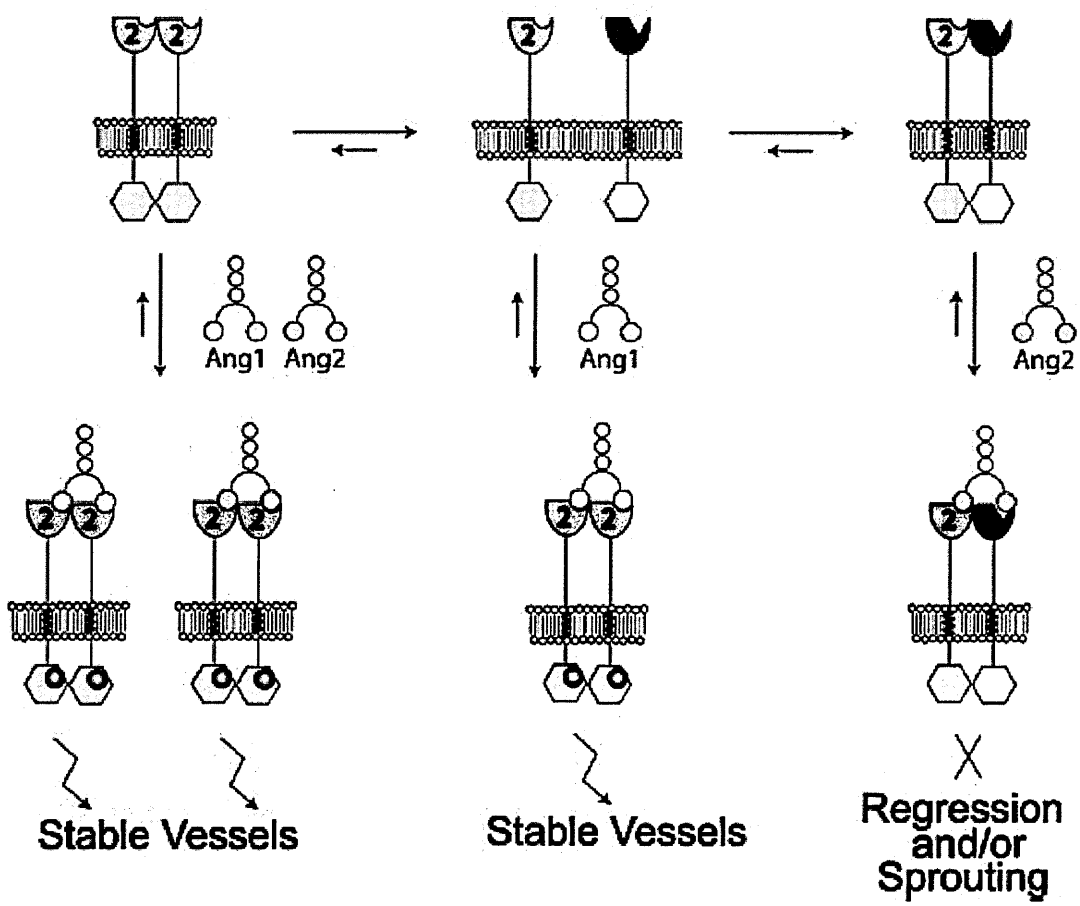

Illustration 10: Model for Angiopoietin-Mediated TIE2 Signaling. Left: expression of TIE2 in the absence of TIE1 at sites of vessel quiescence and maturity. In the absence of TIE1, TIE2 can be activated with either ANG1 or ANG2. Both ligands stimulate receptor clustering, tyrosine kinase activity, and downstream signaling events, effectively become unresponsive to vessel sprouting and branching cues. Middle and right: within sites of active angiogenesis, TIE1 and TIE2 associate to form a complex prior to ligand stimulation. Upon addition of ANG2 (right), TIE1 and TIE2 association and localization remain unchanged. Under these conditions, ANG2 fails to activate the TIE2 receptor and opposes the activation of downstream signaling generated by ANG1. However, upon addition of ANG1 (middle), the opposite is observed. ANG1 stimulates TIE2 clustering, tyrosine kinase activity, and downstream signaling events similar to those observed in the absence of Tie1. Angiopoietins are depicted as dimers for illustration purposes, although they are known to exist as higher-order clusters. (from Seegar et al. 2010)

performed in ECs and it is not known if it holds true also in HCs.

4.2 Regulation of vascular homeostasis

ANG1 is constitutively expressed by many different cell types such as pericytes, smooth muscle cells and fibroblasts (Sundberg et al. 2002). Constitutive ANG1 expression and low level TIE2 phosphorylation in the adult vasculature suggest that ANG1-mediated TIE2 signaling functions as the default pathway to control vascular quiescence. ANG1 exerts a protective effect on the endothelium, limits its ability to be activated by exogenous cytokines and growth factors and inhibits vascular leakage. For these reasons, it has an anti-inflammatory action.

On the other hand, ANG2 is almost exclusively expressed by ECs (Fiedler et al. 2004). *Angpt2* mRNA is almost undetectable in the quiescent vasculature and dramatically upregulated in tumor blood vessels (Stratmann et al. 1998). ANG2 expression is regulated by several different cytokines (FGF2, VEGFs and TNF) and environmental cues (hypoxia, high glucose levels and superoxides) (Fiedler & Augustin 2006). ANG2 protein is stored in EC Weibel-Palade bodies and thus is readily available following endothelial stimulation. The release of ANG2 results in rapid destabilization of the endothelium, suggesting that ANG2 functions as an autocrine negative regulator of the quiescent resting endothelium (Scharpfenecker et al. 2005). In contrast to ANG1, ANG2 triggers an inflammatory response by activating the endothelium and inducing vascular permeability (Roviezzo et al. 2005).

4.3 Regulation of TEM biology

Although it has been shown that TIE2 mediates quiescence in HSCs (De Palma et al. 2005; Arai et al. 2004), the significance of TIE2 expression by TEMs is currently unknown, but it is possible to speculate on the possibility that TEMs are recruited to tumors via ANG2/TIE2 interaction. Of note, expression of ANG2 is known to be

up-regulated in tumors and inflamed tissues as compared to normal, quiescent tissues (Nasarre et al. 2009), and activated ECs appear to be a major source of ANG2, at least in the mouse (Fiedler et al. 2004). In support of a putative chemoattractant role of ANG2, Lewis et al. showed that human peripheral blood-derived monocytes respond to ANG2 with both chemotaxis and altered cytokine release (Murdoch et al. 2007). Similarly, work from our laboratory suggests that human peripheral blood mononuclear cells enriched in TIE2+ monocytes migrate towards ANG2 in vitro. Because ANG2-induced chemoattraction of monocytes is inhibited by anti-TIE2 neutralizing antibodies (Venneri et al. 2007), it is likely that this response is mediated by engagement of the TIE2 receptor. Recently, to investigate the effects of ANG2 on the phenotype and function of TEMs in tumors, Lewis and co-workers (Coffelt et al. 2010b) used a transgenic mouse model in which ANG2 was specifically over-expressed by endothelial cells. Syngeneic tumors grown in these ANG2 transgenic mice were more vascularized and contained greater numbers of TEMs than those in wild-type mice. However, it is currently unknown whether ANG2 directly regulates TEM homing/function in tumors, and whether targeting ANG2 or its receptor, TIE2, could represent a therapeutic strategy to impair TEM activity in tumors.

Aim of the work

In this work, I studied monocyte and macrophage heterogeneity in blood and tumors, in order to identify molecular pathways regulating the pro-angiogenic activity of TEMs and their lineage relationships with distinct monocyte and TAM subsets. Furthermore, I investigated the role of TIE2 receptor in TEM biology and pro-angiogenic activity.

The first aim of this work was to identify the best-performing TEM purification protocol. Flow sort is the gold standard to isolate highly purified cell subsets in case multiple markers are required for their isolation (Dirks 2008). I flow sorted TEMs, TIE2– TAMs and ECs from tumors grown subcutaneously in Tie2p/e-GFP transgenic mice. In this model, GFP expression can be conveniently used to discriminate TEMs from other tumor-infiltrating myeloid cells. However, the low frequency of TEMs among tumor-infiltrating CD11b+ cells and their weak GFP expression level represent technical challenges for the purification of GFP+ TEMs from tumors grown in Tie2p/e-GFP transgenic mice. Moreover, in Tie2p/e-GFP transgenic mice both TEMs and ECs express GFP. These factors together contribute to increase the risk of contamination from other cell types, ECs in particular. Consequently, I compared different sorting strategies to test the presence of contaminating ECs in TEM preparations and identified the best sorting formula to isolate EC-free, tumor-derived macrophage subsets.

The second aim of this work was to determine the gene expression signature of tumor-infiltrating TEMs. To gene profile TEMs, TIE2– TAMs and ECs I employed a quantitative PCR (qPCR) approach because it allows for identifying low-abundance transcripts from small amounts of mRNA. I used low-density qPCR arrays with standardized fluidics, which ensure reproducibility, inter-sample

comparison and high-throughtput analysis. I analysed ~300 genes previously implicated in angiogenesis, tissue remodeling, immune response, cell adhesion, chemotaxis, neural guidance and vascular morphogenesis. TEM specific markers have been validated by FACS analysis and immunofluorescence staining in two different tumor models: N202 tumors grown subcutaneously in Tie2p/e-GFP transgenic mice (De Palma et al. 2005) and mammary tumors spontaneously arising in MMTV-PyMT transgenic mice previously transplanted with Tie2p/e-GFP BM cells (De Palma et al. 2008).

The third aim of this work was to investigate the phenotypic and functional relationships between tumor-infiltrating TEMs and circulating monocytes. Blood monocytes are considered the precursors of tumor-infiltrating macrophages. I then analysed the surface marker and gene expression profiles of blood monocyte subsets and compared them with those of tumor-infiltrating TEMs and TIE2– TAMs.

Finally, the fourth aim of this work was to study the *in vivo* role of the TIE2 receptor in TEM biology. To investigate this, I implemented a LV platform, recently developed in our laboratory (Amendola et al. 2009), that allows for stable and safe delivery of siRNA sequences to primary cells. I selected a highly effective siRNA sequence, which I employed to knock down TIE2 *in vivo*. Since hematopoietic stem/progenitor cells require TIE2 for their maintenance in the stem cell niche (Arai et al. 2004), I implemented advanced features in the LV platform, including conditional expression and post-transcriptional regulation of the siRNA expression cassette. Such modifications of the LV platform enabled highly efficient *Tie2* gene knock down in TEMs *in vivo* and helped to unveil the role of the angiopoietin/TIE2 pathway in the regulation of tumor angiogenesis by TAMs.

Results

5 Isolation of highly purified tumor macrophage subsets

To gene profile TEMs and TIE2– TAMs, I chose a quantitative PCR (qPCR) approach because it allows for identifying low-abundance transcripts from small amounts of mRNA. I used low-density qPCR arrays with standardized fluidics, which ensure reproducibility, inter-sample comparison and global analysis. I sorted TEMs, TIE2– TAMs and ECs from N202 mammary tumors grown subcutaneously in Tie2p/e-GFP transgenic mice (De Palma et al. 2005); in this model, GFP expression can be conveniently used to discriminate TEMs from other tumor-infiltrating myeloid cells.

5.1 Identification of the best-performing cell sorting formula

Purification of GFP+ TEMs from tumors grown in Tie2p/e-GFP transgenic mice presents with several technical challenges, due to the low frequency of TEMs among tumor-infiltrating CD11b+ cells and their weak GFP expression level. Moreover, in Tie2p/e-GFP transgenic mice both TEMs and ECs express GFP. These factors together contribute to increase the risk of contamination from other cell types, ECs in particular. To address this issue, I first developed a model to test the presence of contaminating ECs in TEM preparations. I sorted TEMs as GFP+ CD45+ CD11b+ cells (n=2) and ECs as GFP+ CD45– CD11b– cells (n=2), and analyzed a panel of genes by qPCR analysis. To test for ECs contamination, I took into account only the genes whose expression was up-regulated more than 4-fold in ECs as compared to TEMs (*Agtr2, C3, Ccl19, Cd34, Csf1, Ece1, Edn1, Fn1, Il12b, Il6, Il7, Nos2, Smad7, Angpt1, Angpt2, Tie2, VEGFR1, VEGFR2*) and found a striking correlation in the expression level of such genes in the two cell

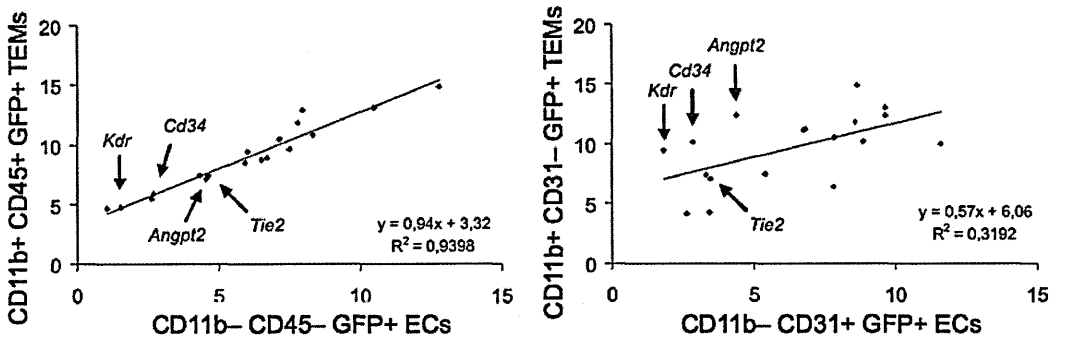

Illustration 11: Identification of the best-performing cell sorting formula for TEM isolation. qPCR analyses of a gene panel (see heading 5.1 for details) in TEMs sorted as Tie2p/e-GFP+ CD45+ CD11b+ (left) or Tie2p/e-GFP+ CD11b+ CD31–/low (right) cells. Gene expression in TEMs was compared with that of tumor-derived ECs sorted as Tie2p/e-GFP+ CD45– CD11b– (left) or Tie2p/e-GFP+ CD31+ CD11b– (right). In the graph on the left, the slope of the regression line was approximately equal to one, suggesting that ECs substantially contaminated the TEM sample. The graph at right shows that inclusion of CD31 as a negative (TEMs) or positive (ECs) gating marker eliminated the source of EC gene contamination in the TEM sample, thus providing for accurate isolation of TEMs from tumors.

populations (Illustration 11). The slope of the regression line was approximately equal to one, which suggested that either these genes were coordinatedly expressed at a constant ratio by the two cell types, which is very unlikely, or that ECs substantially contaminated the TEM sample. By assuming that TEMs and tumor ECs contain the same amount of mRNA per cell, the extent of contamination estimated by the intercept value of the regression line corresponded to $2^{3.32}$ (about 10% ECs in the TEM preparation).

I then implemented the sorting strategy by introducing a dump channel to exclude PECAM1/CD31+ ECs. After vital staining and exclusion of 7-Amino-Actinomycin D+ (7AAD) cells, I sorted TEMs as Tie2p/e-GFP+ CD11b+ CD31–/low cells. The improved sorting strategy eliminated the source of EC gene contamination in the TEM sample (Illustration 11) and provided for accurate isolation of TEMs from tumors. Concerning the potential contamination of the two cell fractions by other

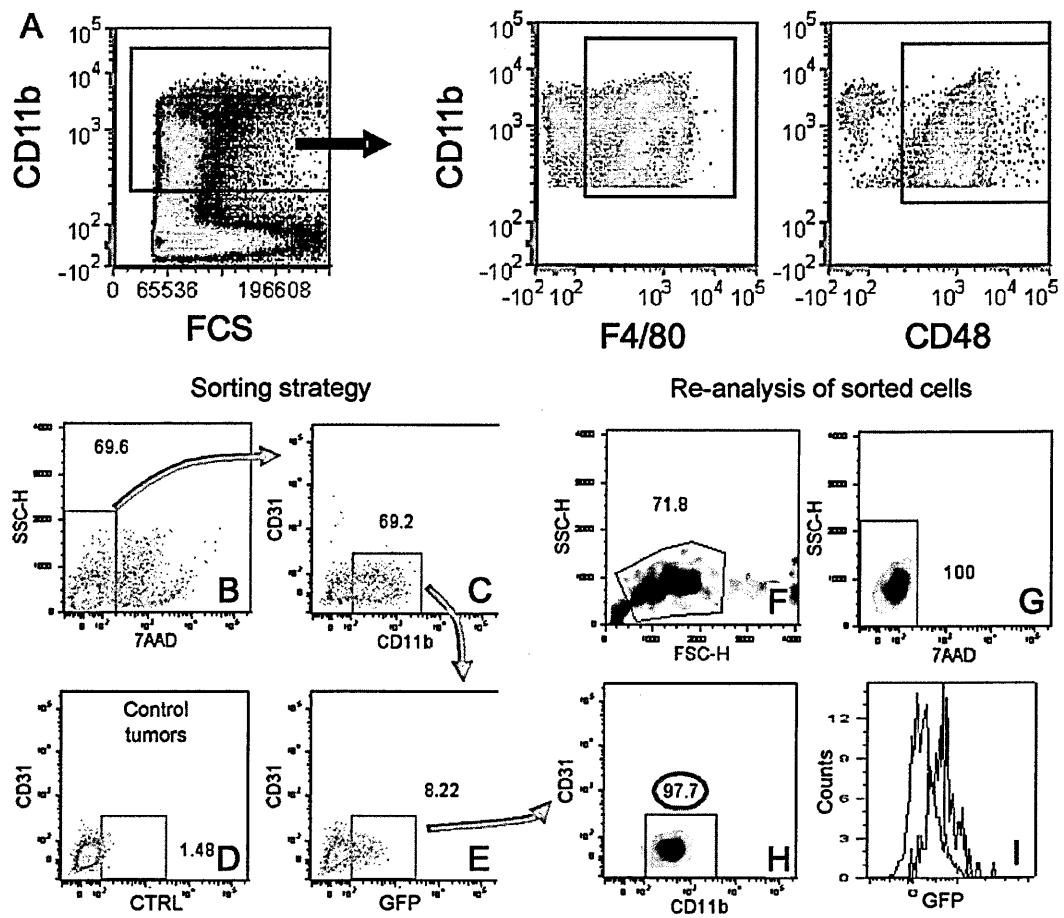

Illustration 12: A. Flow cytometry analyses of N202 tumors grown subcutaneously in wild-type FVB mice (n=4) and made into single cell suspensions shows that the vast majority of tumor-infiltrating myeloid cells (gated as CD11b+ cells, dot plot on the left) are highly enriched in F4/80+ or CD48+ macrophages (dot plots on the right). One representative experiment is shown. To sort TEMs, N202 mammary tumors were grown subcutaneously in Tie2p/e-GFP transgenic mice and made into single-cell suspensions. Before cell sorting, CD11b+ myeloid cells were magnetically enriched (shown in panels B and C after magnetic enrichment). The sorting procedure is shown in the dot plots at left. The GFP+ 7AAD− CD11b+ CD31− TEMs were then sorted (E; panel D shows cells obtained from tumors inoculated in wild-type mice and processed as above). Right panels show re-analysis of sorted TEMs (F), that were virtually all 7AAD− (G), CD11b+ CD31− (H) and GFP+ (open black line in I; open blue line indicates sorted 7AAD− GFP− CD11b+ CD31− cells, i.e. TIE2− TAMs).

cell types, the cytospin data confirmed the flow cytometry data (Illustration 16 on page 45) that sorted TEMs are >94% pure monocytes/macrophages and TIE2−

TAMs are >93% monocyte/macrophage cells, with rare neutrophils/eosinophils accounting for up to 5-6% of the total cells.

5.2 Validation of sorted tumor macrophage subsets

In N202 tumors, the vast majority of the tumor-infiltrating CD11b+ cells were F4/80+ and CD48+ (77±6% and 88±5%, respectively; mean frequency of marker positive cells ± SD; n=4), thus representing myeloid cells highly enriched in TIE2– TAMs (Illustration 12A). I sorted TEMs as Tie2p/e-GFP+ CD11b+ CD31low/–, TIE2– TAMs as Tie2p/e-GFP– CD11b+ CD31low/– and ECs as Tie2p/e-GFP+ CD11b–CD31+ cells (Illustration 12B-I). To validate the sorted cell populations, I measured the expression of the hematopoietic lineage-specific marker *Ptprc/Cd45*, the macrophage-specific marker *F4/80*, the EC-specific marker *Vegfr2* (*Flk1*), and *Tie2*, in TEMs, TIE2– TAMs and ECs (n=2-4 biological samples) by qPCR (Illustration 13). Both TEMs and TIE2– TAMs expressed high-level C*d45* and *F4/80*, which confirmed their hematopoietic origin and monocyte/macrophage identity. Of note, *Tie2* expression was significantly higher in TEMs than in TIE2– TAMs (~20-fold; t-test: $p<0.05$; n=4).

To analyze the presence of hematopoietic progenitors in sorted cell populations, I

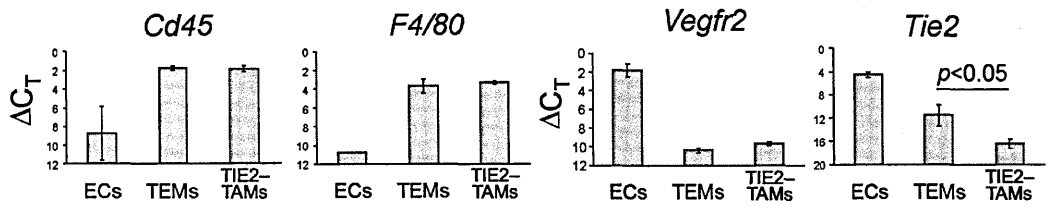

Illustration 13: Gene expression analysis of FACS-purified TEMs (n=4), TIE2– TAMs (n=4) and ECs (n=2). Results show ΔC_T values (mean ± SEM) over reference gene Gapdh. The lower the ΔC_T, the higher the expression level. TEMs and TIE2– TAMs express Cd45 (pan-hematopoietic-specific marker) and F4/80 (macrophage-specific marker) to similar extent. Vegfr2 (endothelial-specific marker) is expressed robustly only by ECs. TEMs express Tie2 to a significantly higher extent than TIE2– TAMs ($p<0.05$).

	Number of plated cells		
	5,000	20,000	100,000
TEMs	0	0	0
TIE2– TAMs	0	0	3
Unfractioned BM cells	3	19	112
lineage negative BM cells	36	132	confluent

Table 1: Number of colony forming cells (CFC) arising from sorted TEMs and TIE2– TAMs

studied the clonogenic activity of TEMs and TIE2– TAMs in colony-forming cell (CFC) assays. Sorted TEMs did not generate hematopoietic colonies (Table 1), indicating that they are virtually devoid of hematopoietic progenitors. Exceedingly few colonies formed upon seeding of TIE2– TAMs (Table 1).

6 Tumor TEMs are monocytes/macrophages expressing a distinguishing gene signature

To investigate the nature of TEMs, I measured the expression of 280 genes previously implicated in angiogenesis, tissue remodeling, immune response, cell adhesion, chemotaxis, neural guidance, vascular morphogenesis, in TEMs (n=3), TIE2– TAMs (n=3) and ECs (n=1). I extended the gene expression analysis to

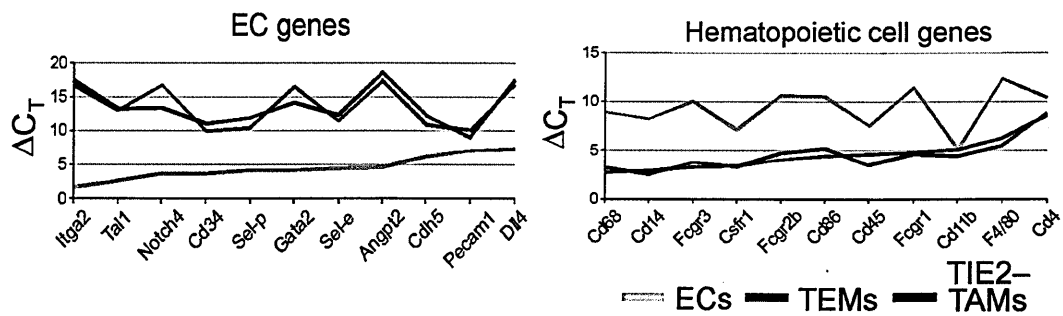

Illustration 14: qPCR-based, multi-gene array analysis of TEMs (n=3), TIE2– TAMs (n=3) and ECs (n=1) showing the expression level (ΔC_T vs. β2m) of relevant EC (left panel) and hematopoietic/myeloid (right panel) genes. TEMs and TIE2– TAMs robustly express classic hematopoietic/myeloid genes, but not EC genes.

resting peritoneal macrophages (PMs; sorted as 7AAD– CD11b+ F4/80+ $CD31^{LOW}$ cells; n=2) and neutrophils/MDSCs isolated from the spleen of N202 tumor-bearing mice (sorted as 7AAD– CD11b+ GR1+ cells; n=2).

6.1 Genes highly expressed in TEMs

The expression profile of TEMs clearly indicated that they belong to the monocyte/macrophage lineage and are distinct from ECs. Indeed, TEMs robustly express typical myeloid genes, but low to negligible amounts of EC genes (Illustration 14). A list of the genes highly expressed in TEMs and grouped by function is shown in Illustration 15. Among the highly expressed monocyte-macrophage genes, were CSF1 receptor (*Csf1r/Cd115*), Fc receptors (*Fcgr1*; *Fcgr2b*; *Fcgr3*), fractalkine receptor (*Cx_3cr1*), macrosialin (*Cd68*), *F4/80*, *Cd14*, scavenger receptors (mannose receptor *Mrc1*; macrophage scavenger receptors *Msr1* and *Msr2*; hemoglobin-haptoglobin scavenger receptor *Cd163*; membrane-bound scavenger receptor/cytokine *Cxcl16*), endopeptidases (metalloproteases, cathepsins) and several integrins. In addition, TEMs express

Myeloid markers		Endopeptidases		Scavenger receptors		Cytokines		Chemokines		Adhesion		Transcription factors	
Gene	*ΔCt*	*Gene*	*ΔCt*	*Gene*	*ΔCt*	*Gene*	*ΔCt*	*Gene*	*ΔCt*	*Gene*	*ΔCt*	*Gene*	*ΔCt*
Cd68	2.5	Ctss	0.8	Mrc1	3.0	Il1b	2.4	Ccl4	1.8	Itgb5	4.7	Stat1	3.7
Cd14	2.9	Ctsb	2.0	Msr1	4.1	Tnf	4.0	Ccl2	2.4	Itgb1	5.0	Stat3	5.1
Fcgr3	3.1	Ctsz	2.3	Msr2	4.4	Tgfb1	4.2	Cxcl10	2.9	Itgam	5.2	Nfkb2	5.9
Csf1r	3.2	Ctsl	3.8	Cxcl16	4.7	Il10	4.4	Cxcl9	4.3	Itga5	7.6	Ski	6.1
Ptprc	3.7	Mmp14	5.7	Cd163	6.3	Vegfa	4.5	Ccl5	4.3	Itgav	7.8	Nfkb1	6.4
Fcgr2b	3.9	Adam17	6.0			Il6	5.1	Cxcl16	4.7	Itga6	8.1	Fli1	6.8
Fcgr1	4.2	Adam15	6.1			Il1a	5.2	Cxcl13	5.1	Itgax	8.1	Ikbkb	7.9
Cd86	4.4	Mmp12	6.5			Sema4d	6.1	Ccl3	5.4	Itga4	8.8	Smad7	8.2
Itgam	5.2	Mmp13	8.4			Pdgfb	7.2	Cxcl11	6.6	Pecam1	9.8	Smad3	9.0
Cx3cr1	5.2	Mmp2	8.5			Ifnb1	7.7	Cxcl14	7.7	Sell	10.3	Stat4	10.7
Emr1	5.3	Mmp9	9.6			Csf1	7.8	Cxcl12	10.6				
Cd4	7.9	Mmp3	9.9			Il18	8.2						
						Vegfb	8.2						
						Mfge8	8.4						
						Il15	8.6						
						Csf3	9.1						
						Igf1	9.3						
						Ecgf1	9.5						
						Pgf	10.5						

Illustration 15: Genes highly expressed in TEMs and grouped by function. ΔC_T was measured vs. B2m. The lower the ΔC_T the higher the expression level.

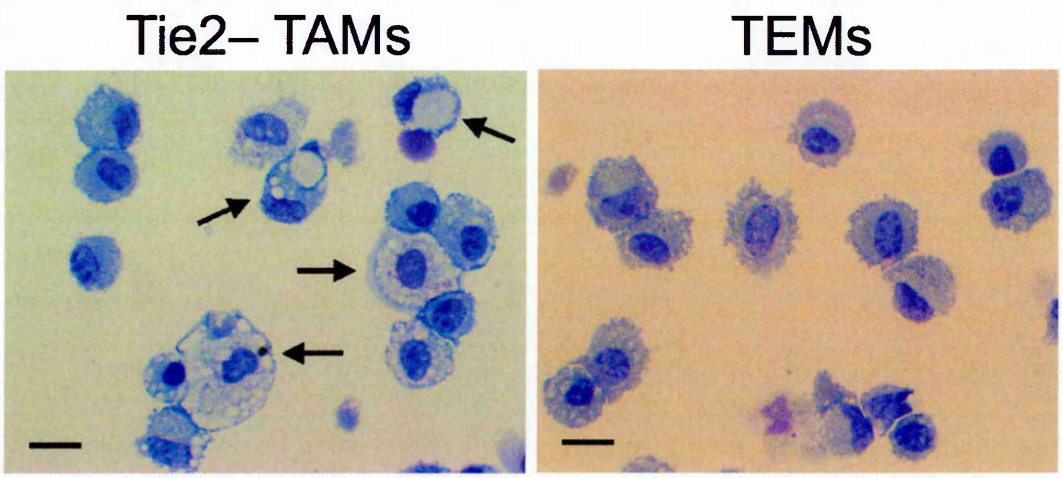

Illustration 16: Morphology (May-Grünwald-Giemsa staining) of TIE2– TAMs (left panel) and TEMs (right panel) FACS-sorted from N202 tumors grown in Tie2p/e-GFP transgenic mice (n=2). Arrows indicate large macrophages containing conspicuous cytoplasmic phagosomes. Scale bar: 30µm. Photos are representative of n=25 photos/sample.

monocyte/macrophage-derived cytokines (*Il1a*; *Il1b*; *Il6*; *Tnf*; *Tgfb1*), chemokines (*Ccl4*; *Ccl3/Mip1a/b*; *Cxcl10*; *Cxcl9*; *Cxcl11*) and classic pro-angiogenic factors (*Vegfa*; *Vegfb*; *Sema4d*; *Pdgfb*; lactadherin *Mfge8*; thymidine phosphorylase *Ecgf1*; placental growth factor *Pgf*).

6.2 Morphological analysis of tumor macrophage subsets

Morphological analysis of FACS-sorted cells (n=2; Illustration 16) showed that TEMs are a homogeneous cell population with typical monocyte/macrophage morphology (>94% of the cells with bean-shaped nucleus and large cytoplasm). On the other hand, TIE2– TAMs displayed a greater extent of morphological heterogeneity and contained both monocyte-like cells and large macrophages with features of activated phagocytes (rounded nucleus; large cytoplasm with numerous vacuoles). The cell morphology corroborated the gene expression data that both TEMs and TIE2– TAMs belong to the monocyte/macrophage lineage.

6.3 *Genes differentially expressed between TEMs and TIE2– TAMs*

A comparison between the gene expression profile of TEMs and TIE2– TAMs revealed that the two monocyte/macrophage subsets were highly related (Illustration 17). However, TEMs differed significantly from spleen-derived GR1+ CD11b+ neutrophils/MDSCs, PMs and tumor-derived ECs.

Statistical analysis of the data (see heading 6.3.a for details) revealed several differentially expressed genes between TEMs and TIE2– TAMs (29% at $p<0.05$; Table 2 and Table 3). Among these, Arginase1 (*Arg1*) and several scavenger receptors (*Cd163*; stabilin-1 (*Stab1*); *Mrc1*; *Msr2 (Taylor et al. 2005)*) were up-regulated, while *Nos2*, pro-inflammatory and anti-angiogenic molecules (*Il1b*;

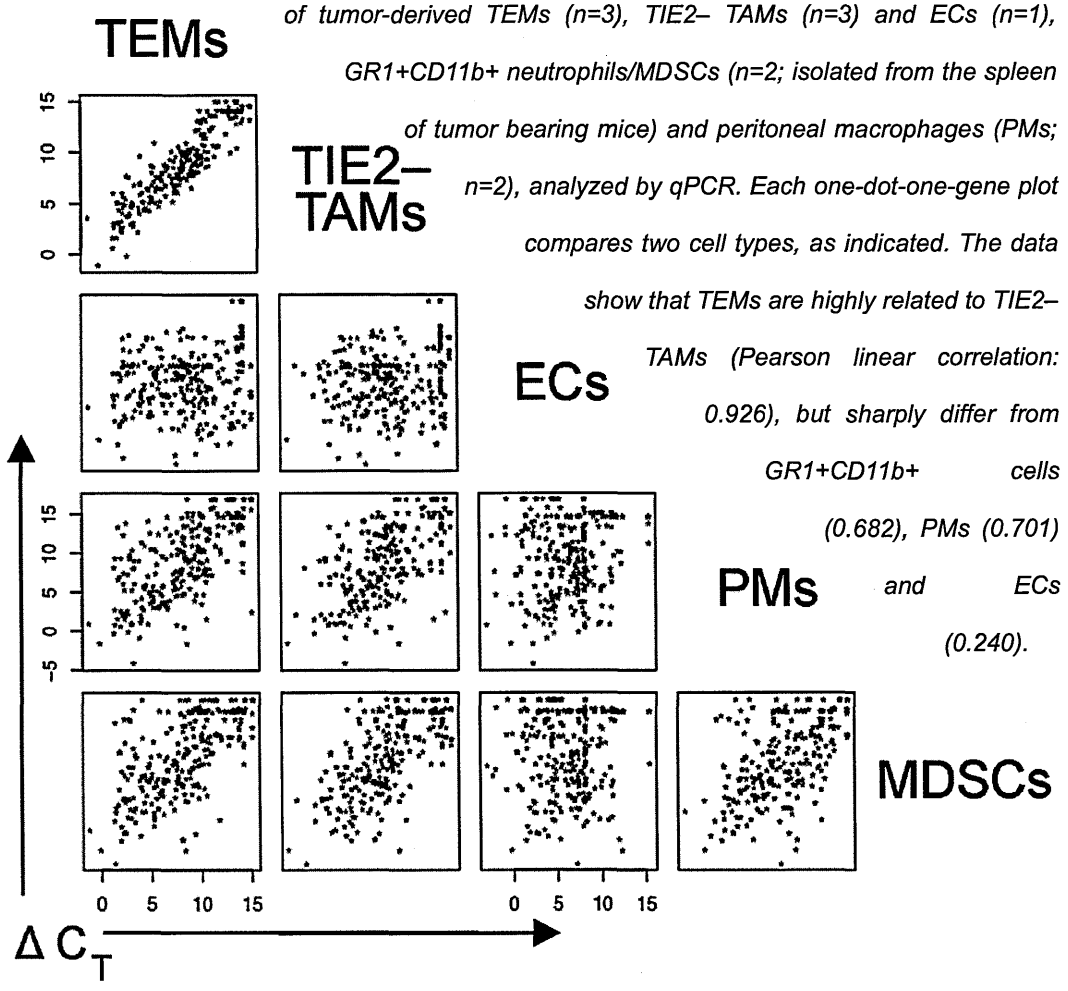

Illustration 17: One-dot-one-gene representation of the expression profile (280 genes analyzed) of tumor-derived TEMs (n=3), TIE2– TAMs (n=3) and ECs (n=1), GR1+CD11b+ neutrophils/MDSCs (n=2; isolated from the spleen of tumor bearing mice) and peritoneal macrophages (PMs; n=2), analyzed by qPCR. Each one-dot-one-gene plot compares two cell types, as indicated. The data show that TEMs are highly related to TIE2– TAMs (Pearson linear correlation: 0.926), but sharply differ from GR1+CD11b+ cells (0.682), PMs (0.701) and ECs (0.240).

Ptgs2/Cox2; *Il12a*; *Tnf*; *Ccl5*; *Cxcl10*; *Cxcl11*) were down-regulated in TEMs vs. TIE2– TAMs. With reference to the M1-M2 polarization paradigm proposed by some authors (Mantovani et al. 2002), the enhanced expression of scavenger receptors and the down-regulation of inflammatory mediators by TEMs would place them at the M2-extreme of the polarization window (i.e. TEMs are significantly more M2-skewed that TIE2– TAMs), consistent with their marked pro-angiogenic and pro-tumoral activity (De Palma et al. 2005; De Palma et al. 2007). Among the most differentially expressed genes were also the hyaluronan receptor-1 (*Lyve1*), neuropilin-1 (*Nrp1*), stromal cell derived factor-1 (*Cxcl12/Sdf-1*), insulin growth factor-1 (*Igf1*) and Toll-like receptor-4 (*Tlr4*), all of which were upregulated in TEMs. The finding of several differentially expressed genes strongly suggests that TEMs represent a distinct subset or differentiation state of TAMs.

Up-regulated genes						
	Fold more	**ΔCt**	**p value**		**Fold more**	**ΔCt**	**p value**
Cd163	15.8	6.3	***	*Timp2*	2.8	4.5	**
Lyve1	14.1	6.1	***	*Plxnd1*	2.8	6.2	**
Igf1	8.2	9.3	***	*Efna1*	2.7	12.6	**
Stab1	6.4	5.5	***	*Slamf1*	2.6	14.6	*
Mrc1	5.3	3.0	***	*Fcgr3*	2.6	3.1	*
Sema6d	5.2	15.2	***	*Angpt1*	2.6	14.2	*
Nrp1	4.6	6.3	***	*Sema3c*	2.6	12.3	*
Cxcl12	4.4	10.6	***	*Timp3*	2.5	12.2	*
Thbs3	4.3	12.1	***	*Kit*	2.5	14.9	*
Cxcl13	4.3	5.1	***	*Sdc2*	2.5	9.1	*
Efnb2	4.2	12.9	**	*Efnb1*	2.5	12.0	*
Neo1	4.1	15.1	**	*Cdh5*	2.4	11.6	*
Plxna3	4.1	12.8	***	*Plxnb2*	2.4	6.3	*
Itga2	4.0	16.3	*	*Il4ra*	2.3	5.1	*
Plxna1	3.6	8.1	***	*Il10ra*	2.2	6.5	*
Msr2	3.5	4.4	***	*Arg1*	2.2	5.7	*
Tlr4	3.5	7.8	**	*Hpse*	2.1	5.6	*
Plxna4	3.1	10.9	**	*Serpinb2*	2.1	9.8	*

Up-regulated genes						
	Fold more	ΔCt	p value		Fold more	ΔCt	p value
Edg1	3.0	8.1	**	*Itgb1*	2.1	5.0	*
Fcgr2b	2.9	3.9	**				

Table 2: Genes up-regulated in tumor-derived TEMs as compared to TIE2– TAMs.

Down-regulated genes						
	Fold less	ΔCt	p value		Fold less	ΔCt	p value
Il1b	-6.6	2.4	***	*Ptprc*	-2.7	3.7	**
Ptgs2	-5.0	5.5	***	*Ctss*	-2.7	0.8	**
Il4	-4.0	12.0	***	*Tgfb1*	-2.6	4.2	*
Nos2	-3.9	8.8	***	*Il18*	-2.6	8.2	*
Ccr7	-3.8	7.6	***	*Sell*	-2.5	10.3	*
Il12a	-3.6	16.2	**	*Ccr2*	-2.5	5.8	*
Smad7	-3.6	8.2	***	*Il12b*	-2.5	11.8	*
Bcl2l1	-3.2	6.6	**	*Nfkb2*	-2.5	5.9	*
Stat4	-3.1	10.7	**	*Fas*	-2.4	9.8	*
Tnf	-3.1	4.0	**	*Gusb*	-2.4	4.9	*
Il13	-3.1	12.8	**	*Smad3*	-2.4	9.0	*
Actb	-3.0	1.0	**	*Socs1*	-2.4	6.6	*
Edn1	-3.0	11.0	**	*Bax*	-2.4	6.2	*
Ccl5	-3.0	4.3	**	*Pgk1*	-2.4	4.1	*
H2-Ea	-3.0	5.1	**	*Ski*	-2.3	6.1	*
Vegfa	-2.9	4.5	**	*Csf1*	-2.3	7.8	*
Il1a	-2.9	5.2	**	*Ctla4*	-2.2	12.9	*
Cxcl10	-2.8	2.9	**	*Stat1*	-2.1	3.7	*
Cd80	-2.8	9.1	**	*Tnfrsf18*	-2.1	12.0	*
Ece1	-2.7	13.1	*	*Tbx21*	-2.1	12.1	*
Cxcl11	-2.7	6.6	**				

Table 3: Genes down-regulated in tumor-derived TEMs as compared to TIE2– TAMs.

6.3.a Statistical model

To rigorously identify differences between TEMs and TIE2– TAMs, in collaboration with the institutional center for statistics at the *Vita-Salute* San Raffaele university,

I implemented in R (http://www.R-project.org) a multivariate regression model, similarly to the model implemented in sas (Yuan et al. 2006), which computes over the whole dataset and estimates the fold-change in gene expression for each single target gene. This model jointly evaluates the role of different variables of interest providing for: (i) statistical significance of the observed differences in expression level across the whole set of experimental samples; (ii) identifying the experimental variables that significantly contribute to explain the differences in expression levels; (iii) subtracting experimentally introduced biases to obtain a stringent estimate of the actual biological differences. Detailed statistical methods are presented in material and methods section.

6.3.b Validation by FACS and IF staining

I then validated the gene expression results by protein analysis, either by immunofluorescence staining (IFS) and confocal microscopy of tumor sections (Illustration 18) or by flow cytometry of tumor-derived cell suspensions (Illustration 19). I employed two different tumor models: N202 tumors grown subcutaneously in Tie2p/e-GFP transgenic mice (De Palma et al. 2005) (n=5 for IFS; n=3-7 for flow cytometry); and mammary tumors spontaneously arising in MMTV-PyMT transgenic mice (Lin et al. 2003) previously transplanted with Tie2p/e-GFP BM cells (n=4 tumors from 4 mice for IFS), as described (De Palma et al. 2008). Whereas in Tie2p/e-GFP transgenic mice both TEMs and ECs express GFP (Illustration 18A), in Tie2p/e-GFP BM-transplanted mice only TEMs are GFP+ (Illustration 18B). GFP+ F4/80+ TEMs were frequently located in stromal tumor areas, whereas GFP– F4/80+ TAMs were evenly distributed throughout the tumor mass (Illustration 18B).

IFS and/or flow analyses showed differential expression of LYVE1, MRC1, TLR4, interleukin-4 receptor-alpha (IL4RA), CD163 and STAB1 – but not of F4/80, TLR2,

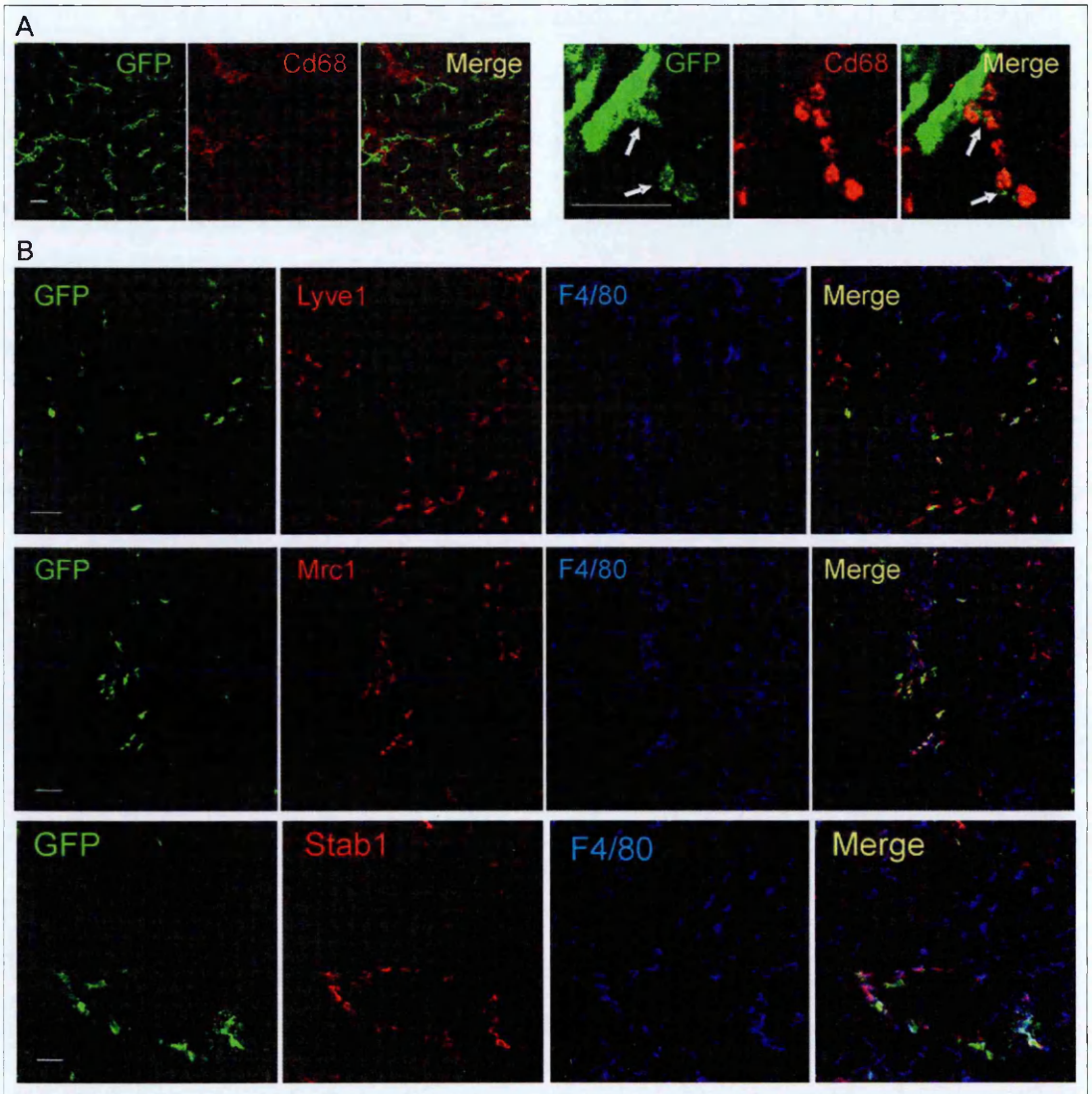

Illustration 18: Confocal immunofluorescence analysis of mouse tumors. (A) N202 mammary tumors (n=5) grown s.c. in Tie2p/e-GFP transgenic mice. The left panels show GFP+ blood vessels and abundant CD68+ macrophages (scale bar: 120µm). High-magnification photos (right panels) show perivascular Tie2p/e-GFP+ CD68+ TEMs (arrows); scale bar: 60µm. For each tumor, at least 3 sections were analyzed. (B) Mammary tumors spontaneously arising in MMTV-PyMT transgenic mice (n=4) previously transplanted with Tie2p/e-GFP BM cells. Abundant F4/80+ macrophages are evenly distributed within the tumor mass, whereas Tie2p/e-GFP+ LYVE1+ or Tie2p/e-GFP+ MRC1+ or Tie2p/e-GFP+ STAB1+ TEMs are mainly found in stromal septa surrounding tumor cell nests. Virtually all the Tie2p/e-GFP+ cells express LYVE1, MRC1 and STAB1. Note that some of the Tie2p/e-GFP− LYVE1+, MRC1+ or STAB1+ cells may represent host-derived, non-transgenic TEMs. Scale bar: 60µm. For each tumor, at least 10 sections were analyzed for each marker.

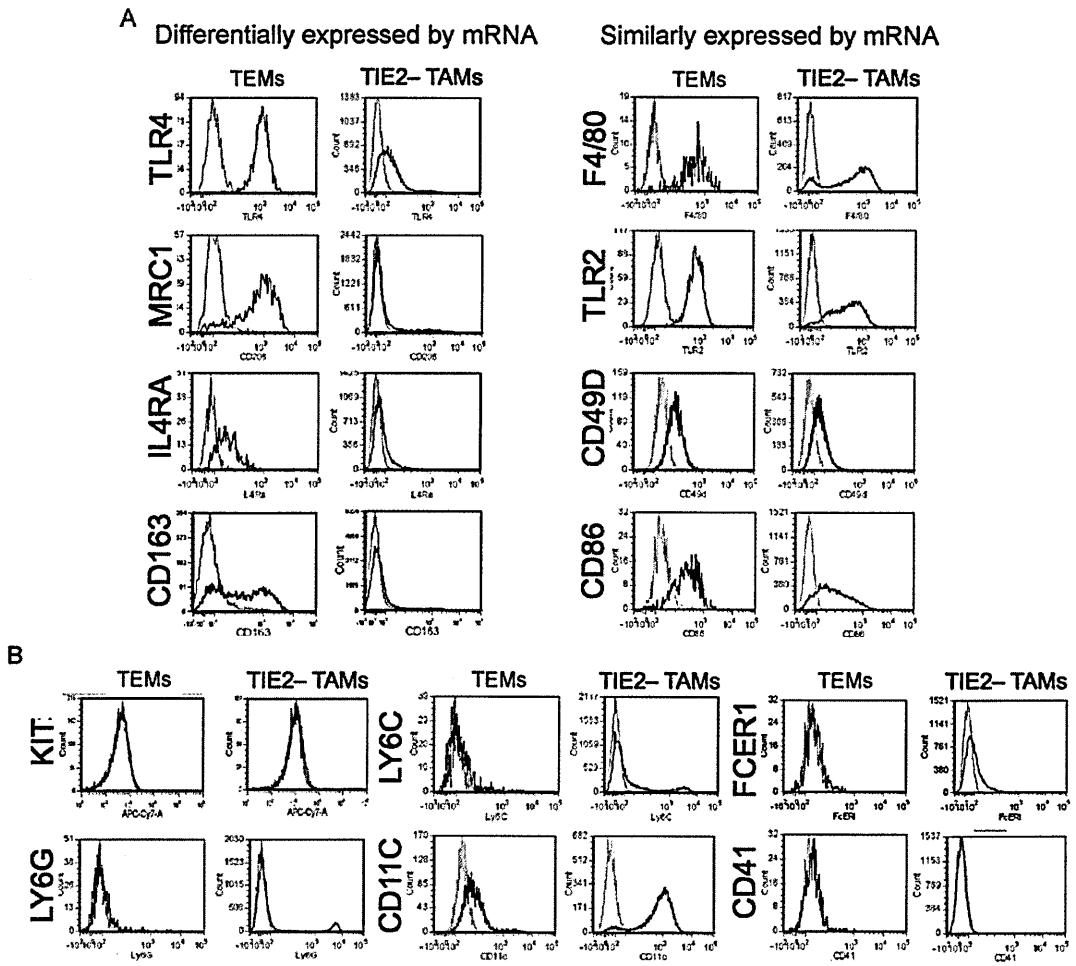

Illustration 19: Flow cytometric analysis of N202 mammary tumors identifies a distinguishing TEM signature. A) Flow analysis of some of the genes that were either differentially expressed or not differentially expressed between TEMs and TIE2– TAMs, gated as Tie2p/e-GFP+ CD11b+ 7AAD– and Tie2p/e-GFP– CD11b+ 7AAD– cells, respectively. In agreement with the mRNA data, TEMs but not TIE2– TAMs robustly and uniformly express TLR4, MRC1, IL4RA and CD163 (left panels, n=3). Genes not differentially expressed by qPCR are similarly expressed by TEMs and TIE2– TAMs (right panels, n=3). B) Further phenotypic characterization of TEMs and TIE2– TAMs. Note that TEMs do not express KIT, granulocyte (LY6G), inflammatory monocyte (LY6C), dendritic cell (CD11c), mast cell (FCER1) and megakaryocyte/platelet (CD41) markers (n=3).

ITGA4 (CD49d) and CD86 – between TEMs and TIE2– TAMs, in agreement with the RNA data (Illustration 18B, Illustration 19). Although the *Itgax* (*Cd11c*) mRNA was expressed similarly in TEMs and TIE2– TAMs (not present in Table 2 and 3), TEMs were CD11c– and TIE2– TAMs markedly CD11c+ by flow cytometry and IFS

(Illustration 19B). TEMs were KIT– and did not express FCER1, LY6G, LY6C and CD41, which are mast cell-, neutrophil-, inflammatory monocyte-, and megakaryocyte/platelet-specific markers, respectively (Illustration 19B). Together with the mRNA data, these results identify a unique TEM surface marker profile, which distinguishes them from TIE2– TAMs and related myeloid-lineage cells.

6.4 TEMs are refractory to pro-inflammatory stimuli

The gene expression data indicated that TEMs have a Th2/M2 phenotype. I wondered whether Th1 stimulation could modulate this phenotype. To this aim, I stimulated (or left unstimulated) tumor-derived TEMs, TIE2– TAMs and PMs with

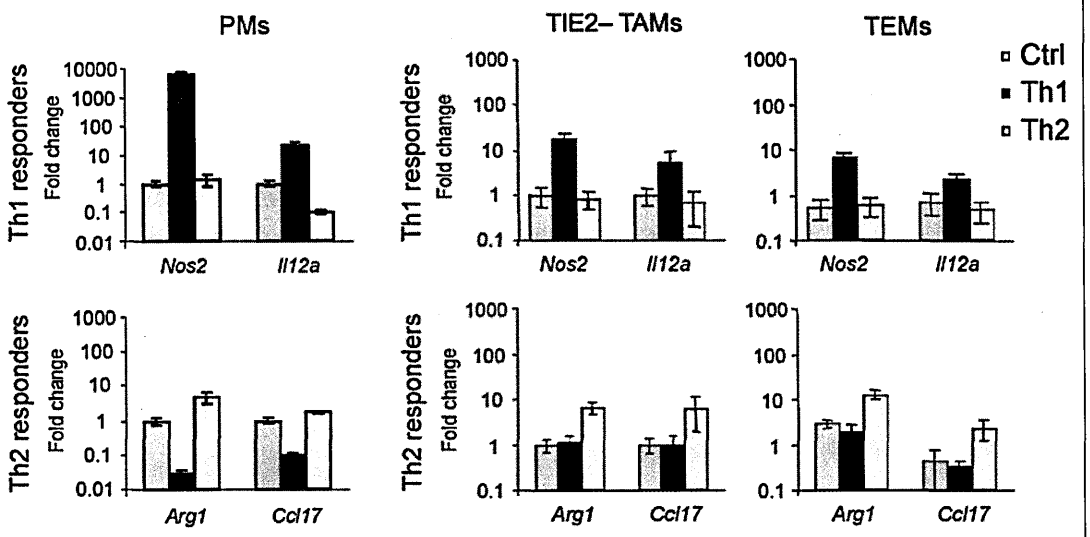

Illustration 20: TEMs, like TIE2– TAMs, are refractory to pro-inflammatory stimuli. In vitro stimulation of PMs, TEMs and TIE2– TAMs with Th1 (LPS + IFNg; black bars) and Th2 (IL4; red bars) cytokines, or the same cells left unstimulated (Ctrl; grey bars). Upper and lower panels show the expression of Th1 (Nos2, Il12a) and Th2 (Arg1, Ccl17) responder genes, respectively. The expression of each gene is indicated as fold-change (mean ± 2•SD, n=3) over its expression in unstimulated PMs (for PMs) or unstimulated TIE2– TAMs (for TEMs and TIE2– TAMs). Note that TEMs and TIE2– TAMs are much less responsive than PMs to Th1 cytokine treatment. Conversely, Th2 cytokine stimulation elicits a greater response in TEMs and TIE2– TAMs than in PMs. Error bars represent a 95% confidence intervals (CI = 2•SD), thus non-overlapping CI denote a statistically significant difference ($p < 0.05$).

either Th1 (LPS + IFNg) or Th2 (IL4) cytokines (n=3 independent experiments) and evaluated the expression of established responder genes (Mantovani et al. 2002) (*Nos2* and *Il12a* for Th1 responses; *Arg1* and *Ccl17* for Th2 responses). Th1 stimulation elicited minor responses in TEMs and TIE2– TAMs, as compared to PMs (Illustration 20). Conversely, TEMs and TIE2– TAMs were more responsive than PMs to Th2 stimulation. These results indicated that both tumour-derived TEMs and TIE2– TAMs display defective Th1 responses but can respond to Th2 stimuli. Of note, both unstimulated and Th2-stimulated TEMs had higher *Arg1* and lower *Nos2* expression than TIE2– TAMs, in agreement with the gene profile data.

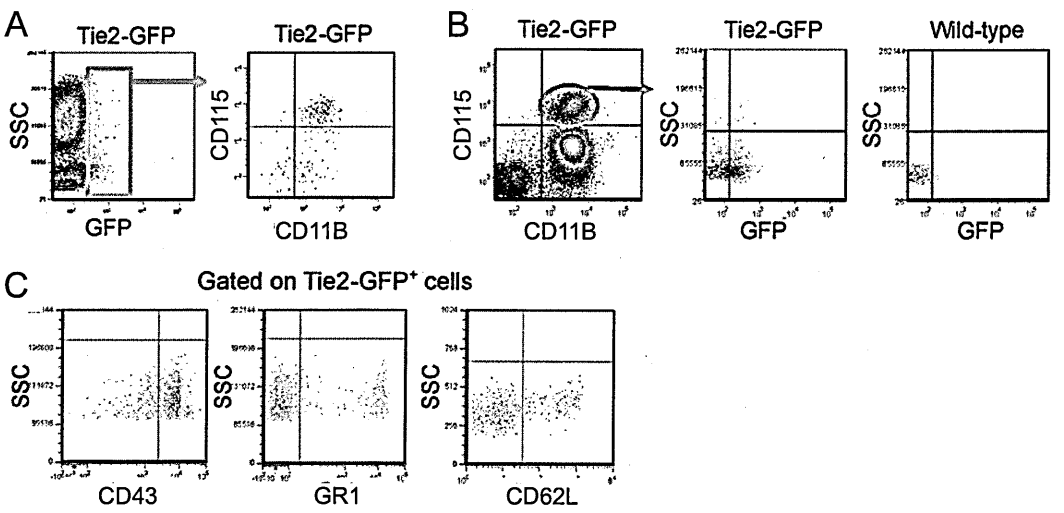

Illustration 21: Flow cytometry analysis of the blood of Tie2p/e-GFP transgenic mice. A) Virtually all the Tie2p/e-GFP+ TEMs (green gate in the dot plot on the left; n=16) are CD11b+ CD115+ 7AAD– monocytes (dot plot on the right). B) Only a fraction (~30%; n=13) of the CD11b+ CD115+ 7AAD– monocytes (dot plot on the left) are Tie2p/e-GFP+ (dot plot in the middle). Monocytes from wild-type mice (n=5) were used to set the gate for GFP+ events (dot plot on the right). C) Dot plots show the expression of surface markers that can distinguish resident from inflammatory monocytes (n=7-10). The CD115+ GFP+ 7AAD– cells were gated and the expression of CD43, GR1 and L-selectin (CD62L) analyzed. The vast majority of Tie2p/e-GFP+ CD115+ 7AAD– TEMs are CD43+ GR1– CD62L– resident monocytes.

7 Blood TEMs are a subset of monocytes

Blood monocytes are commonly considered the natural precursors of macrophages. To investigate the origin of tumor-infiltrating TEMs, I analysed circulating TEMs, which may be the precursors of their tumor-infiltrating counterpart (De Palma et al. 2005). We previously speculated that circulating TEMs belong to the myeloid lineage based on their expression of CD11b and CD14 in mice and humans, respectively (De Palma et al. 2005; Venneri et al. 2007). However, some cell surface-associated markers are co-expressed by endothelial- and hematopoietic-lineage cells (De Palma & Naldini 2006).

7.1 TEMs express resident monocyte marker profile

To better characterize the phenotype of circulating TEMs, I extended the phenotypic analysis to the most specific monocyte marker (i.e. CSF1R/CD115, (Hume et al. 2002)) and to markers able to distinguish between the two monocyte subsets (Sunderkötter et al. 2004). The vast majority of circulating GFP+ cells in Tie2p/e-GFP mice were positive for CD115 (84±5%, mean ± SD; n=16; Illustration 21A). Of note, only 30±6% (n=13) of the total CD115+ monocytes were GFP+, indicating that TEMs represent a subset of circulating monocytes (Illustration 21B). The GFP+ TEMs were mostly GR1– (84±5%, n=10), CD62L– (74±6%, n=7) and CD43+ (80±6%, n=10), thus expressing a resident monocyte marker profile (Illustration 21C).

7.2 Common gene signature of circulating resident monocytes and tumor-infiltrating TEMs

I then analyzed gene expression (39 genes of interest, selected among those analyzed in tumor-derived cells) in CD115+ GR1– resident and CD115+ GR1+ inflammatory monocytes obtained from the blood of tumor-free mice (n=4), and

Up-regulated

	Fold more	ΔCt	p value
Arg1	58,7	11,5	***
Cxcl12	20,5	15,1	***
Lyve1	14,7	12,8	***
Stab1	14,1	16,7	***
Igf1	13,6	15,3	***
Cd163	5,2	13,3	***
Edg1	4,7	9,0	***
Il10	4,4	16,0	***
Mmp9	3,1	12,3	*
Mrc1	2,7	9,9	*
Il12a	2,6	14,0	*
Mmp2	2,5	17,6	*

Down-regulated

	Fold less	ΔCt	p value
Chi3l3/Ym1	-18,0	6,4	***
Sell	-9,5	8,1	***
Ccr2	-5,6	7,6	***
Ptgs2	-4,5	18,1	***

Not differentially expressed

Angpt1	*Cx3cr1*	*Itga4*	*Tbx21*
Angpt2	*Egf*	*Il4*	*Tgfb1*
Ccr7	*Fgf2*	*Vegfr2*	*Tlr4*
Csf1R	*Flt1/Vegfr1*	*Mmp12*	*Tnf*
Cd80	*Ifng*	*Nos2*	*Tnfrsf18*
Cd86	*Il1b*	*Nrp1*	

= Concordant expression in resident vs. inflammatory monocytes and TEMs vs. TAMs
= Significantly upreg./downreg. either in res. vs. inflam. monocytes or TEMs vs. TAMs
= Discordant expression in resident vs. inflammatory monocytes and TEMs vs. TAMs

Illustration 22: Genes expressed either differentially or not between resident and inflammatory monocytes. The concordant (or less) gene expression in blood-derived resident vs. inflammatory monocytes and tumor-derived TEMs vs. TIE2– TAMs is shown by a colour code, as indicated.

****: $p < 0.001$; **: $p < 0.01$; *: $p < 0.05$*

compared the results with those obtained with tumor-derived TEMs and TIE2– TAMs (Illustration 22). Remarkably, 22 out of 39 genes displayed concordant expression in resident vs. inflammatory monocytes and TEMs vs. TIE2– TAMs (exact binomial test p=0.003). These included *Arg1*, *Igf1*, *Cxcl12*, *Lyve1*, *Stab1*, *Cd163*, *Edg1*, *Mrc1* (up-regulated in resident monocytes and TEMs vs. inflammatory monocytes and TIE2– TAMs, respectively) and *Sell*, *Ccr2*, *Ptgs2/Cox2* (down-regulated). Only one gene, *Il12a*, displayed discordant expression, whereas the remainder genes were differentially expressed in either resident vs. inflammatory monocytes or TEMs vs. TIE2– TAMs. The association of the TEM gene expression signature, which enriches for tissue remodeling vs. pro-inflammatory genes, with resident monocytes suggests that resident and inflammatory blood monocytes represent two functionally distinct subsets that may be differentially committed to generate tumor-infiltrating TEMs and TIE2– TAMs, respectively.

8 Tie2 knock down in hematopoietic cells

The function of the TEM distinguishing marker, *Tie2*, is still unknown. To investigate the role of TIE2 receptor in TEMs I employed a lentiviral platform recently developed in our laboratory (Amendola et al. 2009). This platform enables the expression of one or more artificial micro-RNAs (amiR) together with a reporter gene from polymerase-II promoters. By replacing the stem sequence of a primary micro-RNA (pri-miR) with a sequence targeting the gene of interest (i.e. a siRNA sequence, in red in Illustration 23), it is possible to obtain robust expression of the amiR in several cell types and to reach the concentration and activity typical of highly expressed natural miR without perturbing endogenous miR maturation or regulation. Moreover, the option to co-express two amiR in a single LV allows the targeting of two different sites in the target transcript, which increase the repression of the protein at single vector copy number (VCN) (Amendola et al. 2009).

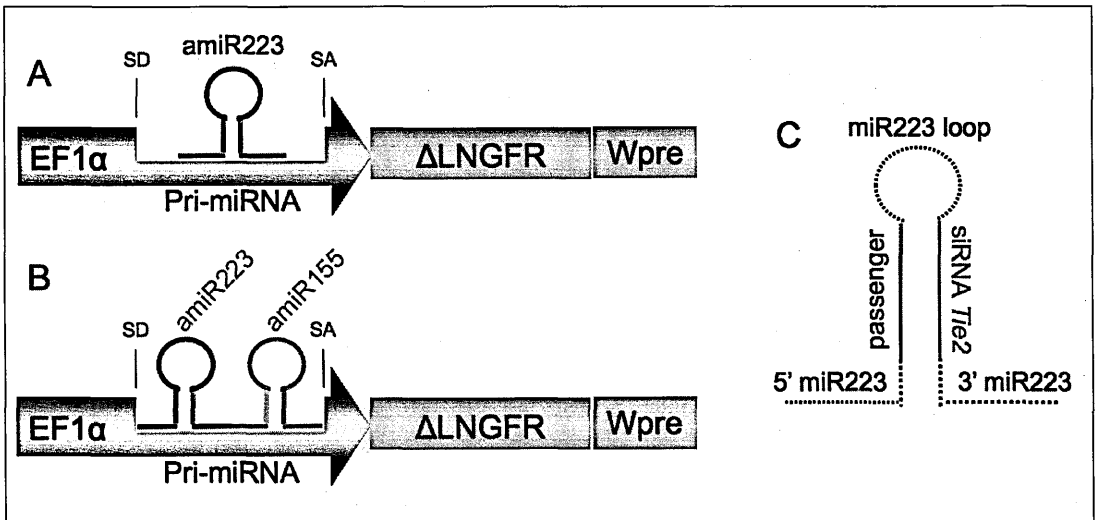

Illustration 23: Design of LVs constitutively expressing either a monocistronic (A) or a bicistronic (B) artificial micro-RNA cassette and a marker gene (NGFR) from the EF1α promoter. C: Detailed structure of the amiR223(Tie2) showing endogenous sequences from pri-miR223 (dotted lines), siRNA sequence against Tie2 (red line) and the passenger strand (blue line).

8.1 Identification of the most effective RNAi sequence against Tie2

Selection of an efficient siRNA sequence still requires empirical validation (Takasaki 2009). In order to find a siRNA sequence able to consistently knock down the murine TIE2 receptor, I tested five candidate sequences targeting *Tie2* suggested by The RNAi Consortium, a public-private consortium based at the Broad Institute of MIT and Harvard (http://www.broadinstitute.org/rnai/trc), and five candidate sequences designed against *Tie2* using the on-line tool from Invitrogen Inc. (http://rnaidesigner.invitrogen.com). No overlapping sequences were present between the two groups. To improve gene knock down, I also generated bicistronic amiR. I then selected two different pri-miR backbones, because recombinations within the LV genome are frequent when tandem repeats longer than ~200 bases (like pri-miR) are present in the same LV genome (Amendola et al. 2009). I chose pri-miR-223 (Amendola et al. 2009) and pri-miR-155 (Chung et al. 2006) backbones to clone the selected *Tie2* siRNA sequences and generated the amiR223(Tie2) and amiR155(Tie2) cassettes, respectively. As control, I employed siRNA sequences targeting unrelated genes (amiR223(Luc) and amiR155(LacZ), targeting luciferase and β-galactosidase, respectively). Finally, these amiR constructs were separately cloned into the intron of an expression cassette made of the elongation factor 1α (EF1α) promoter and first intron, and a cDNA for the truncated form of the low affinity nerve growth factor receptor (NGFR; Illustration 23).

To select the best performing anti-*Tie2* sequence, I transduced brain endothelial cells (bEnd), which express the TIE2 receptor endogenously, with amiR223(Tie2) and control amiR223(Luc) LVs. The most effective amiR223(Tie2) LV almost completely shut off *Tie2* expression as shown by FACS, and reduced its mRNA level by 7-fold as compared to the amiR223(Luc) LV (Illustration 24A). To quantify

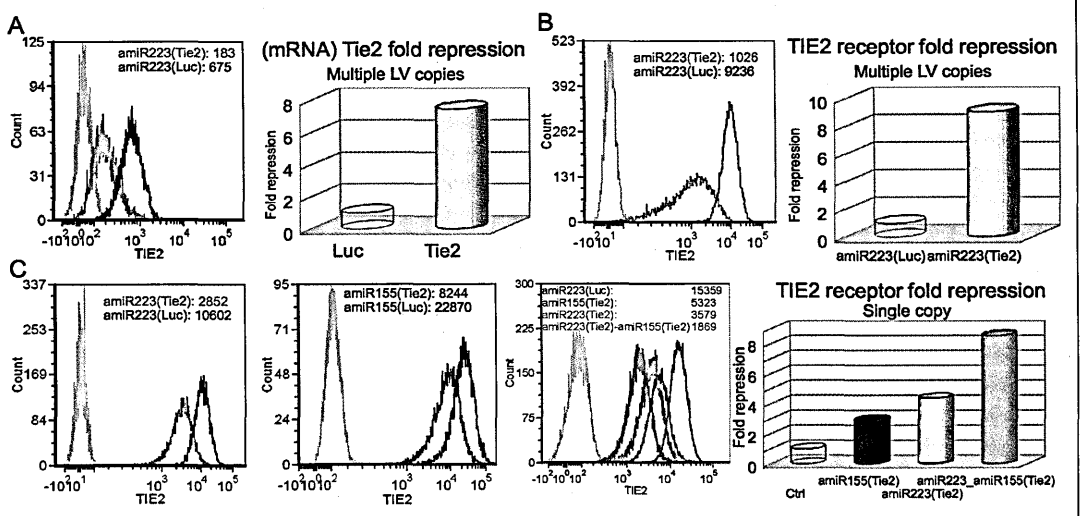

Illustration 24: Selection of siRNA sequences against TIE2 in vitro. bEnd (A) and U937-TIE2 (B) cells expressing the best performing amiR223(Tie2) (or control sequence, Luc). Right plot in A shows Tie2 transcript repression, right plot in B shows TIE2 receptor repression. C) Comparison at single LV copy of the best performing amiR223(Tie2) (red) with the best performing amiR155(Tie2) (blue) and with the bicistronic amiR223(Tie2)_amiR155(Tie2) (pink) in U937-TIE2

the extent of protein suppression of the different siRNA sequences, I performed additional experiments using U937 myelomonocytic cells over-expressing the murine TIE2 receptor (U937-TIE2) from a LV cassette containing the phospho-glycerate kinase 1 (PGK1) promoter and the *Tie2* cDNA. In these cells, the high expression level of TIE2 ensures a wide dynamic range of gene expression to measure gene knock down. The TIE2 receptor was down-regulated by ~10 fold (vs. amiR223(Luc)) when the best performing amiR223(Tie2) LV was used at multiple copies per genome (Illustration 24B). To compare the best performing amiR223(Tie2) LV with the best performing amiR155(Tie2) LV, I monitored cells transduced at single LV copy over a long period of time. Both amiR223(Tie2) and amiR155(Tie2) LVs achieved a 3 to 4 fold repression in U937-TIE2 cells (Illustration 24C).

In order to improve gene knock down even at single VCN, I finally generated bicistronic LVs encoding for the two most effective amiR(Tie2) cassettes. I

compared the performance of this bicistronic amiR223(Tie2)_amiR155(Tie2) LV with that of each monocistronic amiR(Tie2) and monocistronic or bicistronic amiR(Ctrl) LVs. U937-TIE2 cells were transduced with these vectors at single VCN and analysed by FACS. The bicistronic amiR223(Tie2)_amiR155(Tie2) LV repressed TIE2 expression about 10 fold, twice as much as the best monocistronic amiR(Tie2) LV, at single VCN (Illustration 24C).

In summary, I have identified two highly efficient siRNA sequences against *Tie2*, each allowing 4-fold repression of TIE2 at single VCN, and up to 10-fold repression of TIE2 at single VCN when employed in conjunction.

8.2 Constitutive expression of bicistronic amiR impairs cell growth in-vivo and in-vitro

To study the effect of down-regulating *Tie2* in hematopoietic cells, I performed a BM transplantation experiment. To conveniently track TEMs, Tie2p/e-GFP

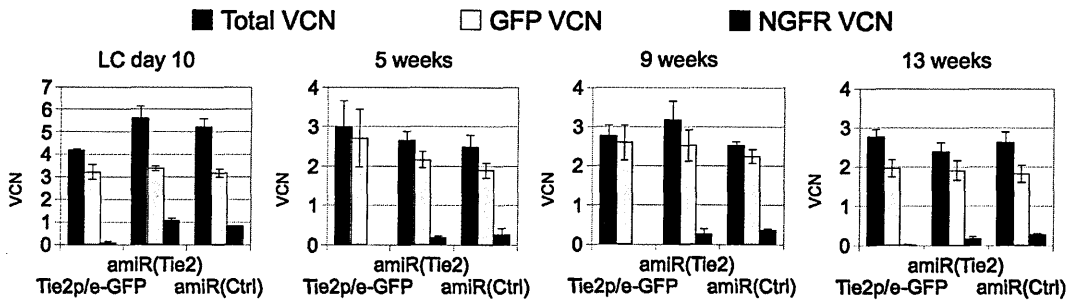

Illustration 25: Vector copy number analysis on day 10 after transduction and on blood leukocytes at different time points after transplant. Tie2p/e-GFP group of mice (n=5) received untransduced Tie2p/e-GFP BM lineage negative cells. amiR(Tie2) group of mice (n=5) received Tie2p/e-GFP BM lineage negative cells transduced with bicistronic amiR(Tie2) LVs. amiR(Ctrl) group of mice (n=5) received Tie2p/e-GFP BM lineage negative cells transduced with bicistronic amiR(Ctrl) LVs. Blue bars: qPCR for HIV (total VCN); yellow bars: qPCR for GFP (donor Tie2p/e-GFP BM); brown bars: qPCR for NGFR (bicistronic amiR LVs). Note that inconsistencies between blue and yellow bars in Tie2p/e-GFP group may be due to differences in qPCR assay efficiencies.

transgenic mice were used as BM donors. BM lineage negative cells were transduced with the bicistronic amiR223(Tie2)_amiR155(Tie2) or amiR223(Luc)_amiR155(LacZ) LVs, and transplanted into lethally irradiated hosts. After hematopoietic reconstitution, the progeny of transduced cells can easily be identified by the expression of the marker gene NGFR. Although the VCN of bicistronic amiR LVs (measured by qPCR for NGFR sequences) was ~1 in liquid culture, it dropped to almost undetectable levels in blood leukocytes of both groups of mice already at 5 weeks after the transplant (Illustration 25).

This trend was further confirmed by FACS analysis for NGFR expression on blood leukocytes at 11 weeks (bicistronic amiR(Tie2): 8.7% SD=1.3% n=5; bicistronic amiR(Ctrl): 10.7% SD=4.2% n=5) and 15 weeks (bicistronic amiR(Tie2): 2.7% SD=1.5% n=5; bicistronic amiR(Ctrl): 4.7% SD=2.4% n=5) post-transplant. (Table 4). Since the chimerism of donor BM (measured as GFP VCN) remained stable throughout the time window of analysis, an engraftment failure can be excluded. Rather, these results suggested the presence of a counter-selection process against bicistronic amiR-transduced cells *in vivo*, regardless of the targeted sequence.

To investigate the long term effect of amiR expression on cell fitness, I transduced U937-TIE2 cells with LVs expressing various combinations of amiR (including mono- and bicistronic LVs), targeting either *Tie2* or unrelated sequences (*Luc* and *LacZ*). During a six weeks period, I measured a steady decrease in the percentage

Bicistronic amiR(Tie2)	**% at 11 weeks**	**% at 15 weeks**	**Bicistronic amiR(Ctrl)**	**% at 11 weeks**	**% at 15 weeks**
Average	8.7	2.7	Average	10.7	4.7
SD	1.28	1.54	SD	4.18	2.39
U-test	0.0120		U-test	0.03	

Table 4: Percentages of NGFR+ blood leukocytes measured by FACS at the indicated time points. U-test: Mann-Whitney test.

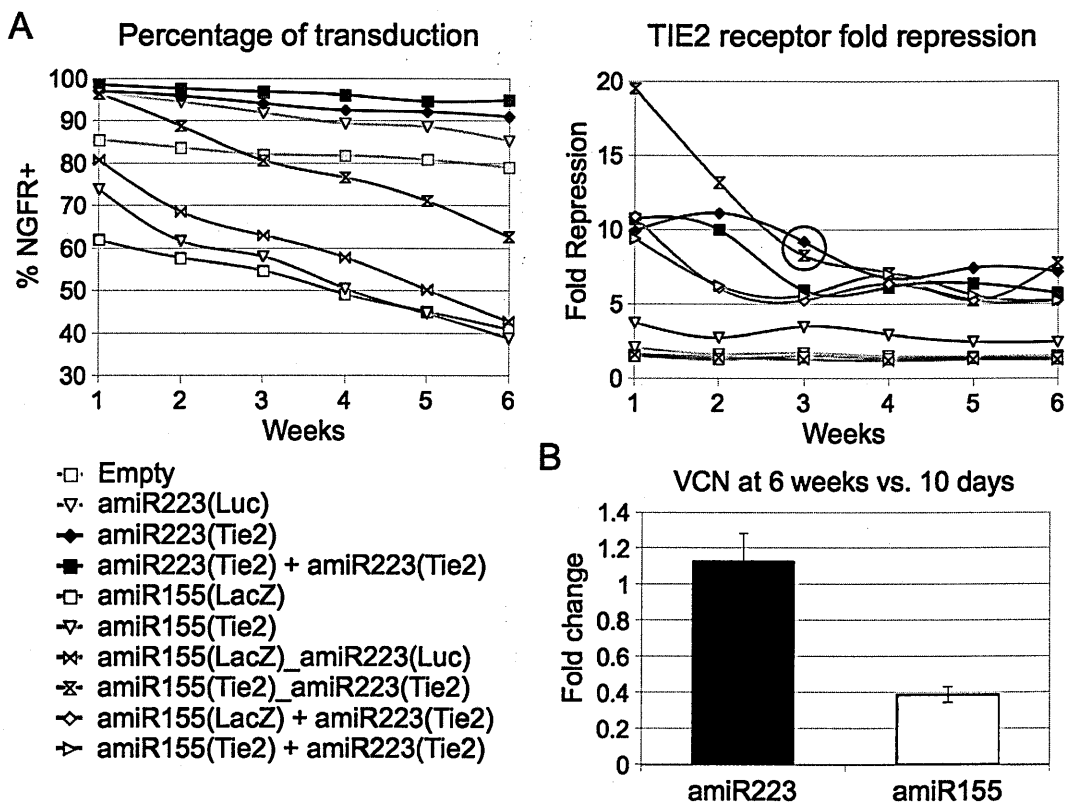

Illustration 26: In-vitro counter-selection of LVs carrying amiR155 cassette in U937-TIE2 cells. A) Time course analysis of cells transduced with the indicated amiR LVs. Percentages of transduced cells (left panel) and TIE2 fold repression (right panel) are reported. Note that cells expressing amiR155 either against Tie2 sequence or control sequence (LacZ) lose the competition with untransduced cells over time (left plot). Fold repression (right plot) is calculated dividing the mean fluorescence intensity (MFI) of TIE2+NGFR– (untransduced) cells by the MFI of TIE2+NGFR+ cells in the same sample (internal control). B) Average fold change in VCN at 6 weeks after transduction as compared to VCN at 10 days after transduction (set equal to 1). A value smaller than 1 indicates a decrease in VCN with time.

of NGFR+ (i.e. transduced) cells carrying a pri-miR155 backbone inside the expression cassette, independently of the target sequence (Illustration 26). Interestingly, *Tie2* gene knock down (measured as fold repression) was very high one week after transduction with the bicistronic amiR155(Tie2)_amiR223(Tie2) LV (19.5 fold vs. amiR223(Luc)_amiR155(LacZ) LVs at multiple LV copies), but dropped down to the same level obtained with monocistronic amiR223(Tie2) LV at 3 weeks after transduction (9.2 fold, Illustration 26A). To discriminate between cell

counter-selection and LV silencing, I compared the VCN at 10 days after transduction with that at 6 weeks after transduction, and found that the VCN decreased, on average, by 3-fold in cells carrying bicistronic amiR cassettes, whereas it remained stable in monocistronic, amiR223 containing cells (Illustration 26B). Overall, these results indicate that amiR155 is detrimental to cell fitness/viability, and the cells which express it are rapidly counter-selected both in-vitro and in-vivo.

9 Conditional Tie2 knock down in mature hematopoietic cells

Although it is reported that the amiR design neither saturates miR pathway (Castanotto et al. 2007; Boudreau et al. 2009) nor triggers type I IFN responses (Ely et al. 2009), some authors suggest that when very high concentrations of RNA duplexes are present inside the cell (whatever method is used to introduce/generate it), nonspecific off-target effects, including activation of the interferon response, become likely (Cullen 2006; Fish & Kruithof 2004). Moreover, hematopoietic stem cells chronically stimulated with type I interferon are functionally compromised (Essers et al. 2009). To overcome toxicity and *in vivo* counter selection of amiR-expressing cells (see paragraph 8.2), I implemented two features in our LV platform:

1. Conditional expression;
2. Post-transcriptional regulation;

in order to finely tune amiR expression level and de-target its expression from HSCs, respectively.

To achieve conditional expression (feature 1) we employed a Tetracycline based genetic switch (Vigna et al. 2005). This switch is composed of a proteinaceous transactivator (reverse Tetracycline transactivator, rtTA) and a synthetic promoter

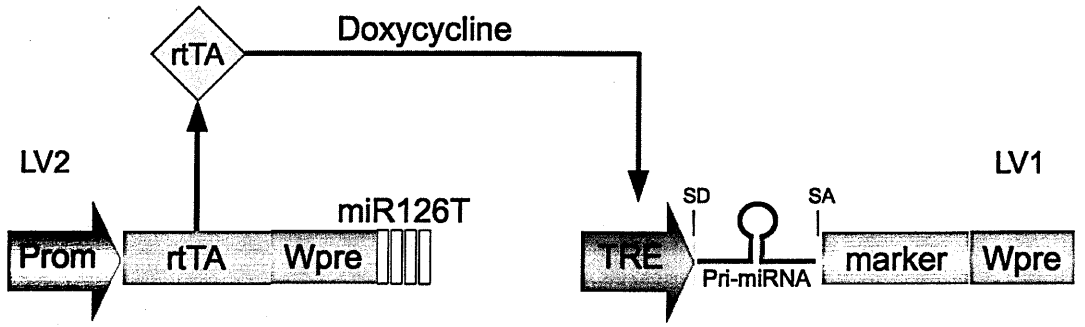

Illustration 27: Conditional LV platform for amiR expression. Prom: promoter of choice; rtTA: reverse Tetracycline transactivator; Wpre: Woodchuck hepatitis virus post-transcriptional regulatory element; miR126T: micro-RNA-126 target sequence; TRE: Tetracycline regulated element; SD/SA: splice donor/acceptor. Red stems inside the primary micro-RNA (pri-miRNA) represents artificially inserted sequences against Tie2 or Luc.

(Tetracycline responsive element, TRE) (Urlinger et al. 2000; Gossen & Bujard 1992). Upon Doxycycline treatment, rtTA binds to TRE and switches on the transcription of the downstream gene silencing cassette (Illustration 27).

In order to suppress rtTA expression (feature 2) and, consequently, *Tie2* gene knock down in HSCs, which require TIE2 for their maintenance in the stem cell niche (Arai et al. 2004), I modified the rtTA expression cassette by incorporating target sequences for miRNA-126 (miR-126T) in the UTR (Illustration 27). By this strategy (Brown & Naldini 2009), rtTA expression is suppressed specifically in HSCs via miRNA-mediated mRNA degradation, as only HSCs express high-level miR-126 among hematopoietic-lineage cells (Gentner and Naldini, unpublished data).

9.1 Tie2 knock down in primary cells

To obtain inducible gene silencing, I placed the rtTA-m2 under the control of the ubiquitously active *PGK* promoter and generated FVB/*PGK*-rtTA-miR-126T (LV2; Illustration 27) transgenic mice by LV-mediated transgenesis, as previously described (De Palma et al. 2005). LV2-transgenic mice carrying more than 3

vector copies per genome were then used as donors of BM cells in all subsequent experiments. We transduced LV2-transgenic, BM-derived lineage-negative cells (BM-Lin$^-$ cells, which comprise cKIT+ SCA1+ long-term repopulating HSCs; Illustration 28A) with LV1 (Illustration 27) either expressing amiR(Tie2) or amiR(Luc), together with a marker gene (orange fluorescent protein, OFP), enabling the identification of the induced cells. I cultured a small aliquot of the transduced cells *in vitro* for 2 weeks, or transplanted them into irradiated FVB mice, to obtain amiR(Tie2) and amiR(Luc) mice (n = 3/group), respectively.

Both amiR(Tie2)- and amiR(Luc)-transduced BM-Lin$^-$ cells efficiently upregulated OFP expression (> 80% OFP+ cells) as early as 2 days after doxycycline treatment *in vitro* (Illustration 28B). To detect if the primary amiR(Tie2) is not only expressed, but also correctly processed inside the cells, I employed a custom qPCR-based assay, which detects the 21 nucleotide long ncRNA corresponding to the mature form of amiR(Tie2). Two days after doxycycline treatment, amiR(Tie2)-transduced cells up-regulated the mature amiR(Tie2) sequence by > 30-fold by qPCR (vs. untreated, amiR(Tie2)-transduced cells; Illustration 28C) and concomitantly down-regulated the endogenous *Tie2* mRNA by > 4-fold (corresponding to a 75% reduction) as compared to untranduced or amiR(Luc)-transduced cells (Illustration 28D). These results indicate efficient and inducible expression, as well as correct maturation, of the primary amiR(Tie2) that generates siRNA sequences against *Tie2* inside the cells.

9.2 The conditional gene silencing platform is safe in vivo

I then tested if cell counter-selection occurs upon induction of amiR expression. Three weeks after BM-Lin$^-$ cell transplant, I treated amiR(Tie2) and amiR(Luc) mice with doxycycline every third day in order to activate LV1 in BM-derived cells. One week and 4 weeks after the first doxycycline administration, I collected the

blood of the mice from the tail vein and analyzed their blood to score for OFP expression and potential hematopoietic counter-selection of OFP+ cells (Illustration 29A). At both time points, I measured very similar percentages of OFP+ monocytes and granulocytes of both amiR(Tie2) and amiR(Luc) mice (indicated by a time ratio equal to 1; Illustration 29B). As expected, at 4 weeks after BM-Lin$^-$ cell transplant, the chimerism of lymphocytes is not yet complete,

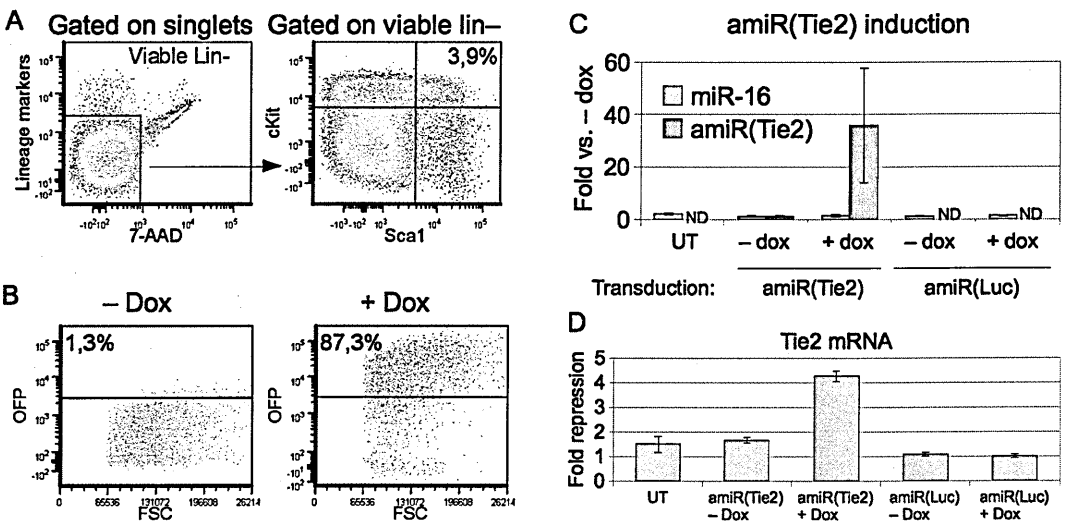

*Illustration 28: Ex vivo validation of conditional Tie2 gene knock down. A: Flow cytometry of LV1-transduced BM-Lin$^-$ HSPCs. Panels show freshly isolated, LV2-transgenic, BM-Lin$^-$ HSPCs stained with 7AAD, lineage markers (B220; Gr1; Ter119; CD11b), c-KIT, and SCA1. Note that viable (7AAD–) BM-Lin$^-$ cells contain bona fide HSCs (Lin$^-$ c-KIT+ SCA1+) at the expected frequency (ca. 2-4%). B: Panels show LV2-transgenic, BM-Lin$^-$ HSPCs analyzed 5 days after transduction with LV1 (carrying the amiR(Tie2)/OFP expression cassette). Cells were treated with doxycycline (or left untreated) starting at day 1 post-transduction. Note that OFP is robustly induced in doxycycline-treated cells. C: Doxycycline-mediated induction of the amiR(Tie2) sequence in LV2-transgenic, BM-Lin$^-$ cells at day 2 post-transduction with LV1, measured by qPCR (fold-change vs. untreated cells). Let7a (a ubiquitously expressed miRNA) was used to normalize gene expression. Note that the amiR(Tie2) sequence is not detected in untransduced cells (UT) and amiR(Luc)-transduced cells either treated with doxycycline or left untreated. D: Tie2 gene knock down in LV2-transgenic, BM-Lin$^-$ cells at day 2 post-transduction with LV1, measured by qPCR (fold-change vs. amiR(Luc)-transduced cells treated with doxycycline (*)). Error bars represent 95% confidence interval (1.96*SEM).*

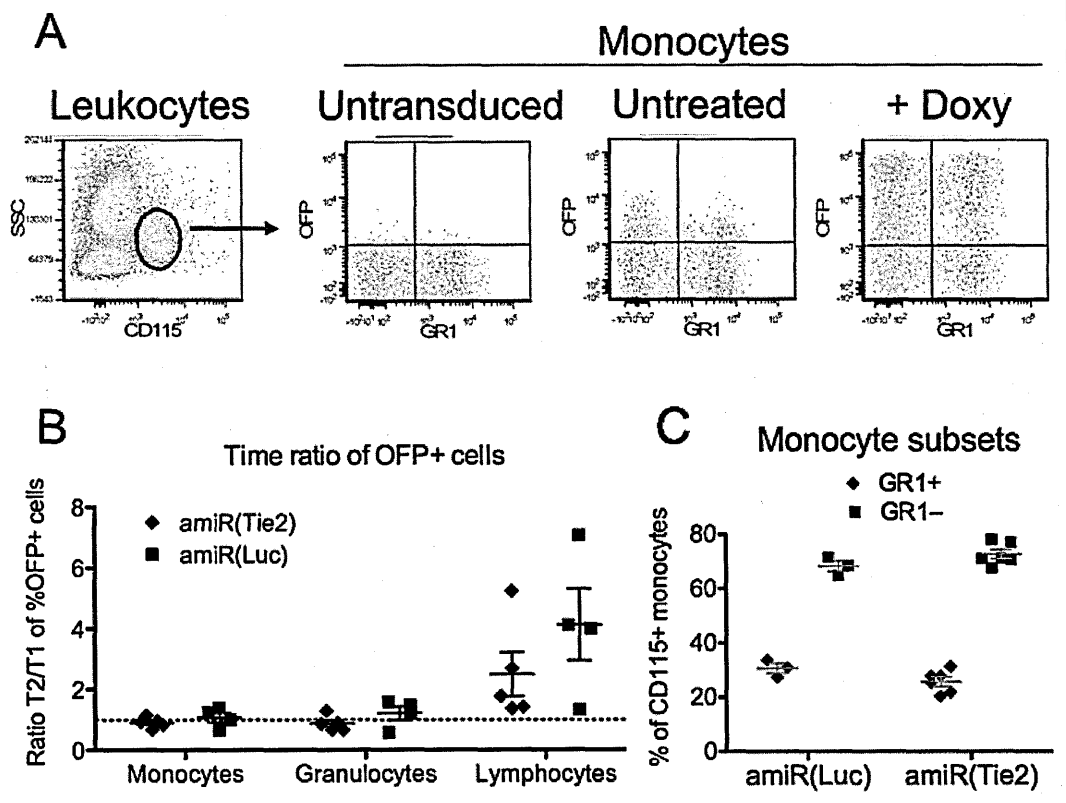

Illustration 29: The conditional gene silencing platform is safe in vivo. A: Representative flow cytometry analysis of OFP in blood monocytes from mice transplanted with LV2-transgenic, BM-Lin⁻ HSPCs transduced with LV1. From left to right: CD115+ monocytes are gated from total viable leukocytes and are further analyzed for GR1 and OFP expression; monocytes from a mouse transplanted with LV2-transgenic, untransduced BM-Lin⁻ HSPCs; mouse transplanted with LV2-transgenic, BM-Lin⁻ HSPCs transduced with LV1 and left untreated (– doxy); mouse transplanted with LV2-transgenic, BM-Lin⁻ HSPCs transduced with LV1 and treated with doxycycline for one week in vivo before analysis (+ doxy; right). B: Flow cytometry analysis of blood leukocyte subsets (monocytes: 7AAD– CD115+; granulocytes: 7AAD– CD115– GR1+; lymphocytes: 7AAD– CD115– GR1–) from amiR(Tie2) and amiR(Luc) mice. The ratio between the percentages of OFP+ cells in the indicated leukocyte subset at T2 (7 weeks after transplant; 3 weeks after doxycycline administration) and T1 (4 weeks after transplant; 1 week after doxycycline administration) is shown. Note that lymphocyte chimerism is not yet complete at 4 weeks after transplant. C: Blood monocyte subsets (inflammatory monocytes: 7AAD– CD11b+ GR1+ CD115+; resident monocytes: 7AAD– CD11b+ GR1– CD115+) in MMTV-PyMT/amiR(Tie2) and MMTV-PyMT/amiR(Luc) mice 3 weeks after doxycycline treatment (7 weeks of age).

since they require at least 6 weeks to develop from donor HSCs. Thus, amiR expression is safe for hematopoietic cells *in vivo*.

As shown in paragraph 7.1, circulating TEMs are *bona fide* resident monocytes. To test if *Tie2* knock down affects monocyte subset ratios, I measured blood monocyte subsets by flow cytometry in amiR(Tie2) and amiR(Luc) mice, 3 weeks after doxycycline treatment (7 weeks of age). I found that *Tie2* knock down did not change the percentages of monocyte subsets (Illustration 29C). Moreover, expression of the amiR(Tie2) did not perturb cell counts and leukocyte composition

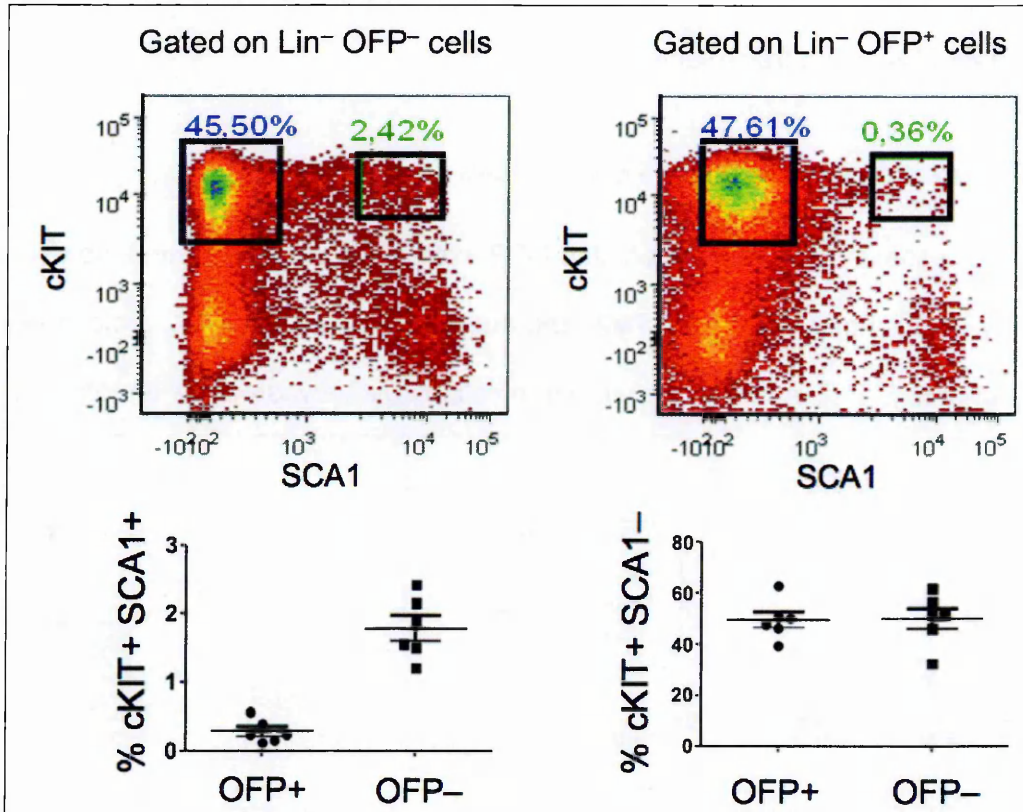

Illustration 30: Efficient de-targeting of amiR expression from BM-Lin⁻ cKIT+ SCA1+ HSCs in vivo. Flow cytometric analyses of cKIT and SCA1 expression in either OFP+ or OFP– BM-Lin⁻ cells obtained from amiR(Tie2) and amiR(Luc) mice 7 weeks after BM-Lin⁻ transplantation and 1 week after the first doxycycline administration. Note that OFP– but not OFP+ BM-Lin⁻ cells contained cKIT+ SCA1+ HSCs at the expected frequency (2-4%), whereas both OFP– and OFP+ BM-Lin⁻ cells contained cKIT+ SCA1– HPCs at the expected frequency (ca. 50%). Error bars in the scatter plots represent SEM (n = 6).

in the blood of transplanted mice (vs. amiR(Luc) mice; data not shown).

To assess if the miR126T-mediated post-transcriptional regulation was effective *in vivo*, I measured OFP expression in BM-Lin$^-$ HSPCs from amiR mice. I found that OFP expression was virtually absent in primitive HSCs, identified as cKIT+ SCA1+ BM-Lin$^-$ cells, but not in cKIT+ HPCs and their prospective progeny (Illustration 30). These data suggest that rtTA is efficiently suppressed in HSCs but not in HPCs, closely recapitulating the expression pattern of miR126.

Overall, these findings indicate robust, safe doxycycline-mediated expression of the amiR/OFP expression cassette in the mature progeny of BM-Lin$^-$ cells, but not *bona fide* HSCs, in the transplanted mice.

9.3 Tie2 knock down in tumor TEMs impairs angiogenesis

In order to assess doxycycline-mediated OFP expression and *Tie2* knock down in TAMs, we challenged both amiR(Tie2) and amiR(Luc) mice with N202 tumor cells subcutaneously. Three weeks post-tumor injection, we harvested the tumors and

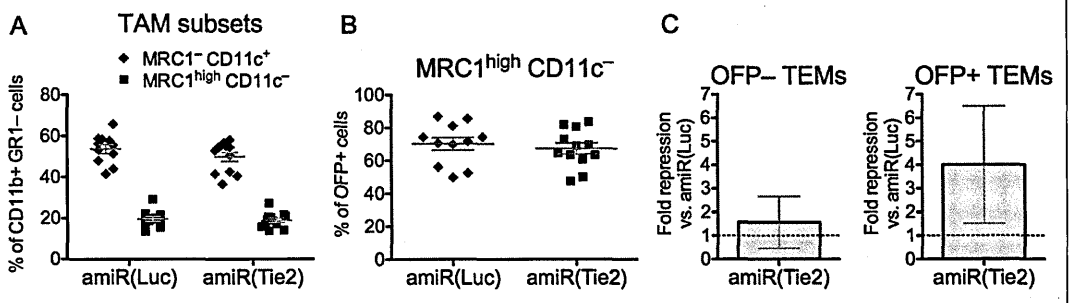

Illustration 31: Efficient conditional Tie2 gene knock down in tumor-infiltrating myeloid cells. Percentages of A: TAM subsets (TEMs: 7AAD– CD11b+ GR1– MRC1high CD11c–; TIE2– TAMs: 7AAD– CD11b+ GR1– MRC1low CD11c+); B: OFP+ cells within TEMs in MMTV-PyMT/amiR(Tie2) and MMTV-PyMT/amiR(Luc) mice at 15.5 weeks of age. C: Conditional Tie2 gene knock down in MRC1high/CD11c– TEMs infiltrating N202 tumors. TEMs from doxycycline-treated amiR(Tie2) mice (fold-change vs. doxycycline-treated amiR(Luc) mice) were fractionated into OFP– (left panel) and OFP+ (right panel) cells. Note that Tie2 is silenced only in OFP+ but not in OFP– TEMs.

measured by flow cytometry the percentages of TAM subsets. As shown in Illustration 31A, the relative amounts of TEMs ($MRC1^{HIGH}$ CD11c–) and TIE2– TAMs ($MRC1^{LOW}$ CD11c+) were unaffected by *Tie2* knock down. Importantly, TEMs from both amiR(Tie2) and amiR(Luc) mice expressed similarly high levels of OFP (Illustration 31B), indicating comparable expression of the amiR in either groups of mice. To quantify the level of *Tie2* gene knock down in TEMs, I isolated the OFP+ and OFP– fractions of TEMs ($CD31^{LOW}$ $MRC1^{HIGH}$ CD11c–) by cell sorting. Statistical modeling of qPCR data (Pucci et al. 2009) showed that the *Tie2* mRNA was specifically knocked-down in the OFP+ TEMs of amiR(Tie2) mice (Illustration 31C; 4-fold vs. OFP+ TEMs of amiR(Luc) mice; $p < 0.01$). These results represent molecular evidence for efficient *in vivo Tie2* gene silencing in tumor-infiltrating TEMs and suggest that *Tie2* gene knock down do not detectably alter TEM recruitment to the tumors.

To study the effects of *Tie2* gene knock down in a model of spontaneous tumorigenesis, I generated MMTV-PyMT/amiR(Tie2) and MMTV-PyMT/amiR(Luc) mice by BM transplantation (2 independent experiments; n = 12-14 mice/group). We treated the mice with doxycycline starting at 4 weeks post-transplant (9.5 weeks of age), when the angiogenic switch and malignant conversion occur in this tumor model (Lin et al. 2006). At 15 weeks of age we euthanized the mice and analyzed tumor angiogenesis by flow cytometry and IFS of frozen sections. I observed significant differences between MMTV-PyMT/amiR(Tie2) and MMTV-PyMT/amiR(Luc) mice. The CD31+ blood vessels of amiR(Tie2) tumors appeared smaller, fewer and less perfused (lectin+) than in the controls (Illustration 32A). To quantify these observations, we measured the CD31+ or lectin+ area in the tumors. Both the relative CD31+ vascular area and the relative lectin+ (perfused) vascular area, measured by IFS of tumor sections, were significantly lower in amiR(Tie2) than amiR(Luc) mice (Illustration 32B). Flow cytometric analyses

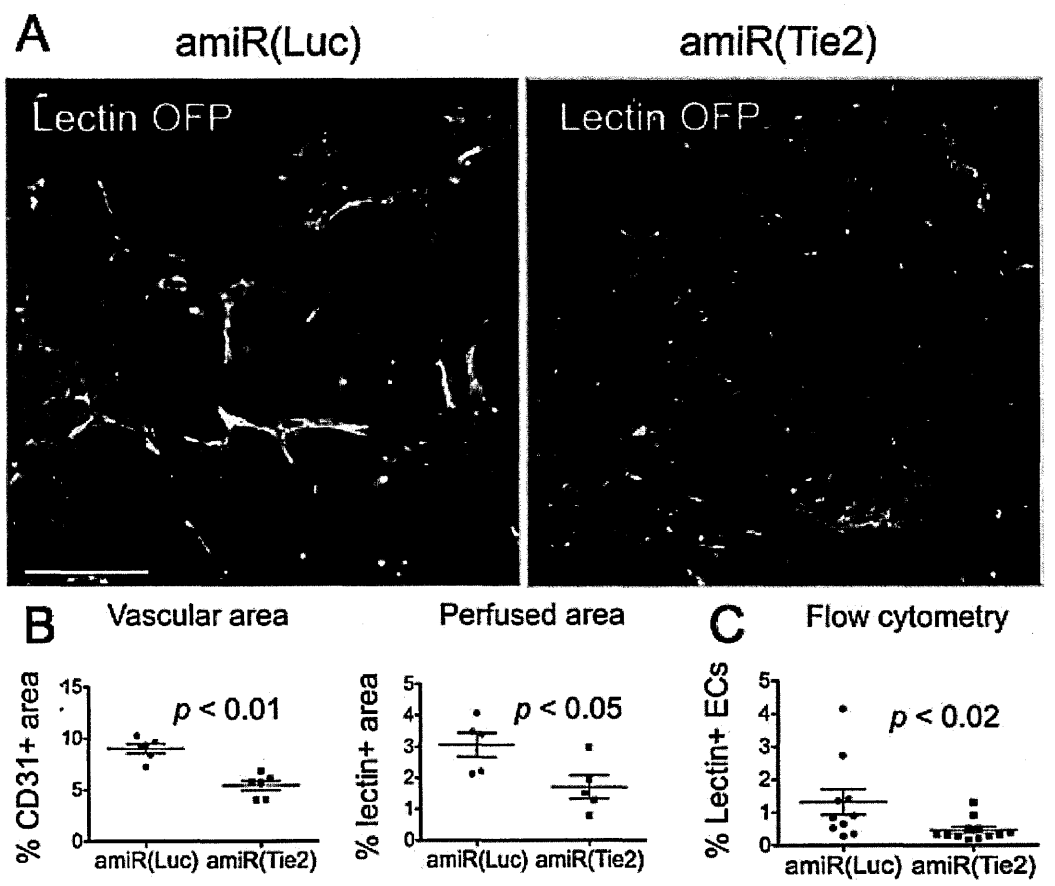

Illustration 32: Conditional Tie2 gene knock down in TEMs inhibits angiogenesis and impairs blood vessel functionality in spontaneous breast tumors. A: Lectin (green), OFP (red) and CD31 (blue) immunostaining of representative tumor sections of MMTV-PyMT mice transplanted with BM-Lin⁻ cells either transduced with amiR(Tie2) or amiR(Luc) LV1 and analyzed at 15 weeks of age. Note the presence of several perfused (lectin+) CD31+ blood vessels in the control, amiR(Luc) tumor; the lectin+ CD31+ blood vessels are fewer in the amiR(Tie2) tumor. Note that abundant OFP+ cells are present in both amiR(Luc) and amiR(Tie2) tumors; Scale bar: 150 μm. Results are representative of 2 independent experiments and 10 tumors/group analyzed. For each tumor, multiple sections (3-5) were analyzed. B: Morphometric analyses of the vascular and perfused tumor area in sections obtained from same tumors as in A. C: Flow cytometry analysis of lectin+ CD31+ CD45– ECs in same tumors as in A. Each dot in B and C indicates one individual tumor analyzed; for each tumor, multiple sections (3-5) were analyzed. Scatter plots show mean values ± SEM. Statistical analyses by Mann-Whitney U test. Results combine 2 independent experiments.

confirmed the lower frequency of lectin+ CD31+ CD45– ECs in the tumors of amiR(Tie2) mice (Illustration 32C). I observed decreased angiogenesis also in FVB/amiR(Tie2) mice challenged with subcutaneous N202 mammary tumors (data not shown).

I noted that the distribution of OFP+ and OFP– tumor-infiltrating cells differed in MMTV-PyMT/amiR(Tie2) and MMTV-PyMT/amiR(Luc) mice. Indeed, there were fewer OFP+ (i.e., *Tie2* knocked-down) cells associated with perfused (lectin+ CD31+) tumor blood vessels in amiR(Tie2) than amiR(Luc) mice (Illustration 33A), whereas similar amounts of OFP+ cells surrounded the non-perfused (lectin– CD31+) immature vessels in either group of mice. These findings suggest that the association of OFP+ myeloid cells (i.e. *Tie2* knocked-down TEMs) with newly

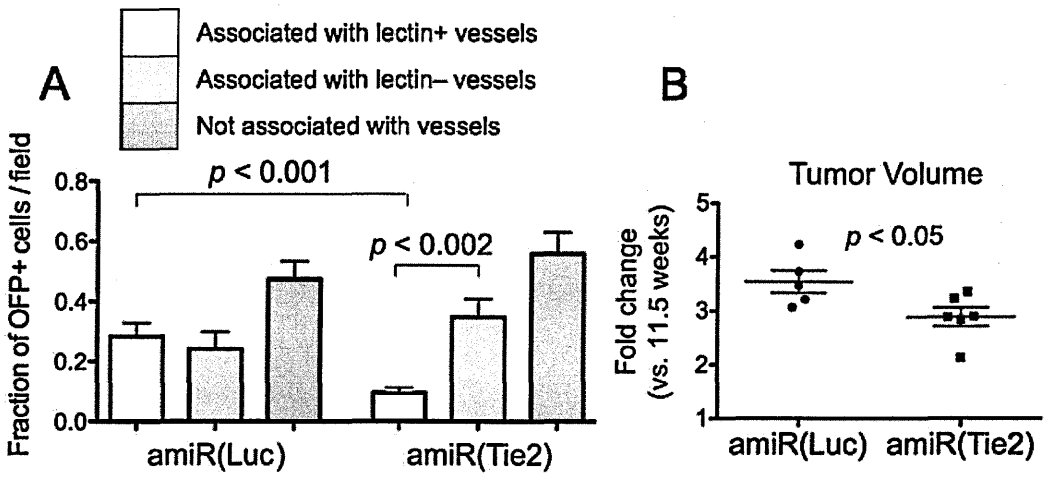

Illustration 33: A: Morphometric analysis of OFP+ cells and their association with CD31+ or lectin+ CD31+ blood vessels in tumors of MMTV-PyMT mice transplanted with BM-Lin⁻ cells either transduced with amiR(Tie2) or amiR(Luc) LV1 and analyzed at 15 weeks of age. Results combine 2 independent experiments. 611 individual OFP+ cells from 10-11 digital images/group acquired at x200 magnification were scored, and their association with blood vessels analyzed. Bars show mean value ± SEM. Digital images were obtained from 5-6 tumors from 2 independent experiments. B: Mammary tumor growth (mean volume ± SEM at 14.5 weeks of age, shown as fold-change vs. tumor volume at 11.5 weeks of age in each individual mouse) by MRI-based volumetry of the 10 mammary glands. One experiment is shown. Statistical analyses in A and B by Mann-Whitney U test.

forming blood vessels impeded their maturation to functional (i.e., perfused) tumor blood vessels. It should be noted that the frequency of OFP+ TEMs ranged from 50% to 90% in the tumors of both amiR(Tie2) and amiR(Luc) mice (Illustration 31B on page 68), indicating that *Tie2* gene knock down occurred in the majority but not all tumor-infiltrating hematopoietic cells. Nevertheless, *Tie2* gene silencing in TEMs produced statistically significant tumor growth inhibition in 1 of the 2 independent experiments performed (26% inhibition measured by MRI-based volumetry at 11.5 and 14.5 weeks of age; $p < 0.05$; Illustration 33B), supporting the relevance of the observed vascular changes. In summary, *Tie2* knock down by RNAi reduced tumor angiogenesis and blood vessel functionality in MMTV-PyMT spontaneous breast tumors. Thus, TIE2 represents a crucial effector of the pro-angiogenic activity of TEMs.

Discussion

10 TEMs are distinct from ECs

Our gene expression data demonstrate that TEMs are distinct from endothelial-lineage cells and represent a subset of tumor infiltrating macrophages expressing a distinguishing gene signature, which is consistent with enhanced pro-angiogenic and tissue-remodeling activity and lower pro-inflammatory activity. The carefull choice of surface markers which made it possible to highly purify TEMs was instrumental in the identification of their gene expression signature. In particular, a negative selection marker for ECs was crucial to avoid EC contamination in the TEM preparation. This apparent link between TEMs and ECs can be explained by the reported close association of TEMs with blood vessels (De Palma et al. 2003).

Several studies have reported that mononuclear cells expressing a reporter gene from *Tie2* transcription regulatory elements are recruited to tumors and ischemic tissues (De Palma et al. 2003; Asahara et al. 1997; Ahn & Brown 2008). Based on the assumption that *Tie2* expression is specific for ECs, these TIE2+ cells were often interpreted as EPCs, even if they expressed hematopoietic or myeloid markers (Modarai et al. 2005) and were often found outside of the vessel wall (Asahara et al. 1999). By implementing stringent combinations of gene marking and imaging approaches, previous work from our lab showed that these TIE2+ mononuclear cells indeed represent myeloid cells (De Palma et al. 2005). Here, I conclusively demonstrate that *Tie2* expressing cells recruited to tumors do not belong to the EC lineage and are *bona fide* monocytes/macrophages. By comparing tumor-derived TEMs, TAMs and ECs, I show that the gene expression profile of TEMs is similar to that of TAMs but clearly distinct from that of ECs. Further data support the non-EC nature of TEMs. Indeed, TEMs (i) robustly

express hematopoietic-specific markers (e.g. CD45, F4/80 and miR-142, the latter shown by using a microRNA-regulated reporter transgenic mouse line); (ii) express low-to-negligible levels of EC-specific genes (e.g. *Vegfr2* and VE-Cadherin/*Cdh5*); (iii) do not incorporate in the tumor endothelium and often reside in perivascular spaces. These findings strongly support the notion that BM-derived *Tie2* expressing cells repeatedly observed in tumors are not EPCs. Whether true EPCs contribute to tumor angiogenesis is still a matter of debate, with recent reports showing a contribution limited to selected experimental conditions, such as tumors treated by vascular-disrupting agents or chemotherapy (Shaked et al. 2008).

11 Overlapping function and phenotype between TEMs and other mononuclear subsets

Although TEMs do not physically incorporate in the tumor endothelium, they seem required for tumor angiogenesis (De Palma et al. 2007). Within the panel of interrogated genes, many genes previously implicated in tumor angiogenesis were among the most differentially expressed between TEMs and TAMs. One such gene is *Lyve1* (14-fold up), which encodes for the hyaluronan receptor-1 expressed on lymphatic ECs and subsets of macrophages. Because TEMs also express *Stab1* (stabilin-1, a hyaluronan receptor (Politz et al. 2002); 6.4-fold up) and *Cd163* (hemoglobin/haptoglobin scavenger receptor; 15.8-fold up), it is likely that the previously described LYVE1+ STAB1+ CD163+ macrophages observed in tumors, wounds, placenta and remodeling adipose tissue (Schledzewski et al. 2006; Cho et al. 2007; Böckle et al. 2008), indeed represent TEMs. In these reports, a common feature of the described LYVE1+ STAB1+ CD163+ macrophages is the juxtaposition with sprouting ECs, which suggests a functional role as cellular chaperones for endothelial tip cells (Fantin et al. 2010).

In the last months, a very interesting paper reported that the tumor microenvironment hosts functionally distinct TAM subsets (Movahedi et al. 2010). The Authors identified 2 subsets among CD11b+ F4/80+ TAMs based on MHC-II expression. MHC-II^{LOW} TAMs have striking similarities with TEMs when compared with the other TAM subset (MHC-II^{HIGH} TAM and TIE2– TAMs respectively); indeed both 1) show a superior pro-angiogenic activity; 2) share the same gene expression signature (high levels of *Lyve1*, *Cd163*, *Stab1*, *Mrc1*, *Arg1*, *Il4ra*, and low levels of *Mhc-II* (alias *H2-Ea*), *Il1b*, *Nos2*, *Ptgs2*, *Ccl5*, *Cxcl10*, *Cxcl11)*; 3) can be distinguished from the other respective subset by the same surface marker profile (MRC1+ CD11c– MHC-II^{LOW}); 4) are bigger (as measured by light scatter); 5) accumulate during progression of several cancer. Unfortunately, the Authors did not find differences in *Tie2* expression levels between MHC-II^{LOW} and MHC-II^{HIGH} TAMs. It is very likely that, since the FACS panel employed by the Authors to isolate the TAM subsets did not include a negative selection marker for ECs (which express high levels of *Tie2*), a small contamination of ECs in both MHC-II^{LOW} and MHC-II^{HIGH} TAMs may have masked the difference in expression of *Tie2*. Still, an independent lab fully reproduced and expanded my work on TAM subsets.

12 Functional considerations

The identification of a TEM gene signature allows us to formulate some hypotheses on the molecular mechanisms of TEM pro-angiogenic activity.

12.1 Extra-cellular matrix and TEMs

As stated before, *Lyve-1* and *Stab1* are up-regulated in TEMs. *Tlr4*, a toll-like receptor implicated in tumorigenesis (Chen et al. 2008), is also preferentially expressed by TEMs (3.5-fold up). Whereas LYVE1 and STAB1 binds hyaluronic acid (HA), TLR4 binds to its low-molecular weight fragmentation products (Termeer

et al. 2002; Politz et al. 2002). Interestingly, *Tlr4* expression by macrophages has been found to mediate remodeling of the lung microenvironment and favor subsequent colonization by tumor cells (Hiratsuka et al. 2008). Moreover, HA fragments stimulate MMP production, cell migration and angiogenesis in tumors (Toole 2004), and up-regulate *Irak-M* expression by monocytes, deactivating them and down-regulating their expression of the anti-angiogenic molecules *Tnfa* and *Il12a* (del Fresno et al. 2005). The preferential expression of *Lyve1, Stab1* and *Tlr4* by TEMs among tumor macrophages suggests a role of TEM-HA interactions in tumor angiogenesis (Genasetti et al. 2008).

12.2 Soluble mediators

Another gene upregulated in TEMs is *Cxcl12* (4.4-fold up), encoding for the stromal cell derived factor-1 (SDF1). SDF1 released by TEMs may promote angiogenesis by attracting CXCR4+ ECs and other pro-angiogenic cells in the tumor microenvironment (Petit et al. 2007). Interestingly, unpublished work from our lab indicates that ANG2 neutralization by a novel ANG2-specific monoclonal antibody (Brown et al. 2010) impedes the transcriptional up-regulation of *Cxcl12* in tumor-infiltrating TEMs (Pucci, Mazzieri). Thus, it is possible that the TEM specific expression of *Cxcl12* may increase their ability to support tumor blood vessel morphogenesis in an ANG2-dependent manner.

Angpt1 (angiopoietin-1, a Tie2 ligand; 2.6-fold up) expressed by TEMs may also promote tumor angiogenesis, as Angpt1-expressing hematopoietic cells stimulate EC sprouting in embryonic tissues (Takakura 2006).

Interestingly, the CXC chemokines *Cxcl10* and *Cxcl11* were down-regulated in TEMs (2.8- and 2.7-fold down, respectively). These chemokines are transcribed upon Irf3/Stat1 activation and are potent inhibitors of angiogenesis (Strieter et al. 2005). Overall, the enhanced expression of several pro-angiogenic molecules by

TEMs, together with the down-regulation of potent anti-angiogenic mediators (also including *Il12a*, 3.6-fold down; *Il12b*, 2.5-fold down; *Tnfa*, 3.1-fold down), may account for their non-redundant pro-angiogenic activity in tumors (De Palma et al. 2007).

12.3 TEMs as cellular chaperones

Vegfa, which is among the most expressed genes in TEMs, was however down-regulated in TEMs vs. TAMs (2.9-fold down). This apparent paradox can be explained by taking into consideration the preferential localization of TEMs in peritumoral areas and their exclusion from necrotic, avascular regions (De Palma et al. 2005), suggesting that TEMs are exposed to a less hypoxic microenvironment in tumors. Of note, the targeted deletion of *Vegfa* alleles in all myeloid cells (including TAMs) did not decrease the overall amounts of VEGFA expressed in the tumors and failed to inhibit tumor angiogenesis and growth (Stockmann et al. 2008). These results may thus challenge the notion that TAMs represent a non-redundant source of VEGFA in experimental tumors and that the cellular localization may be more crucial then the total amount of VEGFA. Indeed, it is likely that TEMs exert a requisite pro-angiogenic function by supporting tumor blood vessel morphogenesis downstream to VEGF-induced vascular activation and EC tip formation. One can envision that TIE2 expression by TEMs regulates blood vessel formation in tumors by non-canonical angiogenic mechanisms, such as cell-to-cell adhesive interactions (Illustration 34 on page 83). Indeed, the finding of a poor association between Tie2 knocked down (i.e., OFP+) TAMs and functional (i.e., lectin+) tumor vessels in MMTV-PyMT tumors supports this view. Such scenario is in agreement with a recent study that shows that perivascular, TIE2+ macrophages physically interact with the tip cells of nascent blood vessels, which also express TIE2, and are essential to promote vascular anastomosis

during embryonic development (Fantin et al. 2010). Furthermore, it was previously shown that, during embryonic development, TIE2 expression by hematopoietic cells promotes their adhesion to TIE2+ ECs, and that such interaction stimulates angiogenesis in para-aortic splanchnopleural mesoderm explant cultures (Takakura et al. 1998).

12.4 Miscellanea

The expression of *Nrp1* (Neuropilin-1, a VEGF co-receptor; 4.6-fold up) by TEMs might enhance angiogenesis by clustering VEGF in contact with VEGFR2+ ECs, as previously described (Takakura 2006). *Efnb2* (Ephrin-B2; 4.2-fold up) encodes a transmembrane ligand of Ephrin receptors expressed on ECs; the bidirectional signaling between ephrin-B2 and Ephrin receptors modulates angiogenesis and the development of arteries and veins (Carmeliet & Tessier-Lavigne 2005). Semaphorin 6D (*Sema6d*; 5.2-fold up), a transmembrane protein that binds to membrane-bound PlexinB1, may also have pro-angiogenic activity in tumors, as it activates VEGFR2-mediated signal transduction (Neufeld & Kessler 2008). The enhanced expression of *Nrp1*, *Efnb2* and *Sema6d* by TEMs may suggest activation of ECs by cell-to-cell contacts.

TEMs display up-regulated expression of *Edg1* (sphingosine-1-phosphate receptor; 3.0-fold up). *Edg1* null embryos are hemorrhagic and die *in utero*, a phenotype associated with impaired vascular maturation and defective recruitment of perivascular cells to angiogenic blood vessels (Liu et al. 2000). Moreover, sphingosine-1-phosphate induces macrophages to acquire an anti-inflammatory phenotype (high *Arg1*, low *Nos2* activity (Hughes et al. 2008)), which is consistent with TEM phenotype.

13 TEM precursors

Both mouse and human monocytes can be grouped into functional subsets (Geissmann et al. 2010). I found that circulating TEMs belong to the GR1– CD62L– CD43+ resident monocyte subset. In addition to previous data from our lab showing that TEMs are pro-angiogenic (De Palma et al. 2005; De Palma et al. 2007), a recent report indicated that resident monocytes promote tissue angiogenesis in the post-ischemic myocardium (Nahrendorf et al. 2007). Together, these data may suggest a developmental and functional relationship between circulating resident monocytes and tumor-infiltrating TEMs. New findings described here further show that resident monocytes isolated from the blood of tumor-free mice and tumor-derived TEMs display a coordinated expression profile, which points to a commitment of TEM phenotype/function in the peripheral blood. *Arg1*, *Cxcl12*, *Lyve1*, *Igf1*, *Stab1*, *Cd163, Mrc1* and *Edg1*, all significantly up-regulated in tumor-derived TEMs vs. TIE2– TAMs, were markedly up-regulated in resident vs. inflammatory monocytes. Expression of *Il12a* (an anti-angiogenic molecule) was down-regulated in TEMs vs. TIE2– TAMs but unexpectedly up-regulated in resident vs. inflammatory monocytes. However, two recent reports have shown that both mouse and human resident monocytes rapidly down-regulate *Il12* expression upon their extravasation *in vivo* (Auffray et al. 2007) or when exposed *in vitro* to experimental conditions mimicking the hypoxic tumor microenvironment (Murdoch et al. 2007). The coordinated expression profiles of resident monocytes/TEMs and inflammatory monocytes/TIE2– TAMs suggest that monocyte heterogeneity in the peripheral blood may reflect the existence of precursor populations that are committed to distinct, non-redundant functions in tumors and growing/regenerating tissues. Of note, this commitment is present even in the absence of tumor burden, as monocyte subsets were isolated from

tumor-free mice.

The developmental relationship between the two main monocyte subsets remains to be clarified. It has been proposed that resident monocytes derive from GR1+ inflammatory monocytes (Varol et al. 2007), implying that the two phenotypes may represent distinct developmental stages along the monocyte lineage. However, neither a genetic defect in nor antibody-mediated depletion of GR1+ monocytes affected the generation of GR1– monocytes (Mildner et al. 2007; Alder et al. 2008; Scatizzi et al. 2006), suggesting that a direct developmental pathway from a multipotent precursor to GR1– monocytes may exists (Yona & Jung 2010). Therefore, a better characterization of monocyte precursors and new lineage tracking studies will be needed to establish the developmental relationship between monocyte subsets and to clarify whether TEMs represent a distinct resident monocyte subset.

Taken together, our findings suggest that TEMs represent a circulating reservoir of monocytes actively recruited to extra-vascular tissues by non-inflammatory signals produced not only by tumors, but also by developing or regenerating tissues. Future studies will identify the signals that govern the lineage determination of TEMs and their recruitment to sites of active tissue morphogenesis. Live imaging analysis (Egeblad et al. 2008) of monocyte/macrophage subsets expressing the newly identified cell surface markers (e.g. MRC1, CD11c, LYVE1, TLR4, MHC-II) may better clarify macrophage heterogeneity and dynamics in tumors.

14 Role of TIE2 in TEMs

To knock down Tie2 in BM-derived hematopoietic cells, I developed a novel gene knock-down platform that effectively protects the hematopoietic compartment from potential toxicity consequent to Tie2 silencing in HSCs. Indeed, our previous

attempts to knock down Tie2 using constitutive LVs did not allow for efficient and stable gene silencing in BM-derived cells because of counter selection of transduced cells. By using inducible LVs and HSC de-targeting, I demonstrated that Tie2 knock-down in BM-derived cells significantly inhibited angiogenesis and microvascular perfusion in MMTV-PyMT mice, but did not affect hematopoiesis detectably. Remarkably, by targeting the TIE2 receptor in TEMs, I recapitulated several features of TEM elimination (De Palma et al. 2005), including: 1) reduced, although not drastically, tumor growth; 2) decrease in tumor vascular area; 3) unaltered myeloid cell infiltration in tumors. Together, these results suggest that TIE2 is a pivotal biological effector and therapeutic target in TEMs.

TIE2 is expressed at very low level in circulating monocytes, but is strongly upregulated (up to 100-fold) specifically in perivascular TEMs (De Palma et al. 2008). Unpublished work from our lab indicates that ANG2 neutralization by a novel ANG2-specific monoclonal antibody (Brown et al. 2010) impedes the transcriptional up-regulation of Tie2 in tumor-infiltrating TEMs (Pucci, Mazzieri). By using a conditional genetic knock down strategy, I show here that the up-regulation of the TIE2 receptor in peri-vascular TEMs is required for the functional maturation of angiogenic blood vessels. ANG2 may thus signal both autocrinally on ECs (Augustin et al. 2009) and juxtacrinally on peri-vascular, TIE2+ macrophages, the latter scenario being supported by experimental evidence that ANG2 agonistically enhances the pro-angiogenic activity of human blood-derived TIE2+, but not TIE2– monocytes in vitro (Coffelt et al. 2010b). One can envision that ANG2 expression by angiogenic blood vessels (such as those of expanding tumors or developing tissues) mediates a self-reinforcing signal on peri-vascular TEMs via the up-regulation of the TIE2 receptor, and that such feedback may be essential for the execution of productive angiogenesis (Illustration 34 on page 83). Although it cannot be excluded that TIE2 up-regulation in TEMs is mediated indirectly by

ANG2, the specific modulation of the Tie2 mRNA among other angiogenic genes observed in TEMs upon ANG2 blockade (Pucci, Mazzieri, unpublished data) supports the view that this response is intimately linked to TIE2 signalling. Of note, several growth factors – including ANGs – can regulate the expression of their receptor tyrosine kinases at the transcriptional level via auto-regulatory feedback loops (Hashimoto et al. 2004).

Tie2 silencing in TEMs, although consistently inhibiting angiogenesis and tumor vessel function by almost 50%, did not reproducibly inhibit tumor growth in MMTV-PyMT mice. In this regard, previous reports have shown that the genetic deletion of pro-angiogenic factors in ECs or myeloid cells may reduce angiogenesis in tumors without decreasing tumor growth rates (Nasarre et al. 2009; Stockmann et al. 2008). It should be noted that in my Tie2 silencing studies, as a consequence of the chimeric nature of repopulating cells in a BM transplantation setting, a significant proportion of the tumor blood vessels were surrounded by enough TIE2-competent (OFP–) TEMs to enable sufficient blood vessel growth and consequent tumor perfusion in the tumors of amiR(Tie2) mice, thus allowing for unimpeded tumor growth. Thus, it cannot be excluded that fully exhaustive Tie2 targeting in tumor-infiltrating macrophages would impair angiogenesis and tumor vessel functionality to an extent critical for tumor oxygenation, nourishment and growth.

In summary, *Tie2* gene silencing data indicate that the TIE2 receptor expressed by peri-vascular TEMs is a critical regulator of ANG2-mediated pro-angiogenic programs in tumors (Illustration 34 on page 83). Because tumor infiltrating myeloid cells are known to convey pro-tumoral and pro-angiogenic programs that can counteract the efficacy of anti-angiogenic treatments (Bergers & Hanahan 2008), the combined targeting of angiogenic ECs and pro-angiogenic TAMs by selective ANG2/TIE2-pathway inhibitors may significantly extend the reach of anti-

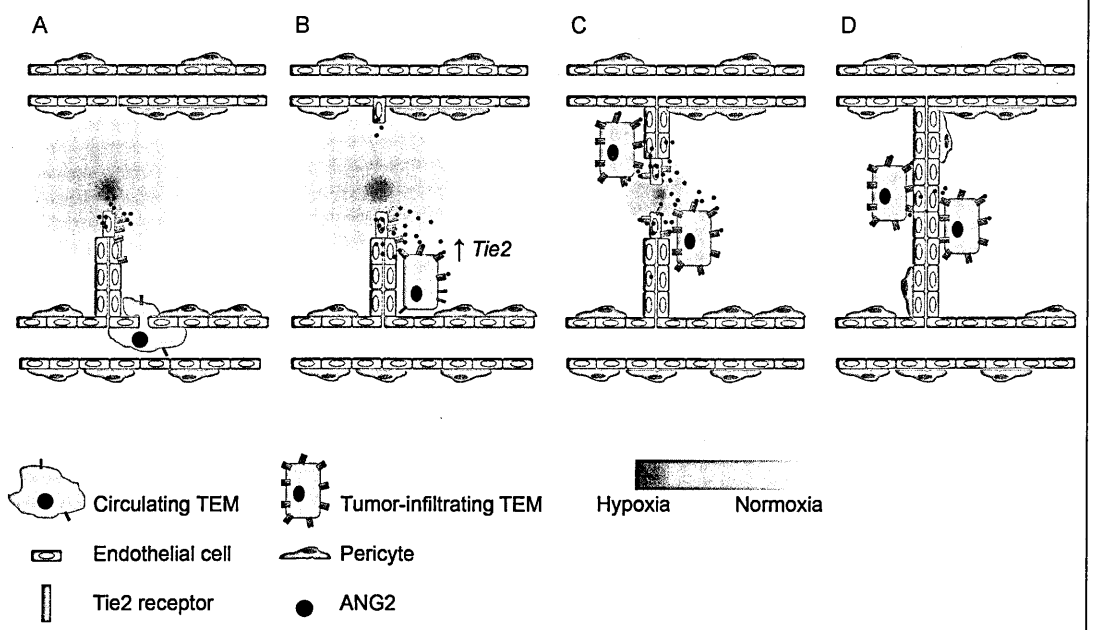

Illustration 34: Model of ANG2-TIE2 interactions modulating the pro-angiogenic activity of TEMs. Circulating TEMs express low-level TIE2, but the receptor is up-regulated upon their extravasation in the tumor microenvironment. Once in the tumor stroma, TEMs adhere to sprouting blood vessels, which secrete high-level ANG2. In the presence of ANG2, TEMs promote vascular growth and anastomosis. Upon genetic knock-down of Tie2, TEMs fail to promote vascular morphogenesis. Because blocking ANG2-TIE2 interactions in TEMs phenocopies the anti-angiogenic effects obtained by depleting TEMs, it is suggested here that the ANG2-TIE2 signaling axis mediates juxtacrine interactions between TEMs and ECs that are required for sprouting angiogenesis.

angiogenic therapy in cancer patients.

Appendix – RNA interference

15 The micro-RNA world

RNA interference (RNAi) is endogenously mediated by microRNA (miR), 21–24 nucleotides non-coding RNA which fine-tunes expression of a large numbers of target genes (Bartel 2004). miRs are generated from primary transcripts (pri-miRs) generally transcribed from polymerase-II (Pol-II) promoters. The genomic location of pri-miRs normally is an intronic sequence of either a coding or non-coding gene, or an intergenic region (Morlando et al. 2008). Pri-miRs are processed in the nucleus by Drosha, an RNase III like enzyme, to ~60–70 nucleotides stem–loop molecules with two-nucleotide 3′ overhangs (pre-miR) (Illustration 35). Drosha cleavage occurs during transcription acting on both independently transcribed (intergenic) and intron-encoded miRNAs (Morlando et al. 2008). Pre-miRs are shuttled by exportin-5, a Ran-GTPase, to the cytosol where Dicer, another RNase III like enzyme, releases a 21–24 double-stranded RNA from the stem. This is loaded into the RNA-induced silencing complex (RISC), which generally selects one of the two strands as the guide strand (mature miR), according to thermodynamic properties. RISC targets mRNA with complementary sequence to the miR and down-regulates their expression decreasing transcript translation and stability by a variety of molecular mechanisms (Eulalio et al. 2008). Because most miR::mRNA pairing in mammalian cells is not perfect, direct RISC-dependent mRNA cleavage is unusual.

16 Exploiting RNAi

RNAi has proven essential for gene function studies and holds promise for the development of new molecular medicines (Chang et al. 2006; Kim & Rossi 2007).

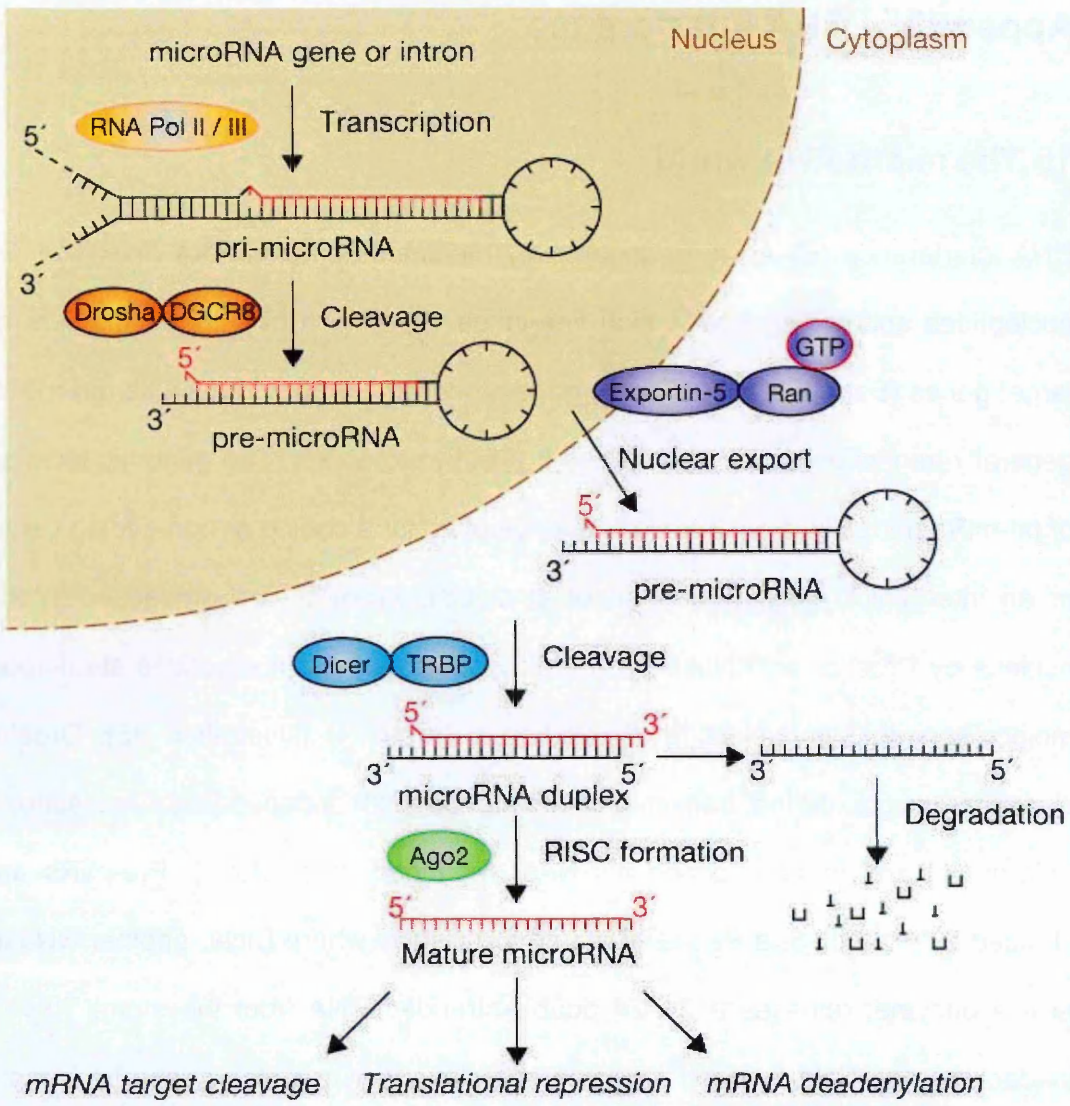

Illustration 35: The miRNA processing pathway. The vast majority of primary miRNA transcripts (pri-miRNA) are synthesized by RNA polymerase II and then cleaved by the microprocessor complex Drosha–DGCR8 (Pasha) in the nucleus. The resulting precursor hairpin, the pre-miRNA, is exported from the nucleus by Exportin-5–Ran-GTP. In the cytoplasm, the RNase Dicer in complex with the double-stranded RNA-binding protein TRBP cleaves the pre-miRNA hairpin to its mature length. The functional strand of the mature miRNA is loaded together with Argonaute (Ago2) proteins into the RNA-induced silencing complex (RISC), where it guides RISC to silence target mRNAs through mRNA cleavage, translational repression or deadenylation, whereas the passenger strand (black) is degraded. From Winter et al. Nat Cell Biol 2009.

Several hurdles still prevent full exploitation of the biological and therapeutic potential of RNAi. Selection of an efficient siRNA sequence still requires empirical

validation, and safe and effective delivery of RNAi molecules remains an active area of investigation (McBride et al. 2008; Li et al. 2007). RNAi off-target effects result from one of three mechanisms: 1) stretches of dsRNA can activate non-specific cellular innate immune responses, such as the interferon and toll-like response (Bridge et al. 2003; Fish & Kruithof 2004; Kleinman et al. 2008); 2) saturation of the cell RNAi machinery and thereby inhibit the function of endogenous miRNAs (Grimm et al. 2006); 3) complementarity to other, non-target mRNAs (Birmingham et al. 2006). Ongoing efforts aim to identify which approach guarantees the best balance between efficacy and off-target effects, toxicity and which expression cassette and delivery vehicle best fit the requirements of stable RNAi delivery (Kim & Rossi 2007). Commonly siRNA are transiently delivered to target cells by transfection approaches, a constraint that limits the possible applications. Hence, other strategies have been pursued to express RNAi precursors from within the target cells. Short hairpin RNA mimic the pre-miR structure and require Dicer processing in order to be functional. A crucial advantage is the possibility to use polymerase-III promoters for high-level expression and stable gene knockdown (Brummelkamp et al. 2002). Although polymerase-III promoters have also been engineered for inducible expression (Szulc et al. 2006), they lack the tissue and developmental specificity of Pol-II promoters. Furthermore, concerns about the potential toxicity of this approach have been reported due to the possible saturation of miR processing steps and consequent interference with endogenous miR regulation (Kleinman et al. 2008; Grimm et al. 2006).

Artificial miRs (amiRs) are natural pri-miR in which the stem sequence of an miR has been substituted with a sequence targeting the gene of interest. In target cells, amiR undergoes the same processing steps of the parental pri-miR (Zeng et al. 2002). Importantly, amiR can be also transcribed by Pol-II promoters, like

endogenous pri-miR, which allows exploitation of state-of-the-art gene expression cassettes and may alleviate concerns for over-expression (Boudreau et al. 2009). Although many examples in the literature of functional amiR and many of the details for making amiR have been worked out, the choice of an optimal pri-miR backbone for robust and versatile amiR expression and the criteria for its validation are still actively pursued (Aagaard et al. 2008; Ely et al. 2009; Chung et al. 2006). In order to co-express RNAi and a selector or therapeutic gene, amiRs have been introduced into the 5′- or 3′-untranslated region (UTR) of the transgene (Stegmeier et al. 2005). This modification, while improving amiR expression, impairs expression of the linked transgene. More recently, amiRs were inserted within an intron to maintain expression of the transgene unaltered (Chung et al. 2006). However, these features of the expression cassette may interfere with delivery by γ-retroviral and lentiviral vectors (LVs), the preferred systems for stable expression in proliferating cells and tissues. Thus, optimization of vector design is still required to perform knock down studies in challenging settings, such as primary cells.

Material and methods

17 Transgenic mice

FVB mice were purchased from Charles River Laboratory (Calco, Milan, Italy). FVB/Tie2p/e-GFP and FVB/Pgk-rtTA-miR-126T transgenic mice were previously generated by lentiviral vector (LV)-mediated transgenesis and established as a colony in 2003 at the San Raffaele animal facility (De Palma et al. 2005). FVB/MMTV-PyMT mice were obtained from the NCI-Frederick Mouse Repository (MD) and established as a colony at the San Raffaele animal facility. Five to 6-week–old female MMTV-PyMT mice were transplanted with BM cells from Tie2p/e-GFP mice, as described (De Palma et al. 2008), and the tumors analyzed 4 or 6 weeks after the transplant. Transgenic mice were screened by qPCR of vector sequences. Tie2p/e-GFP transgenic mice had LV copy number ranging from 5 to 10 LV copies/cell. All animal procedures were performed according to protocols approved by the Animal Care and Use Committee of the Fondazione San Raffaele del Monte Tabor and communicated to the Ministry of Health and local authorities according to the Italian law.

18 Lentiviral vectors

To generate the rtTA-m2 encoding vector (LV2), I cloned four tandem copies of a 21-bp sequence with perfect complementarity to miR-126 (mir-126T) downstream to a PGK-GFP LV, as previously described (Brown et al. 2006). I then replaced the GFP sequence with the rtTA-m2 cDNA, to obtain the PGK-rtTA-m2-mir-126T LV. To generate the amiR encoding vectors (LV1), I replaced the EF1a core promoter of the EF1a-amiR(Tie2)-NGFR and EF1a-amiR(Luc)- NGFR LVs (Amendola et al. 2009) with a tetracycline-responsive element (TRE)-containing promoter, and

further replaced NGFR with OFP, to obtain the TRE-amiR(Tie2)-OFP and TRE-amiR(Luc)- OFP LVs, respectively. In these vectors, the amiR sequence is lodged in the EF1a intronic sequence downstream to the TRE-containing promoter. The siRNA sequences used are: amiR223(Tie2), 5′-TTTGCCCTGAACCTTATAC CG-3′; amiR155(Tie2): 5′-TACAGGTCCTGCCAAATGTGT-3′; amiR223(Luc), 5′-TATTCAGCCCA TATCGTTTCA-3′; amiR155(LacZ), 5′-AAATCGCTGATTTGTGTAGTC-3′. The LVs used in this study and cloning strategy used for their construction will be available upon request. Concentrated VSV.G pseudotyped, third-generation LV stocks were produced and titred as described previously (De Palma & Naldini 2002).

19 Hematopoietic stem/progenitor cell (HSPC) isolation, transduction and transplantation

Six to 12-week–old female FVB/PGK-rtTA-miR-126T (LV2) transgenic mice were killed with CO_2 and their BM was harvested by flushing the femurs and the tibias. Lineage-negative cells (BM-Lin$^-$ cells) enriched in HSPCs were isolated from BM using a cell purification kit (StemCell Technologies) and transduced by concentrated LVs. Briefly, 10^6 cells/ml were prestimulated for 4-6 hours in serum-free StemSpan medium (StemCell Technologies) containing a cocktail of cytokines (IL-3 (20 ng/ml), SCF (100 ng/ml), TPO (100 ng/ml) and FLT-3L (100 ng/ml), all from Peprotech) and transduced with amiR-expressing LVs (LV1) with a dose equivalent to 10^8 LV Transducing Units/ml, for 12 hours in medium containing cytokines. After transduction, 10^6 cells were infused into the tail vein of lethally irradiated, 5.5-week–old, female FVB or FVB/MMTV-PyMT mice (radiation dose: 1150 cGy split in 2 doses). To induce the expression of the amiR(Tie2) and OFP, the transduced cells were cultured in vitro for 2 days in the presence or absence of doxycycline (1 µg/ml; Sigma). Transduced cells were also cultured for 5 days to

measure OFP expression by flow cytometry, or for 9 days to measure the number of integrated LV copies/cell genome.

19.1 In vivo doxycycline administration

Starting at 4 weeks after HSPC transplant (i.e., at 9.5 weeks of age), FVB or MMTV-PyMT mice were moved to doxycycline-containing food (Charles River) and received intra-peritoneal injections of doxycycline (0.5 mg/mouse) every third day, until the end of the experiments (12.5 weeks of age for FVB and 15 weeks of age for MMTV-PyMT mice).

19.2 Magnetic Resonance Imaging (MRI)

MRI examinations of MMTV-PyMT transgenic mice were performed on a 3.0 Tesla human scanner (Achieva 3T, Philips Medical Systems, the Netherlands), equipped with 80 mT/m gradients and a 40 mm volumetric coil (Micro-Mouse 40, Philips Medical Systems, the Netherlands). The mice were anaesthetized with Avertin and maintained on Sevoflurane (2% for maintenance), in a 95-98% O2 mixture. During acquisition, mice were positioned prone on a dedicated temperature control apparatus to prevent hypothermia. For mammary gland imaging, a Turbo Spin Echo T2 (TR = 2500; TE = 80; turbo-factor = 9; FOV = 65x65mm; zero-filled voxelsize 100 x 100 x 800 micron) was acquired at 10.5 and/or 14.5 weeks of age. The larger field of view allowed evaluation of all five couples of mammary glands. Tumor volumes were calculated on a separate workstation (ViewForum 2.0) after manual segmentation of the lesion on the basis of signal intensity variation and enhancement characteristics, by summing individual volumes (calculated as lesion area x slice thickness) in each slice.

20 Tumor models

20.1 Spontaneous MMTV-PyMT tumors

For Tie2 gene knock-down experiments, HSPC transplantation was performed at 5.5 weeks of age, as described above. To induce OFP and Tie2 gene knock-down, the mice received doxycycline administrations (see paragraph 19.1) starting at 4 weeks post-HSPC transplantation (i.e., 9.5 weeks of age). Mammary tumors were monitored at weekly intervals and either measured by magnetic resonance imaging (MRI)- based volumetry (performed 10.5 and/or 14.5 weeks of age; see below) or tumor weight measurements performed at necropsy (15 weeks of age). At the end of the experiments, mice were anesthetized by Avertin and euthanized by intracardiac perfusion of PBS.

20.2 N202 mouse mammary carcinoma

The N202 mammary carcinoma cell line was cultured under standard conditions and $5x10^6$ cells were implanted subcutaneously in 9.5-week–old, female FVB mice transplanted 4 weeks earlier with transduced HSPCs (see above). To induce OFP and Tie2 gene knock-down, the mice received doxycycline administrations (see paragraph 19.1) starting 2 days after tumor cell injection. Tumors were analyzed 3 weeks post-tumor cell injection.

21 Flow cytometry

Flow cytometry either used a CyAn ADP (DAKO) or a BD FACSCanto (BD Bioscience) apparatus.

21.1 Antibodies

Official name	Alias	Origin	Purchased by	Conjugation / Secondary antibodies
Tek	Tie2	Rat	eBiosciences	PE
Csf1r	CD115	Rat	Serotec	PE
Itgam	CD11b	Rat	BD	FITC, PE, APC
Sell	CD62L	Rat	BD	APC
Tlr4	Ly87	Rat	BD	Biotinylated / Streptavidin-PE
Mrc1	CD206	Goat	R&O	Unconj. / Donkey anti-goat Alexa633
Xlkd1	Lyve1	Rat	MBL	PE
Ly6c1	Ly6C	Rat	SouthernBiotech	PE
Ly6g	Ly6G	Rat	BD	PE
Emr1	F4/80	Rat	Serotec	PE, APC
GR1	Ly6C/G	Rat	BD	PE, APC
Pecam1	CD31	Rat	BD	APC
CD163		Rabbit	Santa Cruz	Unconj. / Donkey anti-rabbit Alexa647
CD48	SLAMF2	Rat	BD	PE
114ra	CD124	Rat	BD	PE
Itgax	CD11c	Rat	BD	PE
CD86	B7.2	Rat	BD	PE
Itga4	CD49d	Rat	BD	PE
Fcer1a	FceRI	Rat	eBiosciences	PE
Spn	CD43	Rat	BD	PE
Tlr2	Ly105	Rat	BD	Biotinylated / Streptavidin-PE
Itga2b	CD41	Rat	BD	PE
c-kit	CD117	Rat	BD	APC
c-kit	CD117	Rat	eBiosciences	APC-Alexa750
Sca-1	Ly-6A/E	Rat	BD	PE
IgG1		Rat	eBioscience	PE, APC
IgG2a		Rat	BD	PE, APC
IgG2a		Rabbit	Molecular Probes	Unconj. / Donkey anti-rabbit Alexa647
IgG2a		Goat	Santa Cruz	Unconj. / Donkey anti-goat Alexa633

Table 5: List of antibodies for flow cytometry

21.2 Tumors

N202 mammary tumors were grown subcutaneously for 4-6 weeks in the right flank of 6-8–week old Tie2p/e-GFP transgenic or control FVB mice. For each analysis, 3-5 tumors were excised and made into single cell suspensions by

collagenase IV (0.2 mg/ml, Worthington), dispase (2 mg/ml, Gibco) and DNaseI (0.1 mg/ml, Roche) treatment in IMDM medium supplemented with 5% fetal calf serum (FCS), glutamine and antibiotics. After 1h at 37°C in a shaking bath, the cell suspension was 40 µm-filtered and washed in phosphate buffered saline (PBS) containing 2mM EDTA and 0.5% bovine serum albumin (BSA). Cell suspensions were incubated with rat anti-mouse FcγIII/II receptor (CD16/CD32) blocking antibodies (4 µg/ml), labeled with 7-amino-actinomycin D (7AAD) to stain nonviable cells and then stained using the antibodies listed in Table 5. To gate GFP+ cells, I used cells isolated from wild-type FVB mice.

21.3 Peripheral blood

Peripheral blood was collected from the tail vein of Tie2p/e-GFP transgenic or control FVB mice. After lysis of red blood cells using the TQ-Prep workstation (Beckman-Coulter), leukocytes were stained with 7AAD, incubated with rat anti-mouse FcγIII/II receptor (CD16/CD32) blocking antibodies (4 µg/ml) and then stained using the antibodies listed in Table 5. To gate GFP+ cells, I used cells isolated from wild-type FVB mice.

22 Flow sorting

22.1 Tumor-derived TEMs, TIE2– TAMs and ECs

TEMs and TIE2– TAMs were isolated from N202 mammary tumors grown subcutaneously for 4-6 weeks in the right flank of 6-8–week old Tie2p/e-GFP transgenic mice. For each cell sorting session, 10-30 tumors were excised and made into single-cell suspensions by collagenase IV (0.2 mg/ml, Worthington), dispase (2 mg/ml, Gibco) and DNaseI (0.1 mg/ml, Roche) treatment. Cell suspensions were then stained with PE-conjugated anti-CD11b and APC-

conjugated anti-CD31 monoclonal antibodies (BD Pharmingen), and the CD11b+ myeloid cells magnetically enriched using anti-PE microbeads and LS columns (Miltenyi). After magnetic enrichment, the vast majority of the cells were CD11b+CD31–. To isolate tumor-derived ECs, N202 tumors were processed as above, but the CD11b+ cell enrichment step was omitted. To sort cells, I used a Vantage DiVa apparatus (Becton-Dickinson). Before sorting, single-cell suspensions were labeled with 7-amino-actinomycin D (7AAD) to stain nonviable cells. I isolated TEMs as 7AAD– CD11b+ CD31– GFP+ cells (n=7 independent cell sorting) and TIE2– TAMs as 7AAD– CD11b+ CD31– GFP– cells (n=7). As fluorescence minus one (FMO) sample I used CD11b-enriched cells obtained from tumors grown in wild-type FVB mice. Tumor-derived ECs were sorted as 7AAD– CD11b– CD31+ GFP+ cells (n=3).

22.2 GR1+ CD11b+ myeloid derived suppressor cells (MDSCs)

MDSCs were isolated from the spleen of N202 tumor-bearing Tie2p/e-GFP transgenic mice as GR1+ CD11b+ cells. For each cell sorting session, 3 spleens were made into single-cell suspensions by mechanical treatment and then stained with PE-conjugated anti-CD11b and APC-conjugated anti-GR1 antibodies.

22.3 Peritoneal macrophages (PMs)

PMs were obtained from tumor-free FVB mice by peritoneal lavage with 10 ml/mouse serum-free RPMI. For each cell sorting session, I used 15, 6-to-8–week old mice. Recovered cells were stained with FITC-conjugated anti-CD11b, APC-conjugated anti-CD31 and PE-conjugated anti-F4/80 antibodies before cell sorting. PMs were sorted as F4/80+ CD11b+ CD31– cells (n=2).

22.4 Resident and inflammatory monocytes

For each experiment, blood was collected by cardiac puncture from 20 deeply anesthetized (Avertin) FVB mice. Peripheral blood mononuclear cells were purified with Lympholyte-Mammal (Cedarlane Labs, Canada). After staining with PE-conjugated anti-CD115 and APC-conjugated anti-GR1 antibodies and 7AAD vital staining, resident and inflammatory monocytes were sorted as 7AAD– CD115+ GR1– and 7AAD– CD115+ GR1+ cells, respectively, to a purity > 95% (n=4).

23 Immunofluorescence staining (IFS) and confocal microscopy

Tumors, liver samples and whole embryos (see below) were made into 12-16 µm cryostat sections, as described (Venneri et al. 2007). Briefly, tumors, embryos and organs were fixed for 1-4 hr in paraformaldehyde, equilibrated for 12 hr in PBS containing 15% sucrose, 24 hr in PBS/20% sucrose, and eventually 48 hr in PBS/30% sucrose. The samples were then embedded in O.C.T. compound for quick freezing in liquid nitrogen. Cryostat sections were laid on slides and immediately stained; when required, slides were frozen at -80°C. For immunofluorescence staining, sections were blocked with 5% serum (Vector Laboratories, Burlingame, CA) in PBS containing 1% bovine serum albumin (BSA) and 0.1% Triton X-100 (PBS-T). For staining, I used the antibodies listed in Table 6. Both unconjugated and directly conjugated antibodies were used; secondary antibodies were used to reveal unconjugated antibodies. Nuclei were stained by TO-PRO-3 (Molecular Probes). Confocal microscopy used an Axioskop 2 plus direct microscope (Zeiss) equipped with a Radiance 2100 three-laser confocal device (BioRad, Segrate, Italy). Axioskop 2 microscope used Zeiss W-Pl 10x/0.23 or Zeiss Plan-Neofluor 20x/0.5 numerical aperture objective lens. Fluorescent

signals from the individual fluorophores were sequentially acquired from single optical sections and analyzed by Paint Shop Pro X (Corel, Ottawa, Canada), as described previously (Venneri et al. 2007).

23.1 In vivo labeling of vascular perfusion

To detect perfused blood vessels, 10 min. before anesthesia (Avertin) I intra-venously injected 50 µg/mouse of FITC-conjugated, Lycopersicon esculentum lectin (Vector Labs Inc., Burlingame, CA). Once anesthetized, the mice were perfused by intra-cardiac infusion of 10-15 ml of PBS containing 2% Eparin to wash out blood cells and excess lectin.

23.2 Quantification of vascular parameters

To analyze angiogenesis/vascular perfusion in transgenic MMTV-PyMT models, 3-6 tumors/group, 8-15 sections/tumor and 1- 3 images/section were analyzed. Images were scanned at x400 or x100 magnification by a confocal microscope (Radiance 2100; BioRad) and digitally processed with ImageJ (NIH) to measure the marker-positive area. Counts were averaged to determine the relative vascular area or the marker-positive area. Error bars represent SEM.

23.3 Antibodies

Official name	Alias	Origin	Purchased by	Conjugation / Secondary antibodies
GFP		Rabbit	Molecular Probes	Unconj. / Donkey anti-rabbit Alexa488
GFP		Chicken	Abcam	Unconj. / Donkey anti-chicken Alexa488
Tek	Tie2	Rat	eBiosciences	PE
CD68		Rat	Serotec	Unconj. / Goat anti-rat Alexa546
Ptprc	CD45	Rat	BD	PE
Pecam1	CD31	Rat	BD	PE, APC
Emr1	F4/80	Rat	Serotec	PE, APC
Mrc1	CD206	Goat	R&D	Unconj. / Donkey anti-goat Alexa546
Xlkd1	Lyve1	Rabbit	MBL	Unconj. / Donkey anti-rabbit Alexa488 / 546
CD163		Rabbit	Santa Cruz	Unconj. / Donkey anti-rabbit Alexa488
Stab1		Mouse	NA	Biotinylated / Streptavidin-PE
IgG1		Rat	eBioscience	PE, APC
IgG2a		Rat	BD	PE, APC

Table 6: List of antibodies for IFS

24 Colony-forming cell (CFC) assays

CFC assays were performed from either FACS-sorted cells (tumor-derived TEMs and TIE2– TAMs; Tie2p/e-GFP+ CD11b+ and Tie2p/e-GFP– CD11b+ embryonic macrophages), unfractioned BM cells or BM-derived lineage-negative (Lin^-) cells. Unfractioned BM cells were obtained from 6 week-old mice by flushing their femora and tibiae. Lin^- cells were isolated from unfractioned BM cells using a kit from StemCell Technologies. I plated 5 x 10^3, 2 x 10^4 and 1 x 10^5 cells in a methylcellulose-based medium (MethoCult M3434, from StemCell Technologies) and allow the colonies to grow for 15 days before scoring them under an inverted microscope.

25 May-Grünwald-Giemsa staining

May-Grünwald-Giemsa staining was performed on flow sorted cells (tumor-derived TEMs and TIE2– TAMs; Tie2p/e-GFP+ CD11b+ and Tie2p/e-GFP– CD11b+ embryonic macrophages). Briefly, I prepared 3 slides for each cell population, by centrifuging 1 x 10^5 (2 slides) and 5 x 10^4 (1 slide) sorted cells onto the slide. After cytospin, cells were stained using a standard May-Grünwald-Giemsa staining protocol. For each cell population, at least 25 photos were randomly acquired under a direct microscope (Zeiss) and morphologic analysis of the cells performed with the advice of a professional pathologist.

26 Gene expression analyses and statistical analysis

26.1 Comparison of gene expression profiles between tumor-derived cells vs. circulating monocytes

The expression of a panel of 39 genes (selected among those analyzed in tumor-derived cells) was analyzed in both resident and inflammatory monocytes by qPCR, as described above. The 39 analyzed genes were either upregulated, downregulated or not differentially expressed between tumor TEMs and TIE2– TAMs. Twenty-two out of 39 genes displayed coordinated expression in tumor TEMs/TIE2– TAMs vs. resident/inflammatory monocytes (n=4 independent experiments). To test whether this outcome results by chance, I performed an Exact binomial test. Since the case to have a concordant expression is 1 out of 3 possible situations (upregulated, downregulated, not differentially expressed), the null hypothesis is assumed H_0: p=1/3, p being the probability of a random occurrence of concordant events. The two-sided test for 22 successes in a sequence of 39 independent experiments, with the hypothesized probability of success explained above, is computed, leading to a *p*-value = 0.003. Thus, I reject

the null hypothesis and consider the "concordance" as not random.

27 RNA and DNA extraction and qPCR

27.1 Gene expression (mRNA)

Sorted cells obtained from N202 tumors were lysed for long RNA extraction using the RNeasy Micro kit (Qiagen). Briefly, after cell sorting, 2.5-10 x 10^4 cells were obtained from each independent cell sorting (see above) and washed in low-protein buffer. Long RNA was purified following the RNeasy Micro kit guidelines (Qiagen). RNA was retrotranscribed with SuperScript III (Vilo kit, Invitrogen). All qPCR analyses were performed with TaqMan probes from Applied Biosystems. qPCR was run for 45 cycles in standard mode using an ABI7900HT apparatus (Applied Biosystems).

27.1.a Freshly isolated TEMs, TIE2– TAMs, MDSCs, PMs and ECs

To obtain adequate amounts of cDNA for each gene profiling experiment (interrogating 280 individual genes), 1 to 3 cell sorting sessions were performed. All qPCR analyses were performed with TaqMan probes from Applied Biosystems, apart from Th1-Th2 *in vitro* stimulation experiments, which used Sybrgreen mastermix from Applied Biosystems and designed primers (see paragraph 27.1.b below). I either used individual TaqMan gene expression assays to analyze expression of individual genes, or multi-gene TaqMan low density arrays. I used 2 custom and 1 pre-made (Immune Panel) TaqMan low density arrays, each measuring the expression of 96 genes in 4 technical replicates. One hundred ng – 1 µg of cDNA was loaded on each array. qPCR was run for 35 (low density arrays) or 40-45 cycles (individual gene analyses) in standard mode using an ABI7900HT apparatus (Applied Biosystems).

27.1.b In vitro stimulation of TEMs, TIE2– TAMs and PMs with Th1 and Th2 cytokines

Adherent PMs (purity >95% after cell sorting) and tumor-derived TEMs were incubated for 30 minutes at 37° in complete RPMI with 10% fetal calf serum. Th1 polarization was stimulated by priming cells with IFNg (0.05U/ml, Sigma) for 30 minutes, followed by stimulation with LPS (100ng/ml). Th2 responses were induced by stimulating cells with IL4 (20ng/ml, Peprotech). After 4 hours of stimulation, cells were washed and lysed for RNA extraction and qPCR analysis. qPCR used Sybrgreen mastermix from Applied Biosystems and the primers listed in Table 7.

Gene	Fw	Rv
Arg1	CAGAAGAATGGAAGAGTCAGTG	GCAGCTATGCAGGGAGTCACCC
Ccl17	AGTGCTGCCTGGATTACTTCAAAG	CTGGACAGTCAGAAACACGATGG
Nos2	TGGTCCGCAAGAGAGTGCT	CCTCATTGGCCAGCTGCTT
Il12a	GGAAGCACGGCAGCAGAATA	AACTTGAGGGAGAAGTAGGAATGG
B2m	CATGGCTCGCTCGGTGACC	AATGTGAGGCGGGTGGAACTG

Table 7 Primer sequences

27.1.c Circulating inflammatory and resident monocytes

To perform multiple qPCR assays on the limited amount of starting material obtained from circulating monocyte subsets, a pre-amplification step was done on cDNA using TaqMan PreAmp MasterMix (AppliedBiosystems). Briefly, up to 100 TaqMan assays were pooled and diluted 1:100 in water. This mix has been used to pre-amplify the genes of interest in a PCR as follows: 10 min 95°, 14 cycles of 15 sec at 95° and 4 min at 60° in a 50µl reaction volume. After pre-amplification, the samples were diluted 1:5 and used as template to quantify the genes of interest in

a standard TaqMan-based qPCR. I validated this procedure on non-limiting samples (data not shown) and found that >92% of the genes gave a $\Delta\Delta C_T$ value within ±1.5 with respect to the non-amplified sample. These results indicate that the pre-amplification step did not bias the mRNA composition (i.e. the relative proportion of each mRNA) in our samples.

27.2 Small RNA (including artificial micro RNA) analysis

To purify small RNA from BM-derived, LV2-transgenic/LV1- transduced HSPCs, I followed miRNeasy Mini kit guidelines (Qiagen). Two days after LV1 transduction in the presence or absence of doxycycline, the cultured cells were collected, extensively washed and lysed for total RNA extraction using the miRNeasy Mini kit (Qiagen). To retrotranscribe small RNAs, I used High Capacity cDNA Reverse Transcription Kit (Applied Biosystems) and a custom, small RNA reverse transcription primer specific for the mature form of amiR(Tie2) sequence (Applied Biosystems). To perform qPCR on retrotranscribed small RNAs I used inventoried (for miR-16 and Let7a) or custom (for amiR(Tie2)) TaqMan small RNA assays (Applied Biosystems).

27.3 Vector copy number analysis

For vector copy number (VCN) analysis, I purified genomic DNA from circulating blood or BM cells using a Maxwell-16 instrument (Promega) and performed qPCR using custom TaqMan assays specific for βactin, rtTA-m2 or OFP sequences (Applied Biosystems). Standard curves for the rtTA-m2 and OFP sequences were obtained from PGKrtTA- miR-126T transgenic mice and a cell line transduced with an OFP-expressing LV, respectively. The VCN of genomic DNA standard curves was determined using custom TaqMan assays specific for LVs (Applied Biosystems).

27.4 Collection of raw data and determination of gene expression and LV copy number

The SDS 2.2.1 software was used to extract raw data (C_T) and to perform gene expression or VCN analysis. In the Sybr-based qPCR experiment (see paragraph 27.1.b), after the qPCR run I performed a dissociation curve. Wells with more than one amplicon were discarded. To determine gene expression, the difference (ΔC_T) between the threshold cycle (C_T) of each gene and that of the reference gene (*B2m* for multi-gene arrays and *in vitro* stimulation experiments; *Gapdh* for individual gene assays; both *B2m* and *Gapdh* for analyses of circulating monocytes; *Let7a* for small RNA analysis) was calculated by applying an equal threshold (0.02 for all the genes inside the TaqMan low density arrays, 0.1 for all the pre-amplified genes). The ΔC_T of different genes can be compared only when an equal threshold is applied to calculate the C_T. The lower the ΔC_T, the higher the gene expression level.

To calculate VCN I used the following formula: VCN = VCN(standard curve) * ng of "LV of interest" / ng of βactin; where "LV of interest" is either rtTA-m2 or OFP.

27.5 Calculation of PCR efficiency

The SDS 2.2.1 software was used to extract raw data (C_T and raw fluorescence). For multi-gene arrays, I calculated PCR amplification efficiency using Miner algorithm (http://www.miner.ewindup.info/miner/) and non-baseline subtracted fluorescence data. For each gene, I used the mean PCR efficiency calculated throughout the samples (TEMs, TIE2– TAMs, PMs, MDSCs). Before averaging, single amplification runs that met one of the following conditions have been filtered out, because they could represent background amplification: (i) less than 5 regression windows; (ii) LogA value less than 0.5; (iii) LogPvalue equal to 0; (iv) C_T greater than 35.

27.6 Statistical analysis of gene expression data (fold change)

To calculate the fold-change of gene expression, I implemented an analysis of covariance model (ANCOVA). This multiple regression approach is aimed at modelling jointly the impact of different explicative covariates on the outcome of interest. The implemented model leads to a procedure equivalent to test the $\Delta\Delta C_T$ (Yuan et al. 2006). The advantage of this procedure with respect to two-by-two t-test comparisons lies in the joint nature of the modeling of all covariates, which allows minimizing type I errors (false positive results). Estimation technique is based on Likelihood Ratio Test. The model is implemented in R-statistical software (version 2.6.1; see http://www.R-project.org). Significance level is chosen at α = 0.05.

27.6.a TEMs vs TIE2– TAMs and Ly6C– vs Ly6C+ monocytes

In this case, the outcome variable is ${}^{E}C_T$, the efficiency-corrected C_T, and the covariates are the Sample type (i.e. TEMs or TIE2– TAMs; X_{sample}), the Experiment (i.e. biological replicates; X_{Exp}), the Card (i.e. individual array; X_{card}), the Gene (X_{gene}) and the pre-amplification (only for the analysis of gene expression in monocytes; Table 2 in the main text). The multiple regression formula is $C_T \cdot log_2(1+E) = {}^{E}C_T = \beta_0 + \beta_1 \cdot X_{Sample} + \beta_2 \cdot X_{Exp} + \beta_3 \cdot X_{Card} + \beta_4 \cdot X_{Gene} + \beta_5 \cdot X_{Gene \cdot Sample} + \varepsilon$, where C_T is the threshold cycle, E is the gene-specific PCR efficiency, ${}^{E}C_T$ is the efficiency-corrected C_T, β_i are the coefficients calculated by the model that represents the impact of the respective qualitative variable X_i, ε is the residual error. X_i is set to zero when Sample=TIE2– TAMs, Exp = "first replicate", Card = "first array" and Gene = *B2m*. I chose *B2m* as the most stable gene by GeNorm analysis.

27.6.b OFP+ vs. OFP– TEMs

In this case, I measured the *Tie2* and *β2m* (reference gene) mRNA in 2 (amiR(Tie2)) or 3 (amiR(Luc)) biological samples and 6 (for Tie2) or 3 (for *β2m)* technical replicates/biological sample. Being the C_T the outcome variable, the covariates are the sorted subset (TEMs and TIE2– TAMs), the mouse (i.e., biological replicate), the qPCR plate (multi-plate experiment), the gene (*Tie2* or *B2m*) and the amiR (i.e., amiR(Tie2) or amiR(Luc)). The multiple regression formula reads as follows:

$$C_T = \beta_0 + \beta_1 \cdot X_{Subset} + \beta_2 \cdot X_{Mouse} + \beta_3 \cdot X_{Plate} + \beta_4 \cdot X_{Gene \cdot amiR} + \varepsilon$$

where C_T is the threshold cycle, β_i are the coefficients calculated by the model that represents the impact of the respective qualitative variable X_j, with j being each of the covariates, and ε the residual error.

27.6.c Hematopoietic stem/progenitor cell cultures

In these cases the analyses were performed using qBase excel macro (BioGazelle). Calculation of amiR(Tie2) levels in HSPC liquid cultures, either treated with doxycycline or left untreated (calibrator). Let7a was used as a reference miR. Calculation of Tie2 mRNA levels in HSPC liquid cultures, either treated with doxycycline or left untreated (calibrator). β2m was used as reference gene. In these experiments, doxycycline was added after washing out LV1; cells were analyzed 2 days after transduction. Error bars represent 95% confidence interval (1.96*SEM).

Acknowledgements

I would like to express my gratitude to my supervisor, Dr. Michele De Palma, whose expertise, understanding and patience added considerably to my Ph.D. experience. I am also in debt with Dr. Luigi Naldini, the lab head, whose ability to focus on relevant data is admirable. I would like to thank present and past members of the Angiogenesis and Tumor Targeting Research Unit (ATTRU), coordinated by Dr. De Palma. In particular, Dr. Mary Anna Venneri, who, together with Dr. De Palma, welcomed me in the laboratory. A big thank also to the other ATTRU members, Daniela, Roberta, Erika, Davide and Leonardo, without them my laboratory life would have not been as good as it was. I am particularly obliged to Dr. Mario Amendola, a former post-doc in Dr. Naldini's laboratory. I appreciated very much his sense of humor and his vision of reality. I can not forget Dr. Anna Zingale, who introduced me to qPCR technique. I recognize the invaluable work of Dr. Fabrizio Benedicenti, the laboratory manager, and the help of Dr. Lucia Sergi Sergi for LV production. Many thanks to: Dr. Alessio Palini, Dr. Emanuele Canonico and Dr. Chiara Villa, from in house flow cytometry facility, for their ability with cell sorting apparatuses; to the Office of Ph.D. Studies for organizing seminars, courses and annual meetings; to Student Secretariat for support with Ph.D. program regulations; to all DIBIT brats: Saverio&Sara, Biasco&Alice, Alex&Franz, Anto, PIM, Nurayev†, Annarita, Aresu, Pota, Mattia, Marco&Stefi, Jak, Nicola. I acknowledge the "Vita-Salute" San Raffaele University for a 3 years Ph.D. fellowship.

Eternal gratitude to my parents, Paolo and Silvana, who encouraged me and let me do what I most like. Many thanks also to my younger brother Ruggero for allowing me to be the older brother, and to Emma, Loki and Zelda, my cats. Last but not least, my precious half, Sara, who endured sharing life with me in Milan.

Acronym Index

7AAD – 7-Amino-Actinomycin D

amiR – artificial micro-RNAs

ANG – angiopoietin

bEnd – brain endothelial cells

BM – bone marrow

BM-Lin– – BM-derived lineage-negative cells

CFC – Colony-forming cell

Csf1 – colony stimulating factor-1

DCs – dendritic cells

deMφs – definitive embryonic Mφs

dpc – days post coitum

ECs – endothelial cells

EF1α – elongation factor 1α

EPCs – endothelial progenitor cells

FGF – fibroblast growth factor

GCV – Gancyclovir

HA – hyaluronic acid

HCs – hematopoietic cells

HSC – hematopoietic stem cells

HSPCs – hematopoietic stem/progenitor cells

IFS – immunofluorescence staining

LacZ – Beta-galactosidase

LCs – Langerhans cells

Luc – luciferase

LVs – lentiviral vectors

MDSCs – myeloid derived suppressor cells

miR – microRNA

MMP – matrix metalloproteinase

MMTV-PyMT – mouse mammary tumor virus promoter-polyoma virus middle T antigen

MP – mononuclear phagocytes

MRI – Magnetic Resonance Imaging

Mφs –macrophages

NGFR – low affinity nerve growth factor receptor

OFP – orange fluorescent protein

peMφs – primitive embryonic Mφs

PGK1 – phospho-glicerate kinase 1

PMs – peritoneal macrophages

pre-miR – precursor miR

pri-miR – primary micro-RNA

RES – reticulo-endothelial system

RISC – RNA-induced silencing complex

RNAi – RNA interference

rtTA – reverse Tetracycline transactivator

SDF1 – stromal cell derived factor-1

siRNA – short interfering RNA

TAMs – tumor-associated Mφs

TEMs – Tie2-expressing macrophages

Tie2p/e – promoter and enhancer from the Tie2 gene

TK – Tymidine Kinase

TRE – Tetracycline responsive element

VCN – vector copy number

VEGF – vascular endothelial growth factor

Author' s publications

1. Andreu P*, M Johansson*, NI Affara*, **F Pucci**, T Tan, S Junankar, L Korets, J Lam, D Tawfik, D DeNardo, L Naldini, KE de Visser, M De Palma, LM Coussens.

   FcRγ activation regulates inflammation-associated squamous carcinogenesis. **Cancer Cell**. 2010 Feb 17;17(2):121-134.

   *: Co-first authors.

   IF: 25.288. Quoted 8 times

2. **Pucci F***, MA Venneri*, D Biziato, A Nonis, D Moi, A Sica, C Di Serio, L Naldini, M De Palma.

   A distinguishing gene signature shared by tumor-infiltrating Tie2-expressing monocytes (TEMs), blood "resident" monocytes and embryonic macrophages suggests common functions and developmental relationships.

   Blood. 2009 Jul 23;114(4):901-14.

   Preview (MC Yoder): Blood, Jul 23;114(4):756-7.

   *: Co-first authors.

   IF: 10.555. Quoted 15 times

3. Amendola M, L Passerini, **F Pucci**, B Gentner, R Bacchetta, L Naldini.

   Regulated and multiple miRNA and siRNA delivery into primary cells by a lentiviral platform.

   Mol Ther. 2009 Jun;17(6):1039-52.

   IF: 6.239. Quoted 2 times

4. De Palma M, R Mazzieri, LS Politi, **F Pucci**, E Zonari, S Mazzoleni, G Sitia, D Moi, MA Venneri, S Indraccolo, A Falini, LG Guidotti, R Galli, L Naldini.

   Tumor-targeted Interferon-α Delivery by Tie2-Expressing Monocytes Inhibits Tumor Growth and Metastasis.

   Cancer Cell, 2008 Oct 7;14(4):299-311.

   IF: 25.288. Quoted 26 times

5. Venneri MA*, M De Palma*, M Ponzoni, **F Pucci**, C Scielzo, E Zonari, R Mazzieri, C Doglioni, L Naldini.

   Identification of Proangiogenic Tie2-Expressing Monocytes (TEMs) in Human Peripheral Blood and Cancer.

   Blood. 2007 Jun 15;109(12):5276-85.

   Preview (G. Coukos): Blood, Jun 15;109(12):5076.

   *: Equal Contribution.

   IF: 10.555. Quoted 60 times

Submitted manuscript

Mazzieri R*, **F Pucci***, D Moi, E Zonari, A Berti, LS. Politi, L Naldini, and M De Palma.

Targeting the Angiopoietin-2/TIE2 axis Inhibits Tumor Progression and Metastasis by Impairing Angiogenesis and Disabling Rebounds of Proangiogenic Myeloid Cells.

*: Equal Contribution.

Bibliography

Aagaard, L.A. et al., 2008. Engineering and optimization of the miR-106b cluster for ectopic expression of multiplexed anti-HIV RNAs. *Gene Therapy*, 15(23), 1536-1549.

Ahn, G. & Brown, J.M., 2008. Matrix metalloproteinase-9 is required for tumor vasculogenesis but not for angiogenesis: role of bone marrow-derived myelomonocytic cells. *Cancer Cell*, 13(3), 193-205.

Ajami, B. et al., 2007. Local self-renewal can sustain CNS microglia maintenance and function throughout adult life. *Nature Neuroscience*, 10(12), 1538-1543.

Alder, J.K. et al., 2008. Kruppel-Like Factor 4 Is Essential for Inflammatory Monocyte Differentiation In Vivo. *J Immunol*, 180(8), 5645-5652.

Amendola, M. et al., 2009. Regulated and multiple miRNA and siRNA delivery into primary cells by a lentiviral platform. *Molecular Therapy: The Journal of the American Society of Gene Therapy*, 17(6), 1039-1052.

Arai, F. et al., 2004. Tie2/angiopoietin-1 signaling regulates hematopoietic stem cell quiescence in the bone marrow niche. *Cell*, 118(2), 149-161.

Asahara, T. et al., 1999. Bone marrow origin of endothelial progenitor cells responsible for postnatal vasculogenesis in physiological and pathological neovascularization. *Circulation Research*, 85(3), 221-228.

Asahara, T. et al., 1997. Isolation of Putative Progenitor Endothelial Cells for Angiogenesis. *Science*, 275(5302), 964-966.

Auffray, C. et al., 2007. Monitoring of blood vessels and tissues by a population of monocytes with patrolling behavior. *Science (New York, N.Y.)*, 317(5838), 666-670.

Augustin, H.G. et al., 2009. Control of vascular morphogenesis and homeostasis through the angiopoietin-Tie system. *Nat Rev Mol Cell Biol*, 10(3), 165-177.

Balkwill, F. & Mantovani, A., 2001. Inflammation and cancer: back to Virchow? *The Lancet*, 357(9255), 539-545.

Bartel, D.P., 2004. MicroRNAs: Genomics, Biogenesis, Mechanism, and Function. *Cell*, 116(2), 281-297.

Barton, W.A. et al., 2006. Crystal structures of the Tie2 receptor ectodomain and the angiopoietin-2-Tie2 complex. *Nature Structural & Molecular Biology*, 13(6), 524-532.

Bergers, G. et al., 2000. Matrix metalloproteinase-9 triggers the angiogenic switch during carcinogenesis. *Nature cell biology*, 2(10), 737-744.

Bergers, G. & Hanahan, D., 2008. Modes of resistance to anti-angiogenic therapy. *Nat Rev Cancer*, 8(8), 592-603.

Birmingham, A. et al., 2006. 3[prime] UTR seed matches, but not overall identity,

are associated with RNAi off-targets. *Nat Meth*, 3(3), 199-204.

Böckle, B.C. et al., 2008. DC-sign+ CD163+ macrophages expressing hyaluronan receptor LYVE-1 are located within chorion villi of the placenta. *Placenta*, 29(2), 187-192.

Boudreau, R.L., Martins, I. & Davidson, B.L., 2009. Artificial microRNAs as siRNA shuttles: improved safety as compared to shRNAs in vitro and in vivo. *Molecular Therapy: The Journal of the American Society of Gene Therapy*, 17(1), 169-175.

Bournazou, I. et al., 2009. Apoptotic human cells inhibit migration of granulocytes via release of lactoferrin. *The Journal of Clinical Investigation*, 119(1), 20-32.

Bridge, A.J. et al., 2003. Induction of an interferon response by RNAi vectors in mammalian cells. *Nature Genetics*, 34(3), 263-264.

Brown, B.D. & Naldini, L., 2009. Exploiting and antagonizing microRNA regulation for therapeutic and experimental applications. *Nature Reviews. Genetics*, 10(8), 578-585.

Brown, B.D. et al., 2006. Endogenous microRNA regulation suppresses transgene expression in hematopoietic lineages and enables stable gene transfer. *Nature Medicine*, 12(5), 585-591.

Brown, J.L. et al., 2010. A Human Monoclonal Anti-ANG2 Antibody Leads to Broad

Antitumor Activity in Combination with VEGF Inhibitors and Chemotherapy Agents in Preclinical Models. *Molecular Cancer Therapeutics*, 9(1), 145-156.

Brummelkamp, T.R., Bernards, R. & Agami, R., 2002. A system for stable expression of short interfering RNAs in mammalian cells. *Science (New York, N.Y.)*, 296(5567), 550-553.

Capuano, G. et al., 2009. Modulators of arginine metabolism support cancer immunosurveillance. *BMC Immunology*, 10, 1.

Carmeliet, P. & Tessier-Lavigne, M., 2005. Common mechanisms of nerve and blood vessel wiring. *Nature*, 436(7048), 193-200.

Castanotto, D. et al., 2007. Combinatorial delivery of small interfering RNAs reduces RNAi efficacy by selective incorporation into RISC. *Nucleic Acids Research*, 35(15), 5154-5164.

Cavanagh, L.L. & Weninger, W., 2008. Dendritic cell behaviour in vivo: lessons learned from intravital two-photon microscopy. *Immunol Cell Biol*, 86(5), 428-438.

Chang, K., Elledge, S.J. & Hannon, G.J., 2006. Lessons from Nature: microRNA-based shRNA libraries. *Nature Methods*, 3(9), 707-714.

Chang, Z., 2009. Recent development of the mononuclear phagocyte system: in memory of Metchnikoff and Ehrlich on the 100th Anniversary of the 1908

Nobel Prize in Physiology or Medicine. *Biology of the Cell*, 101(12), 709-721.

Chen, R. et al., 2008. Cancers take their Toll--the function and regulation of Toll-like receptors in cancer cells. *Oncogene*, 27(2), 225-233.

Cho, C. et al., 2007. Angiogenic Role of LYVE-1-Positive Macrophages in Adipose Tissue. *Circ Res*, 100(4), e47-57.

Chorro, L. et al., 2009. Langerhans cell (LC) proliferation mediates neonatal development, homeostasis, and inflammation-associated expansion of the epidermal LC network. *The Journal of Experimental Medicine*, 206(13), 3089-3100.

Chung, K. et al., 2006. Polycistronic RNA polymerase II expression vectors for RNA interference based on BIC/miR-155. *Nucleic Acids Research*, 34(7), e53.

Coffelt, S.B. et al., 2010a. Elusive identities and overlapping phenotypes of proangiogenic myeloid cells in tumors. *The American Journal of Pathology*, 176(4), 1564-1576.

Coffelt, S.B. et al., 2010b. Angiopoietin-2 Regulates Gene Expression in TIE2-Expressing Monocytes and Augments Their Inherent Proangiogenic Functions. *Cancer Res*, 0008-5472.CAN-10-0012.

Condeelis, J. & Pollard, J.W., 2006. Macrophages: obligate partners for tumor cell

migration, invasion, and metastasis. *Cell*, 124(2), 263-266.

Coussens, L.M. et al., 1999. Inflammatory mast cells up-regulate angiogenesis during squamous epithelial carcinogenesis. *Genes & Development*, 13(11), 1382-1397.

Coussens, L.M. & Werb, Z., 2002. Inflammation and cancer. *Nature*, 420(6917), 860-867.

Coussens, L.M. et al., 2000. MMP-9 Supplied by Bone Marrow–Derived Cells Contributes to Skin Carcinogenesis. *Cell*, 103(3), 481-490.

Crivellato, E., Nico, B. & Ribatti, D., 2008. Mast cells and tumour angiogenesis: new insight from experimental carcinogenesis. *Cancer Letters*, 269(1), 1-6.

Crofton, R.W., Diesselhoff-den Dulk, M.M. & van Furth, R., 1978. The origin, kinetics, and characteristics of the Kupffer cells in the normal steady state. *The Journal of Experimental Medicine*, 148(1), 1-17.

Cullen, B.R., 2006. Enhancing and confirming the specificity of RNAi experiments. *Nature Methods*, 3(9), 677-681.

Dale, D.C., Boxer, L. & Liles, W.C., 2008. The phagocytes: neutrophils and monocytes. *Blood*, 112(4), 935-945.

Davis, S. et al., 2003. Angiopoietins have distinct modular domains essential for receptor binding, dimerization and superclustering. *Nature Structural*

Biology, 10(1), 38-44.

De Palma, M. & Coussens, L., 2008. Immune cells and inflammatory mediators as regulators of tumor angiogenesis. In Angiogenesis: An integrative approach from science to medicine. In *Angiogenesis: An Integrative Approach from Science to Medicine*. Springer Science, New York, NY USA, pagg. 225-238.

De Palma, M. et al., 2008. Tumor-targeted interferon-alpha delivery by Tie2-expressing monocytes inhibits tumor growth and metastasis. *Cancer Cell*, 14(4), 299-311.

De Palma, M. et al., 2007. Tie2-expressing monocytes: regulation of tumor angiogenesis and therapeutic implications. *Trends in Immunology*, 28(12), 519-524.

De Palma, M. & Naldini, L., 2006. Role of haematopoietic cells and endothelial progenitors in tumour angiogenesis. *Biochimica Et Biophysica Acta*, 1766(1), 159-166.

De Palma, M. & Naldini, L., 2002. Transduction of a gene expression cassette using advanced generation lentiviral vectors. *Methods in Enzymology*, 346, 514-529.

De Palma, M. et al., 2005. Tie2 identifies a hematopoietic lineage of proangiogenic monocytes required for tumor vessel formation and a mesenchymal population of pericyte progenitors. *Cancer Cell*, 8(3), 211-226.

De Palma, M. et al., 2003. Targeting exogenous genes to tumor angiogenesis by transplantation of genetically modified hematopoietic stem cells. *Nature Medicine*, 9(6), 789-795.

Dirks, P.B., 2008. Brain tumor stem cells: bringing order to the chaos of brain cancer. *Journal of Clinical Oncology: Official Journal of the American Society of Clinical Oncology*, 26(17), 2916-2924.

Doerr, W., 1985. [Cohnheim's inflammation doctrine and the current debate]. *Zentralblatt Für Allgemeine Pathologie Und Pathologische Anatomie*, 130(4), 299-306.

Dumont, D.J. et al., 1994. Dominant-negative and targeted null mutations in the endothelial receptor tyrosine kinase, tek, reveal a critical role in vasculogenesis of the embryo. *Genes & Development*, 8(16), 1897-1909.

Dumont, D.J. et al., 1992. tek, a novel tyrosine kinase gene located on mouse chromosome 4, is expressed in endothelial cells and their presumptive precursors. *Oncogene*, 7(8), 1471-1480.

Egeblad, M. et al., 2008. Visualizing stromal cell dynamics in different tumor microenvironments by spinning disk confocal microscopy. *Disease Models & Mechanisms*, 1(2-3), 155-167.

Ehrlich, P., 1908. Partial Cell Functions. In *The Nobel Prize in Physiology or Medicine 1908*. Physiology or Medicine 1901-1921. Amsterdam: Elsevier

Publishing Company. Available at: http://nobelprize.org/nobel_prizes/medicine/laureates/1908/ehrlich-lecture.html.

Ely, A., Naidoo, T. & Arbuthnot, P., 2009. Efficient silencing of gene expression with modular trimeric Pol II expression cassettes comprising microRNA shuttles. *Nucleic Acids Research*, 37(13), e91.

Essers, M.A.G. et al., 2009. IFNalpha activates dormant haematopoietic stem cells in vivo. *Nature*, 458(7240), 904-908.

Eulalio, A., Huntzinger, E. & Izaurralde, E., 2008. Getting to the Root of miRNA-Mediated Gene Silencing. *Cell*, 132(1), 9-14.

Fantin, A. et al., 2010. Tissue macrophages act as cellular chaperones for vascular anastomosis downstream of VEGF-mediated endothelial tip cell induction. *Blood*. Available at: http://www.ncbi.nlm.nih.gov/pubmed/20404134 [Consultato Luglio 9, 2010].

Fiedler, U. & Augustin, H.G., 2006. Angiopoietins: a link between angiogenesis and inflammation. *Trends in Immunology*, 27(12), 552-558.

Fiedler, U. et al., 2006. Angiopoietin-2 sensitizes endothelial cells to TNF-[alpha] and has a crucial role in the induction of inflammation. *Nat Med*, 12(2), 235-239.

Fiedler, U. et al., 2004. The Tie-2 ligand Angiopoietin-2 is stored in and rapidly

released upon stimulation from endothelial cell Weibel-Palade bodies. *Blood*, 103(11), 4150-4156.

Fischer, C. et al., 2007. Anti-PlGF inhibits growth of VEGF(R)-inhibitor-resistant tumors without affecting healthy vessels. *Cell*, 131(3), 463-475.

Fish, R.J. & Kruithof, E.K.O., 2004. Short-term cytotoxic effects and long-term instability of RNAi delivered using lentiviral vectors. *BMC Molecular Biology*, 5, 9.

Folkman, J., 1971. Tumor angiogenesis: therapeutic implications. *The New England Journal of Medicine*, 285(21), 1182-1186.

Folkman, J., Hahnfeldt, P. & Hlatky, L., 2000. Cancer: looking outside the genome. *Nat Rev Mol Cell Biol*, 1(1), 76-79.

del Fresno, C. et al., 2005. Tumor cells deactivate human monocytes by up-regulating IL-1 receptor associated kinase-M expression via CD44 and TLR4. *Journal of Immunology (Baltimore, Md.: 1950)*, 174(5), 3032-3040.

Fry, W.E., 1936. The Reticulo-Endothelial System of the Eye. *Transactions of the American Ophthalmological Society*, 34, 264-283.

van Furth, R. et al., 1972. The mononuclear phagocyte system: a new classification of macrophages, monocytes, and their precursor cells. *Bulletin of the World Health Organization*, 46(6), 845-852.

Gabrilovich, D.I. & Nagaraj, S., 2009. Myeloid-derived suppressor cells as regulators of the immune system. *Nature Reviews. Immunology*, 9(3), 162-174.

Geissmann, F. et al., 2010. Unravelling mononuclear phagocyte heterogeneity. *Nat Rev Immunol*, advance online publication. Available at: http://dx.doi.org/10.1038/nri2784 [Consultato Maggio 17, 2010].

Geissmann, F., Jung, S. & Littman, D.R., 2003. Blood Monocytes Consist of Two Principal Subsets with Distinct Migratory Properties. *Immunity*, 19(1), 71-82.

Geissmann, F. et al., 2010. Development of Monocytes, Macrophages, and Dendritic Cells. *Science*, 327(5966), 656-661.

Genasetti, A. et al., 2008. Hyaluronan and human endothelial cell behavior. *Connective Tissue Research*, 49(3), 120-123.

Giraudo, E., Inoue, M. & Hanahan, D., 2004. An amino-bisphosphonate targets MMP-9-expressing macrophages and angiogenesis to impair cervical carcinogenesis. *The Journal of Clinical Investigation*, 114(5), 623-633.

Goerdt, S. et al., 1996. The mononuclear phagocyte–dendritic cell dichotomy: myths, facts, and a revised concept. *Clinical and Experimental Immunology*, 105(1), 1-9.

Gordon, S. & Martinez, F.O., 2010. Alternative activation of macrophages: mechanism and functions. *Immunity*, 32(5), 593-604.

Gordon, S. & Taylor, P.R., 2005. Monocyte and macrophage heterogeneity. *Nat Rev Immunol*, 5(12), 953-964.

Gossen, M. & Bujard, H., 1992. Tight control of gene expression in mammalian cells by tetracycline-responsive promoters. *Proceedings of the National Academy of Sciences of the United States of America*, 89(12), 5547-5551.

Gounaris, E. et al., 2007. Mast cells are an essential hematopoietic component for polyp development. *Proceedings of the National Academy of Sciences of the United States of America*, 104(50), 19977-19982.

Grimm, D. et al., 2006. Fatality in mice due to oversaturation of cellular microRNA/short hairpin RNA pathways. *Nature*, 441(7092), 537-541.

Hanahan, D. & Folkman, J., 1996. Patterns and Emerging Mechanisms of the Angiogenic Switch during Tumorigenesis. *Cell*, 86(3), 353-364.

Hanahan, D. & Weinberg, R.A., 2000. The Hallmarks of Cancer. *Cell*, 100(1), 57-70.

Hart, K.M. et al., 2009. Phenotypic and functional delineation of murine CX(3)CR1 monocyte-derived cells in ovarian cancer. *Neoplasia (New York, N.Y.)*, 11(6), 564-573, 1 p following 573.

Hashimoto, T. et al., 2004. Regulation of tie2 expression by angiopoietin--potential feedback system. *Endothelium: Journal of Endothelial Cell Research*, 11(3-

4), 207-210.

Hashizume, H. et al., 2000. Openings between defective endothelial cells explain tumor vessel leakiness. *The American Journal of Pathology*, 156(4), 1363-1380.

Hiratsuka, S. et al., 2008. The S100A8-serum amyloid A3-TLR4 paracrine cascade establishes a pre-metastatic phase. *Nature Cell Biology*, 10(11), 1349-1355.

Hoffman, R.M. & Yang, M., 2006. Color-coded fluorescence imaging of tumor-host interactions. *Nature Protocols*, 1(2), 928-935.

Hughes, J.E. et al., 2008. Sphingosine-1-phosphate induces an antiinflammatory phenotype in macrophages. *Circulation Research*, 102(8), 950-958.

Hume, D.A., 2006. The mononuclear phagocyte system. *Current Opinion in Immunology*, 18(1), 49-53.

Hume, D.A. et al., 2002. The mononuclear phagocyte system revisited. *J Leukoc Biol*, 72(4), 621-627.

Hussain, S.P., Hofseth, L.J. & Harris, C.C., 2003. Radical causes of cancer. *Nature Reviews. Cancer*, 3(4), 276-285.

Jain, R.K., 2005. Normalization of tumor vasculature: an emerging concept in antiangiogenic therapy. *Science (New York, N.Y.)*, 307(5706), 58-62.

Kaufmann, S.H.E., 2008. Elie Metchnikoff's and Paul Ehrlich's impact on infection biology. *Microbes and Infection / Institut Pasteur*, 10(14-15), 1417-1419.

Kim, D.H. & Rossi, J.J., 2007. Strategies for silencing human disease using RNA interference. *Nat Rev Genet*, 8(3), 173-184.

Kleinman, M.E. et al., 2008. Sequence- and target-independent angiogenesis suppression by siRNA via TLR3. *Nature*, 452(7187), 591-597.

Landsman, L. & Jung, S., 2007. Lung Macrophages Serve as Obligatory Intermediate between Blood Monocytes and Alveolar Macrophages. *J Immunol*, 179(6), 3488-3494.

Landsman, L., Varol, C. & Jung, S., 2007. Distinct Differentiation Potential of Blood Monocyte Subsets in the Lung. *J Immunol*, 178(4), 2000-2007.

Lemmon, M.A. & Schlessinger, J., 2010. Cell Signaling by Receptor Tyrosine Kinases. *Cell*, 141(7), 1117-1134.

Lewis, C.E. & Pollard, J.W., 2006. Distinct Role of Macrophages in Different Tumor Microenvironments. *Cancer Research*, 66(2), 605-612.

Lewis, J.S. et al., 2000. Expression of vascular endothelial growth factor by macrophages is up-regulated in poorly vascularized areas of breast carcinomas. *The Journal of Pathology*, 192(2), 150-158.

Ley, K. et al., 2007. Getting to the site of inflammation: the leukocyte adhesion

cascade updated. *Nat Rev Immunol*, 7(9), 678-689.

Li, L. et al., 2007. Defining the optimal parameters for hairpin-based knockdown constructs. *RNA (New York, N.Y.)*, 13(10), 1765-1774.

Lin, E.Y. et al., 2003. Progression to malignancy in the polyoma middle T oncoprotein mouse breast cancer model provides a reliable model for human diseases. *The American Journal of Pathology*, 163(5), 2113-2126.

Lin, E.Y. et al., 2006. Macrophages regulate the angiogenic switch in a mouse model of breast cancer. *Cancer Research*, 66(23), 11238-11246.

Lin, E.Y. et al., 2001. Colony-stimulating factor 1 promotes progression of mammary tumors to malignancy. *The Journal of Experimental Medicine*, 193(6), 727-740.

Liu, Y. et al., 2000. Edg-1, the G protein-coupled receptor for sphingosine-1-phosphate, is essential for vascular maturation. *The Journal of Clinical Investigation*, 106(8), 951-961.

Luo, Y. et al., 2006. Targeting tumor-associated macrophages as a novel strategy against breast cancer. *The Journal of Clinical Investigation*, 116(8), 2132-2141.

Lyden, D. et al., 2001. Impaired recruitment of bone-marrow-derived endothelial and hematopoietic precursor cells blocks tumor angiogenesis and growth. *Nature Medicine*, 7(11), 1194-1201.

Maeda, H. & Akaike, T., 1998. Nitric oxide and oxygen radicals in infection, inflammation, and cancer. *Biochemistry. Biokhimiĭa*, 63(7), 854-865.

Mantovani, A., 2009. Cancer: Inflaming metastasis. *Nature*, 457(7225), 36-37.

Mantovani, A. et al., 2008. Cancer-related inflammation. *Nature*, 454(7203), 436-444.

Mantovani, A. & Sica, A., 2010. Macrophages, innate immunity and cancer: balance, tolerance, and diversity. *Current Opinion in Immunology*, 22(2), 231-237.

Mantovani, A. et al., 2002. Macrophage polarization: tumor-associated macrophages as a paradigm for polarized M2 mononuclear phagocytes. *Trends in Immunology*, 23(11), 549-555.

McBride, J.L. et al., 2008. Artificial miRNAs mitigate shRNA-mediated toxicity in the brain: implications for the therapeutic development of RNAi. *Proceedings of the National Academy of Sciences of the United States of America*, 105(15), 5868-5873.

Mechnikov, I., 1908. On the Present State of the Question of Immunity in Infectious Diseases. In *The Nobel Prize in Physiology or Medicine 1908*. Physiology or Medicine 1901-1921. Amsterdam: Elsevier Publishing Company. Available at: http://nobelprize.org/nobel_prizes/medicine/laureates/1908/mechnikov-

lecture.html.

Medzhitov, R., 2007. Recognition of microorganisms and activation of the immune response. *Nature*, 449(7164), 819-826.

Mildner, A. et al., 2007. Microglia in the adult brain arise from Ly-6ChiCCR2+ monocytes only under defined host conditions. *Nat Neurosci*, 10(12), 1544-1553.

Mills, C.D. et al., 2000. M-1/M-2 Macrophages and the Th1/Th2 Paradigm. *J Immunol*, 164(12), 6166-6173.

Modarai, B. et al., 2005. Endothelial progenitor cells are recruited into resolving venous thrombi. *Circulation*, 111(20), 2645-2653.

Morlando, M. et al., 2008. Primary microRNA transcripts are processed co-transcriptionally. *Nature Structural & Molecular Biology*, 15(9), 902-909.

Movahedi, K. et al., 2008. Identification of discrete tumor-induced myeloid-derived suppressor cell subpopulations with distinct T cell-suppressive activity. *Blood*, 111(8), 4233-4244.

Movahedi, K. et al., 2010. Different Tumor Microenvironments Contain Functionally Distinct Subsets of Macrophages Derived from Ly6C(high) Monocytes. *Cancer Research*. Available at: http://www.ncbi.nlm.nih.gov/pubmed/20570887 [Consultato Giugno 24, 2010].

Murdoch, C. et al., 2007. Expression of Tie-2 by Human Monocytes and Their Responses to Angiopoietin-2. *J Immunol*, 178(11), 7405-7411.

Nahrendorf, M. et al., 2007. The healing myocardium sequentially mobilizes two monocyte subsets with divergent and complementary functions. *The Journal of Experimental Medicine*, 204(12), 3037-3047.

Nasarre, P. et al., 2009. Host-Derived Angiopoietin-2 Affects Early Stages of Tumor Development and Vessel Maturation but Is Dispensable for Later Stages of Tumor Growth. *Cancer Res*, 69(4), 1324-1333.

Neufeld, G. & Kessler, O., 2008. The semaphorins: versatile regulators of tumour progression and tumour angiogenesis. *Nature Reviews. Cancer*, 8(8), 632-645.

Nozawa, H., Chiu, C. & Hanahan, D., 2006. Infiltrating neutrophils mediate the initial angiogenic switch in a mouse model of multistage carcinogenesis. *Proceedings of the National Academy of Sciences of the United States of America*, 103(33), 12493-12498.

Ovchinnikov, D.A., 2008. Macrophages in the embryo and beyond: much more than just giant phagocytes. *Genesis (New York, N.Y.: 2000)*, 46(9), 447-462.

Pahler, J.C. et al., 2008. Plasticity in Tumor-Promoting Inflammation: Impairment of Macrophage Recruitment Evokes a Compensatory Neutrophil Response.

Neoplasia (New York, N.Y.), 10(4), 329-339.

Palframan, R.T. et al., 2001. Inflammatory Chemokine Transport and Presentation in HEV. *The Journal of Experimental Medicine*, 194(9), 1361-1374.

Perretti, M. & D'Acquisto, F., 2009. Annexin A1 and glucocorticoids as effectors of the resolution of inflammation. *Nat Rev Immunol*, 9(1), 62-70.

Petit, I., Jin, D. & Rafii, S., 2007. The SDF-1-CXCR4 signaling pathway: a molecular hub modulating neo-angiogenesis. *Trends in Immunology*, 28(7), 299-307.

Plytycz, B. & Seljelid, R., 2003. From inflammation to sickness: historical perspective. *Archivum Immunologiae Et Therapiae Experimentalis*, 51(2), 105-109.

Pober, J.S. & Cotran, R.S., 1990. The role of endothelial cells in inflammation. *Transplantation*, 50(4), 537-544.

Pober, J.S. & Sessa, W.C., 2007. Evolving functions of endothelial cells in inflammation. *Nat Rev Immunol*, 7(10), 803-815.

Politz, O. et al., 2002. Stabilin-1 and -2 constitute a novel family of fasciclin-like hyaluronan receptor homologues. *The Biochemical Journal*, 362(Pt 1), 155-164.

Pollard, J.W., 2009. Trophic macrophages in development and disease. *Nature*

Reviews. Immunology, 9(4), 259-270.

Prater, D.N. et al., 2007. Working hypothesis to redefine endothelial progenitor cells. *Leukemia*, 21(6), 1141-1149.

Pucci, F. et al., 2009. A distinguishing gene signature shared by tumor-infiltrating Tie2-expressing monocytes, blood "resident" monocytes, and embryonic macrophages suggests common functions and developmental relationships. *Blood*, 114(4), 901-914.

Pulaski, H.L. et al., 2009. Identifying alemtuzumab as an anti-myeloid cell antiangiogenic therapy for the treatment of ovarian cancer. *Journal of Translational Medicine*, 7, 49-49.

Qian, B. & Pollard, J.W., 2010. Macrophage Diversity Enhances Tumor Progression and Metastasis. *Cell*, 141(1), 39-51.

Ravichandran, K.S. & Lorenz, U., 2007. Engulfment of apoptotic cells: signals for a good meal. *Nat Rev Immunol*, 7(12), 964-974.

Rock, K.L. et al., 2010. The sterile inflammatory response. *Annual Review of Immunology*, 28, 321-342.

Roviezzo, F. et al., 2005. Angiopoietin-2 causes inflammation in vivo by promoting vascular leakage. *The Journal of Pharmacology and Experimental Therapeutics*, 314(2), 738-744.

Sato, T.N. et al., 1995. Distinct roles of the receptor tyrosine kinases Tie-1 and Tie-2 in blood vessel formation. *Nature*, 376(6535), 70-74.

Scatizzi, J.C. et al., 2006. p21Cip1 Is Required for the Development of Monocytes and Their Response to Serum Transfer-induced Arthritis. *The American Journal of Pathology*, 168(5), 1531-1541.

Scharpfenecker, M. et al., 2005. The Tie-2 ligand angiopoietin-2 destabilizes quiescent endothelium through an internal autocrine loop mechanism. *Journal of Cell Science*, 118(Pt 4), 771-780.

Schledzewski, K. et al., 2006. Lymphatic endothelium-specific hyaluronan receptor LYVE-1 is expressed by stabilin-1+, F4/80+, CD11b+ macrophages in malignant tumours and wound healing tissue in vivo and in bone marrow cultures in vitro: implications for the assessment of lymphangiogenesis. *The Journal of Pathology*, 209(1), 67-77.

Seegar, T.C. et al., 2010. Tie1-Tie2 Interactions Mediate Functional Differences between Angiopoietin Ligands. *Molecular Cell*, 37(5), 643-655.

Serbina, N.V. & Pamer, E.G., 2006. Monocyte emigration from bone marrow during bacterial infection requires signals mediated by chemokine receptor CCR2. *Nat Immunol*, 7(3), 311-317.

Serhan, C.N., Chiang, N. & Van Dyke, T.E., 2008. Resolving inflammation: dual anti-inflammatory and pro-resolution lipid mediators. *Nature reviews. Immunology*, 8(5), 349-361.

Shaked, Y. et al., 2008. Rapid chemotherapy-induced acute endothelial progenitor cell mobilization: implications for antiangiogenic drugs as chemosensitizing agents. *Cancer cell*, 14(3), 263-273.

Shen, H.H. et al., 1983. Functional subsets of human monocytes defined by monoclonal antibodies: a distinct subset of monocytes contains the cells capable of inducing the autologous mixed lymphocyte culture. *Journal of Immunology (Baltimore, Md.: 1950)*, 130(2), 698-705.

Shojaei, F. & Ferrara, N., 2008. Refractoriness to Antivascular Endothelial Growth Factor Treatment: Role of Myeloid Cells. *Cancer Res*, 68(14), 5501-5504.

Shojaei, F. et al., 2008. Role of Bv8 in neutrophil-dependent angiogenesis in a transgenic model of cancer progression. *Proceedings of the National Academy of Sciences of the United States of America*, 105(7), 2640-2645.

Shojaei, F. et al., 2007. Tumor refractoriness to anti-VEGF treatment is mediated by CD11b+Gr1+ myeloid cells. *Nat Biotech*, 25(8), 911-920.

Soehnlein, O. & Lindbom, L., 2010. Phagocyte partnership during the onset and resolution of inflammation. *Nat Rev Immunol*, 10(6), 427-439.

Soehnlein, O. et al., 2008. Neutrophil secretion products pave the way for inflammatory monocytes. *Blood*, 112(4), 1461-1471.

Soucek, L. et al., 2007. Mast cells are required for angiogenesis and macroscopic

expansion of Myc-induced pancreatic islet tumors. *Nature Medicine*, 13(10), 1211-1218.

St Croix, B. et al., 2000. Genes expressed in human tumor endothelium. *Science (New York, N.Y.)*, 289(5482), 1197-1202.

Stark, M.A. et al., 2005. Phagocytosis of Apoptotic Neutrophils Regulates Granulopoiesis via IL-23 and IL-17. *Immunity*, 22(3), 285-294.

Starkey, J.R., Crowle, P.K. & Taubenberger, S., 1988. Mast-cell-deficient W/Wv mice exhibit a decreased rate of tumor angiogenesis. *International Journal of Cancer. Journal International Du Cancer*, 42(1), 48-52.

Stegmeier, F. et al., 2005. A lentiviral microRNA-based system for single-copy polymerase II-regulated RNA interference in mammalian cells. *Proceedings of the National Academy of Sciences of the United States of America*, 102(37), 13212-13217.

Steinman, R.M., Lustig, D.S. & Cohn, Z.A., 1974. Identification of a novel cell type in peripheral lymphoid organs of mice. *The Journal of Experimental Medicine*, 139(6), 1431-1445.

Stockmann, C. et al., 2008. Deletion of vascular endothelial growth factor in myeloid cells accelerates tumorigenesis. *Nature*, 456(7223), 814-818.

Stratmann, A., Risau, W. & Plate, K.H., 1998. Cell type-specific expression of angiopoietin-1 and angiopoietin-2 suggests a role in glioblastoma

angiogenesis. *The American Journal of Pathology*, 153(5), 1459-1466.

Strieter, R.M. et al., 2005. CXC chemokines in angiogenesis relevant to chronic fibroproliferation. *Current Drug Targets. Inflammation and Allergy*, 4(1), 23-26.

Sundberg, C. et al., 2002. Stable expression of angiopoietin-1 and other markers by cultured pericytes: phenotypic similarities to a subpopulation of cells in maturing vessels during later stages of angiogenesis in vivo. *Laboratory Investigation; a Journal of Technical Methods and Pathology*, 82(4), 387-401.

Sunderkötter, C. et al., 2004. Subpopulations of mouse blood monocytes differ in maturation stage and inflammatory response. *Journal of Immunology (Baltimore, Md.: 1950)*, 172(7), 4410-4417.

Swirski, F.K. et al., 2009. Identification of splenic reservoir monocytes and their deployment to inflammatory sites. *Science (New York, N.Y.)*, 325(5940), 612-616.

Szulc, J. et al., 2006. A versatile tool for conditional gene expression and knockdown. *Nature Methods*, 3(2), 109-116.

Takakura, N. et al., 1998. Critical role of the TIE2 endothelial cell receptor in the development of definitive hematopoiesis. *Immunity*, 9(5), 677-686.

Takakura, N., 2006. Role of hematopoietic lineage cells as accessory components

in blood vessel formation. *Cancer Science*, 97(7), 568-574.

Takasaki, S., 2009. Methods for selecting effective siRNA sequences by using statistical and clustering techniques. *Methods in Molecular Biology (Clifton, N.J.)*, 487, 1-39.

Taylor, P. et al., 2005. Macrophage receptors and immune recognition. *Annual Review of Immunology*, 23(1), 901-944.

Termeer, C. et al., 2002. Oligosaccharides of Hyaluronan activate dendritic cells via toll-like receptor 4. *The Journal of Experimental Medicine*, 195(1), 99-111.

Toole, B.P., 2004. Hyaluronan: from extracellular glue to pericellular cue. *Nature Reviews. Cancer*, 4(7), 528-539.

Umemura, N. et al., 2008. Tumor-infiltrating myeloid-derived suppressor cells are pleiotropic-inflamed monocytes/macrophages that bear M1- and M2-type characteristics. *Journal of Leukocyte Biology*, 83(5), 1136-1144.

Urlinger, S. et al., 2000. Exploring the sequence space for tetracycline-dependent transcriptional activators: Novel mutations yield expanded range and sensitivity. *Proceedings of the National Academy of Sciences of the United States of America*, 97(14), 7963-7968.

Valenzuela, D.M. et al., 1999. Angiopoietins 3 and 4: diverging gene counterparts in mice and humans. *Proceedings of the National Academy of Sciences of*

the United States of America, 96(5), 1904-1909.

Varol, C. et al., 2007. Monocytes give rise to mucosal, but not splenic, conventional dendritic cells. *The Journal of Experimental Medicine*, 204(1), 171-180.

Varol, C. et al., 2009. Intestinal Lamina Propria Dendritic Cell Subsets Have Different Origin and Functions. *Immunity*, 31(3), 502-512.

Venneri, M.A. et al., 2007. Identification of proangiogenic TIE2-expressing monocytes (TEMs) in human peripheral blood and cancer. *Blood*, 109(12), 5276-5285.

Vigna, E. et al., 2005. Efficient Tet-dependent expression of human factor IX in vivo by a new self-regulating lentiviral vector. *Molecular Therapy: The Journal of the American Society of Gene Therapy*, 11(5), 763-775.

de Visser, K.E., Korets, L.V. & Coussens, L.M., 2005. De novo carcinogenesis promoted by chronic inflammation is B lymphocyte dependent. *Cancer Cell*, 7(5), 411-423.

Wagers, A.J. et al., 2002. Little evidence for developmental plasticity of adult hematopoietic stem cells. *Science (New York, N.Y.)*, 297(5590), 2256-2259.

Ward, N.L. & Dumont, D.J., 2002. The angiopoietins and Tie2/Tek: adding to the complexity of cardiovascular development. *Seminars in Cell & Developmental Biology*, 13(1), 19-27.

Wijffels, J.F. et al., 1994. Macrophage subpopulations in the mouse spleen renewed by local proliferation. *Immunobiology*, 191(1), 52-64.

Yang, L. et al., 2004a. Expansion of myeloid immune suppressor Gr+CD11b+ cells in tumor-bearing host directly promotes tumor angiogenesis. *Cancer Cell*, 6(4), 409-421.

Yang, L. et al., 2004b. Expansion of myeloid immune suppressor Gr+CD11b+ cells in tumor-bearing host directly promotes tumor angiogenesis. *Cancer Cell*, 6(4), 409-421.

Yona, S. & Jung, S., 2010. Monocytes: subsets, origins, fates and functions. *Current Opinion in Hematology*, 17(1), 53-59.

Youn, J. et al., 2008. Subsets of myeloid-derived suppressor cells in tumor-bearing mice. *Journal of Immunology (Baltimore, Md.: 1950)*, 181(8), 5791-5802.

Yuan, H.T. et al., 2007. Activation of the orphan endothelial receptor Tie1 modifies Tie2-mediated intracellular signaling and cell survival. *The FASEB Journal: Official Publication of the Federation of American Societies for Experimental Biology*, 21(12), 3171-3183.

Yuan, J.S. et al., 2006. Statistical analysis of real-time PCR data. *BMC Bioinformatics*, 7, 85.

Zeng, Y., Wagner, E.J. & Cullen, B.R., 2002. Both natural and designed micro

RNAs can inhibit the expression of cognate mRNAs when expressed in human cells. *Molecular Cell*, 9(6), 1327-1333.

Ziegler-Heitbrock, H.W. et al., 1991. Small (CD14+/CD16+) monocytes and regular monocytes in human blood. *Pathobiology: Journal of Immunopathology, Molecular and Cellular Biology*, 59(3), 127-130.

Ziegler-Heitbrock, L. et al., 2010. Nomenclature of monocytes and dendritic cells in blood. *Blood*, blood-2010-02-258558.